THE INFLUENCE OF PROCESS PARAMETERS ON MICROSTRUCTURES AND MECHANICAL PROPERTIES OF MAGNESIUM ALLOY BY ECAP PROCESS

A THESIS SUBMITTED TO
THE GRADUATE SCHOOL OF NATURAL AND APPLIED SCIENCES
OF
UNIVERSITY OF TURKISH AERONAUTICAL ASSOCIATION

BY

HAITHAM HASHEM AL-JAWAD

IN PARTIAL FULFILLMENT OF THE REQUIREMENTS
FOR
THE DEGREE OF DOCTOR OF PHILOSOPHY
IN
MECHANICAL AND AERONAUTICAL ENGINEERING

DECEMBER 2020

Approval of the thesis:

THE INFLUENCE OF PROCESS PARAMETERS ON MICROSTRUCTURES AND MECHANICAL PROPERTIES OF MAGNESIUM ALLOY BY ECAP PROCESS

submitted by **HAITHAM AL-JAWAD** in partial fulfillment of the requirements for the degree of **Doctor of Philosophy in Mechanical and Aeronautical Engineering, University of Turkish Aeronautical Association** by,

Assoc. Prof. Dr. Suat Dengiz
Dean, Graduate School of **Natural and Applied Sciences** _____

Prof. Dr. İbrahim Halil Güzelbey
Head of the Department, **Mechanical and Aeronautical Eng** _____

Prof. Dr. Çetin Karataş
Supervisor, **Manufacturing Eng, Gazi University** _____

Assist. Prof. Dr. Faruk Mert
Co-Supervisor, **Multi-Dimensional Modelling and Animation, Ankara Yıldırım Beyazıt University** _____

Examining Committee Members:

Prof. Dr. Cihan Karataş
Mechatronics Eng, UTAA _____

Prof. Dr. Çetin Karataş
Manufacturing Eng, Gazi University _____

Assoc. Prof. Dr. Hakan Gürün
Manufacturing Eng, Gazi University _____

Assoc. Prof. Dr. Mustafa Kaya
Aerospace Eng, Ankara Yıldırım Beyazıt University _____

Assist. Prof. Dr. Reza Aghazadeh
Mechatronics Eng, UTAA _____

Date: 25.12.2020

I hereby declare that all information in this document has been obtained and presented in accordance with academic rules and ethical conduct. I also declare that, as required by these rules and conduct, I have fully cited and referenced all material and results that are not original to this work.

Haitham Al-Jawad

Signature:

ABSTRACT

THE INFLUENCE OF PROCESS PARAMETERS ON MICROSTRUCTURES AND MECHANICAL PROPERTIES OF MAGNESIUM ALLOY BY ECAP PROCESS

Al-Jawad, Haitham
Doctor of Philosophy, Mechanical and Aeronautical Engineering
Supervisor: Prof. Dr. Çetin Karataş
Co-Supervisor: Assist. Prof. Dr. Faruk Mert

December 2020, 123 pages

Severe plastic deformation (SPD) is a method of metal forming that uses hydrostatic pressure to put high strains on a work piece with little to no important changes to shapes and dimension in order to achieve excellent refinement of grain size thereby increasing the mechanical properties of strength and ductility. Equal channel angular pressing is one of the most significant processes of the SPD method which is used especially for light metals to improve their properties by using simple dies of two constant cross-sectional channels with bends between them through two distinct angles, namely an outside angle called the curvature angle (ψ) and an inside angle called the channel angle. Hydrostatic pressure is applied with a punch to press the billets from above one channel to exit from the other side of the other channel. Moving through the bending section and pressing leads to changing any coarse grains to very fine grains by repeating this process many times. A great improvement is seen in the material structure without any significant modification to the shape of the work piece. In this study, magnesium alloy AZ31 was used to investigate the effect of punch velocity, number of passes and temperature on required loads, microstructure, grain size and hardness.

Temperatures of T1 = 275°C and T2 = 300°C and velocities of V1 = 14mm/s and V2 = 27 mm/s were used with three passes. The process was performed using MOLY KOTE D321 mineral lubricant. Numerical analysis was conducted using the QForm application and experimental work was performed with suitable manufactured dies containing jacket heaters for the ECAP process that was achieved with a hydraulic press. The die was insulated on all sides to maintain the temperature inside the die high so as to reduce the time of heating. The results showed that increasing the number of passes reduced the grain size to 1.9 at the maximum temperature of T2 = 300°C with the highest velocity of V2 = 27 mm/s. In this field, increasing the temperature T2 = 300°C would increase the hardness to 103 HV, while the hardness was 94 HV at T1 = 275°C with the hardness increasing gradually from pass 1 to pass 3 from 83.5 HV to 103 HV. For the microstructure, it has been shown that on pass 3 with the highest temperature and V2, the grain distribution was more homogeneous and uniform than with the low temperature and low velocity. Many defects appeared during the experimental work, such as broken samples, flakes, non-uniform shapes, sticking with die surfaces and difficulty of extraction from the die. These defects were related to there having been little to no lubrication, occasional high temperatures, high velocities, and the poor surface finishing of the die. Nevertheless, there was good agreement between the numerical analysis and the experimental work.

Keywords: Q Form, ECAP Process, Magnesium Alloy, Microstructure, Velocity.

ÖZ

İŞLEM PARAMETRELERİNİN MAGNEZYUM ALAŞIMININ EKAP İŞLEMİNDE MİKROYAPI VE MEKANİK ÖZELLİKLERİ ÜZERİNE ETKİSİ

Al-Jawad, Haitham
Doktora, Makine ve Uçak Mühendisliği
Tez Yöneticisi: Prof. Dr. Çetin Karataş
Ortak Tez Yöneticisi: Dr. Öğr. Üyesi. Faruk Mert

Aralık 2020, 123 sayfa

Bir metal şekillendirme yöntemi olarak bilinen aşırı plastik deformasyon (SPD), tane boyutu için mükemmel bir düzenleme elde etmek amacıyla boyutlarda herhangi bir değişiklik olmadan veya önemli bir değişiklik olmadan işlenecek parça üzerinde çok yüksek gerilmeler oluşturmak için hidrostatik basıncı kullanır ve bunun sonucunda mukavemet ve esnekliğin mekanik özelliklerini artırır. Eşit kanal açısal presleme, (1) eğrilik açısı (ψ) olarak adlandırılan dış açı ve (2) kanal açısı olarak adlandırılan iç açı olmak üzere iki farklı açı ile aralarında bükülme bulunan iki sabit kesitsel kanalın basit şekillendirme kalıbını kullanarak özellikle hafif metallerin özelliklerini iyileştirmek için kullanılan SPD işlemlerinin en önemlilerinden birisidir. Hidrostatik basınç bir kanalın üstünden kütüğü diğer kanalın öbür tarafından bastırmak için zımba ile uygulanmaktadır. Bükme bölümü boyunca hareket etmek ve presleme, bu işlemi birçok kez tekrarlayarak taneciği çok ince tanelere dönüştürmeye neden olur, ardından işlenecek parçanın şeklinde önemli bir değişiklik olmadan malzeme yapısında yüksek bir geliştirme meydana gelir. Bu çalışmada, magnezyum alaşımı AZ31, zımba hızı, pas sayısı ve sıcaklığın; gerekli yük, mikroyapı, tanecik boyutu ve sertlik üzerindeki etkisini araştırmak için

kullanılmıştır. Üç pas ile iki hız değeri (V1 = 14 mm/s ve V2 = 27 mm/s) ve iki sıcaklık (T1 = 275°C, T2 = 300°C) kullanılmıştır. İşlem, bir mineral yağlama türü (MOLY KOTE D321) kullanılarak yapılmıştır. QForm yazılımının sayısal analizi uygulanmış ve EKAP işlemi için ceket ısıtıcıları içen uygun pres kalıbı üretilerek deneysel çalışma hidrolik pres ile gerçekleştirilmiştir. Kalıbın içindeki sıcaklığı yüksek ve sabit tutmak ve ısıtma süresini düşürmek için, kalıp her yönden yalıtılmıştır. Sonuçlar, artan pas sayısının T2 = 300°C maksimum sıcaklıkta en yüksek V2 = 27 mm/s hızda tane boyutunu 1.9'a düşürdüğünü göstermektedir. Bu alanda artan sıcaklık T2 = 300°C, sertliği 103 HV 'ye çıkarırken, T1 = 275 C' de sertlik 94 HV ‘dir ve sertlik pas 1'den pas 3'e (83.5-103) HV'den kademeli olarak artmaktadır. Mikro-yapı için, pas 3 ‘te, en yüksek sıcaklıkta ve V2 ‘de, tane dağılımının düşük sıcaklık ve düşük hıza oranla daha homojen ve tekdüze olduğu görülmüştür. Deneysel çalışma sırasında (1) numune kırılması (2) çatlama (3) düzgün olmayan şekil (4) kalıp yüzeyine yapışma, (5) kalıptan zor çıkarılması gibi kusurlar ortaya çıkmıştır. Bu kusurlar düşük yağlama, bazen yüksek sıcaklıklar, yüksek hız ve kalıbın zayıf yüzey kaplaması ile ilgilidir. Sayısal analiz ile deneysel çalışma arasında iyi bir uyum vardır.

Anahtar Kelimeler: Q Formu, EKAP İşlemi, Magnezyum Alaşımı, Mikro-yapı, Hız.

I dedicate my work to my family.

ACKNOWLEDGMENTS

My gratitude goes to Allah, Who helped me to reach to this goal.

I would like to thank my supervisor Prof. Dr. Çetin KARATAŞ and Co-Supervisor Assist. Prof. Dr. Faruk MERT for their continuous advice and support during the period of my work.

My thanks go to my Big Family, especially my parents and I would like to express my deepest gratitude appreciation to them.

I wish also to convey my love and gratitude to my small family, especially my wife for her support for me as well as our dear son, for my study from its beginning to its end.

Many thanks also to Assoc. Prof. Dr. Suat DENGİZ and Assist. Prof. Dr. Masoud LATIFI-NAVID from UTAA University for their assistance and support.

Finally, thank you to all my well-wishers.

December 2020

Haitham Hashem AL-JAWAD

TABLE OF CONTENTS

LIST OF TABLES

TABLES

LIST OF FIGURES

FIGURES

LIST OF ABBREVIATIONS

ABBREVIATIONS

ECAP	:	Equal Channel Angular Process
SPD	:	Severe Plastic Deformation Process
TEM	:	Transmission Electron Microscopy
LOM	:	Light Optical Microscopy
EBSD	:	Electron Back Scattering Diffraction
IPF	:	Inverse Pole Figure
CRSS	:	Critical Resolved Shear Stress
3D-RD ECAP	:	Three Dimensional Rotary Die for the Equal Channel Angular Pressing Process
I-ECAP	:	Incremental Equal Channel Angular Pressing
P/M	:	Powder Metallurgy
QForm	:	QForm software
HPT	:	High Pressure Torsion
ARB	:	Accumulative Roll Bonding

LIST OF SYMBOLS

SYMBOLS

ε	:	Strain
N	:	Number of pass
ε_{tot}	:	Total strain
ε_N	:	Strain after (N) passes
P	:	Applied pressure
Φ	:	Channel angle
ψ	:	Angle at the arc of curvature (corner angle)
φ	:	Channel angle
σ	:	Stress
σ_o	:	Yield strength
σ_1	:	Frictional stress
k	:	Hall pitch slope
D	:	Diameter of grains
H_o	:	Hardness of material HV
H_1	:	Constant
HV	:	Vickers Hardness

CHAPTER 1

INTRODUCTION

1.1 Motivation

Magnesium and its alloys have a closely packed hexagonal crystalline with some slip arrangements which can occur at minimum temperatures.

Parts made of magnesium are usually manufactured with a casting process, which limits how products are shaped due to the low ductility of these alloys. Therefore, the need to produce more complex magnesium alloy product shapes has led to the improvement of their manufacturing processes by using equal channel angular pressing, which is one of the severe plastic deformation processes that increases the superplasticity of magnesium alloys and increases the ability of structures to use them with high strain ranges under compression [1].

The ECAP process has many advantages, especially the reduction in grain size and increase in refinement of products in addition to improvements in mechanical properties such as hardness and strength of products. Moreover, this process has the ability to dissolve the second phase when using alloying elements. The differences between any severe plastic deformation and other metal forming processes are the limited shape and dimension changes when applying pressing to achieve high strains. For this reason, it becomes possible to repeat the process many times to increase refinement while the dimension and shape of the product shows no ostensible change. Lubricants are usually is used with the work piece and die in the ECAP process. In the ECAP process, there are two angles channels with constant cross section. The process has many applications in many fields of industry, especially those industries that used magnesium alloys. The most important aspects of this process are the two angles, the channel angle (denoted by

Φ), and the curvature angle (denoted by ψ), both of which have a great influence on the plastic deformation during each pass [2].

1.2 Background

Serve plastic deformation processes (SPDs) are metal forming methods such that wide pressing is applied to produce high strains with little to no change to the form and dimension of a work piece. Over the last few decades, metal forming has improved with the SPD process by adopting equal channel angular pressing, the results of which include decreased deformation, improvements in superplasticity and better mechanical properties. Magnesium attracts great interest due to its broad application in the automotive, military, electronic and aerospace industries [3]. A specific characteristic of magnesium that makes it a significant metal and one of the lighter commercial structural metals is its ability to be cast as well as its hexagonal closed-packed (HCP) crystalline structure which yields a low number of efficient slip systems.

Magnesium alloy is used for its light weight in medical applications. However, magnesium and its alloys are considered to be light metals that need to have their forming properties enhanced by increasing ductility and decreasing grain size during refinement, especially since these alloys work with high or moderate temperatures according to their crystal structures [4]. Hot metal forming for magnesium produces remarkable effects on grain size and grain distribution. In traditional metal forming of magnesium, the distribution of grains is heterogeneous, whereas in severe plastic deformation, a homogeneous fine grain occurs. SPD is usually used to change coarse grains in metallic materials into ultrafine grains (UFGs) that have an average size of less than 1 micrometer [5]. The SPD processes includes ECAP, high pressure torsion, multi-directional forging, twist extrusion and cyclic extrusion compression (ECAP).

The equal channel angular process was first introduced by Segal in 1970. The process would increase strains with low shear. Then this process developed in 1990

when studies improved to achieve sub-micrometer grains and high refinement with uniform properties. This process is important among other SPD processes as it can be used with alloys and metals, simple die designs, and homogeneous grain structures [6].

1.3 Aim of the Study

The study presents the equal channel angular pressing process (ECAP) by designing and manufacturing a suitable die followed by presenting the effects of hardness, tensile strength and ductility on texture and mechanical properties.

The study includes:

- The effect of velocity and a study on the development of microstructure and super plasticity to achieve the optimum velocity for the best refinement of magnesium alloy.
- The effect of the number of passes of the ECAP process and demonstrating its influence on microstructure.
- The effect of temperatures used during the process, such that different temperatures will be used to study their effects on grain refinement as well as improvement of ductility and formability.
- Insight into different past developments in this area of the ECAP process. One of the points discussed in this study is the significant characteristic of magnesium alloy undergoing sever plastic deformation.
- Demonstrations of the importance of numerical solutions to estimate initial results and the advantages of simulations to reduce the time and costs of manufacturing but improve product quality.
- Finding the optimum values of the parameters of the ECAP process for magnesium alloy.

1.4 Thesis Outline

Chapter One: In this chapter, an introduction to ECAP process and severe plastic deformation is discussed and a brief background is explained with the aims of the research.

Chapter Two: Previous studies related to the subject are presented in summary to reveal what has already been studied in addition to noting what has not been discussed or studied. Finally, the reasons for choosing this research are presented.

Chapter Three: In this chapter, all fundamentals and parameters with an analysis of the equal channel angular pressing process are explained. In addition, the chapter presents the types of angles, advantages of ECAP in different routes available.

Chapter Four: Q Form software and numerical analysis are discussed. Die design, boundary condition, work piece material and output with input parameters are also presented.

Chapter Five: In this chapter, the details of experimental work, die manufacturing, billet preparation, process achievement, product shape and defects are explained.

Chapter Six: The results of the numerical analysis in addition to experimental results with tests and a discussion are presented in this penultimate chapter.

Chapter Seven: Finally in this chapter, the conclusion of the study and work are presented, ending finally with a number of suggestions and recommendations for future work.

CHAPTER 2

LITERATURE REVIEW

2.1 Classification of Studies

2.1.1 Work Piece Material

L. Lin et al. studied the development of the microstructures and low temperature super plasticity of magnesium alloy ZK40 by using ECAP. The temperatures used for the process ranged from 473°K to 623°K. To find the microstructure transformation, the Transmission Electron Microscopy (TEM) technique was applied. It was seen that important changes would occur after one pass across the die and ultrafine grains would occur after many passes of the ECAP process until the grain size reached decreased to 0.8 μm and less. This alloy gives minimum temperature superplastic between 473°K and 523°K. Elongation had increased from 260% at 473°K to 612% at 523°K. However, for only one pass, the parallel values were 124% at 473°K and 212% at 523°K. The cause of this low superplastic action through one pass of ECAP was the non-uniform grain boundaries of the rough grains that belonged to the large stresses domain. Another reason for reduction of the superplasticity progress had been the inappropriate contact between the fine and large grains. The results showed that the grain size of the ZK40 alloy after one pass of ECAP process was 5.6 μm and 0.8 μm after three passes. In one ECAP pass, non-uniform microstructures would occur because of the great number of dislocations of the coarse grains and the non-uniform grain boundaries. The areas of small and large grains were moved. For three passes of the ECAP process for ZK40 alloy, superplasticity at low temperatures had related to the effects of fine grains, grain boundaries with large angles and the symmetry of the microstructure [1].

F.S.J. Poggiali et al. studied the influence of the ECAP process on grain refinement for commercial grade pure magnesium. The process was applied at a temperature of 523°K, a temperature lower than every other temperature used in previous papers. The deformation zone was used to measure the grain structure. The benefit such a low temperature was to stop the important growth of the grain. Verification was done by comparing the results of the refinement with other studies. A two modal grain size spread was noticed with an important fraction of the volume of unrefined rough grains. At the beginning of the stage, twinning and grain boundary roughness would occur while small grains nucleated around the center of the grain boundaries and through twins in the second stage [2].

Y. Estrin and A. Vinogradov, demonstrated severe plastic deformation processes and their application and advantages with process principles. The main reasons to use severe plastic deformation (SPD) include grain size control, which is the guide for the microstructure and mechanical properties of the material, especially light metals that have low strength. The goal was to reduce grain size and achieve the best refinement to increase the performance of the alloy. The study defined the SPD process as type of metal forming that occurs when using hydrostatic pressure to produce a very high strain with no important changes to the geometry and dimensions of the billets. These processes included many metal forming processes, such as ECAP, high pressure torsion, multi axial forging, twist extrusion, cyclic extrusion and Con shearing. Grain sizes after the SPD processes were between 100 nm and 1000 nm for sub-micrometer sized grains and less than 100 nm for nanometer sized grains [3].

R.B. Figueiredo and T.G. Langdon, demonstrated the mechanical behavior and grain refinement of AZ31 magnesium alloy by using the equal channel angular pressing (ECAP) process at 473°K. This process has the efficiency to refine the grain structure of magnesium alloys. Moreover, for mild temperatures, it would develop ductility. The differences between the magnesium alloys and other metals are the growth of new grains at the boundaries of the first structure and those recent grains having slow diffusion that resists large grains in subsequent passes to enter

between grain boundaries. The process depended on the basics of dynamic recrystallization such that new grains would grow at the initial boundaries and at the couple of boundaries in which they distributed like the necklace shape. The study provided the idea for many experiments and explained the grain size engineering principles which would facilitate choices of material characteristics in alloys of magnesium. The study showed that the ECAP process applied to magnesium alloy AZ31 would produce a non-uniform grain structure after two passes and after six passes it would give a uniform structure with smooth grains and good diffusion. These smooth grains increase the ductility at medium temperatures [4].

M. Gzyl et al. studied the ECAP process with another magnesium alloy, namely AZ31B, to investigate the influence of temperatures on microstructures and grain sizes during the process. The gradual process of this type of equal channel angular process provided the ability to use longer work pieces than the traditional process. The study dealt with the temperature T = 250°C to show the refinement on grain sizes and its effects on hardness and another mechanical properties with different routes. These routes would have a great influence on grain sizes and metal structure and thus they could control the behavior of the metal while pressing. It was shown that after the process, the ductility of the material increased and made slipping of the metals and deformation easier than before. The research showed that there were improvements in the microstructure and homogeneity of the materials [5].

P. Lukáč et al. discussed the microstructure and mechanical properties of AZ31 and AZ61 magnesium alloys by using rolling and then having the metals undergo equal channel angular pressing. The study calculated the micro hardness, maximum tensile strength and elongation to failure. In the study, light optical microscopy (LOM) was used and the results showed that grain sizes decreased and that the microstructures were inhomogeneous. Transmission electron microscopy (TEM) showed grains with an increase in the heterogeneity of the dislocations and grains without dislocations. In other areas, recrystallized grains were distributed. For the micro hardness test, the values showed another in homogenous. The maximum

tensile strengths of the materials in these two processes were higher than those of the work pieces produced by rolling only [7].

Y. Estrin et al. investigated the microstructure, mechanical properties and texture of magnesium alloy AZ31 after applying the ECAP process to it. To study the effects of this technique, electron backscattering diffraction (EBSD) and neutron diffraction experiments were conducted. These tests had the ability of demonstrate the development of the microstructure and texture with the strain increasing while increasing the number of passes of the equal channel angular process. In addition, other compression tests were performed to explain the microstructure changes. The ECAP processes had a useful influence on the compressive strength and ductility of the alloy. The results showed that after four to eight ECAP passes, homogeneous smooth grains were formed and the grain size was near to 3 µm. The first situation used an extrusion process which offered a good texture and deformation encouraging tensile twins. These tensile twins were reduced to four in the microstructure in the ECAP passes and new structures were formed. By using inverse pole figure (IPF) maps acquired via EBSD, the grain improvement technique was demonstrated to be dynamic recrystallization. The results were verified using neutron diffraction. By taking the ductility and strength into account, the best properties could occur in compression tests for the squeeze cast, hot rolled and extruded + ECAP process materials [8].

R.B. Figueiredo and T.G. Langdon, worked in the field of developing superplasticity using the ECAP process for magnesium AZ31 alloy. Their process improved and reduced the grain size to 2.2 µm; however, by using heat treatment (annealing) at 673°K for 30 minutes, grain sizes increased to 6 µm. Although the microstructure was non-stable, the material had been superplastic under tension at temperatures ranging from 623°K to 723°K with elongations occurring at near to 1,000% and strain rates below 10^{-4} s^{-1}. The results showed that the strain rate sensitivity = 0.5 and the active was near to the amount of the grain boundary spread. A comparison between the experimental work and the model show a big approval for super plasticity related to grain boundary slipping [9].

R.B. Figueiredo and T.G. Langdon, discussed superplastic ductility for magnesium alloy ZK60 undergoing the ECAP process. The grain sizes of the superplastic metals were 3-5 μm, while the methods of severe plastic deformation (SPD) yielded average grain sizes in the sub-micrometer range and that the materials could offer very good superplastic properties if the grains showed consistency at high temperatures. Equal channel angular pressing could produce substantial grain refinements at the sub-micrometer level and increase the superplastic ductility of magnesium alloy. Tensile elongation was 3,050% after two passes of ECAP at 473°K. This large amount of ductility after only a few passes is the reason for using these alloys in industrial superplastic production processes. The elongation refers to the best collection of refined grains and consistency of structure. At that time, the material would show super plasticity at a minimum temperature and it give high impedance to the growth of the damage. In addition, it could increase the instability of the strain rate, resist the tensile sensitivity and increase the next homogeneous deformation. The study showed that grain improvement would increase the likelihood of elongation and enhance the ductility during the initial ECAP passes and after two passes. Superplastic ductility would decrease because of grain growth. The strain rate instability value had a great influence on calculating the properties of the flow for ZK60 alloy [10].

R.B. Figueiredo et al. studied the effects of changing angles during the equal channel pressing process on the development of texture for magnesium alloy ZK60 during one pass. The experimental work included pressing the magnesium alloy through different angled dies (such as 90°, 110° and 135°). The prediction work was performed with a visco plastic self-consistent model. The study showed that the angles of dies affected the development of the texture and there was activity throughout the process beginning with basic slips in magnesium alloys. This important conclusion was related to the fine grain size and severe plastic deformation. The numerical solution showed proof of geometrical softening at the beginning stage of deformation if channel angles of 90° and 110° were used. In the simulation, predictions of the texture were made after four passes. To reveal the best connection between the numerical solution and experimental solution, the

ratios of the critical resolved shear stress (CRSS) for basal and non-basal slip were modified. For good agreement between the experimental and numerical work, the CRSS ratio for the basal and non-basal slips had to be low. The factors affecting the ECAP process were first the texture before ECAP process, then the path of the process and finally the channel angle [11].

2.1.2 Process Conditions

R. Ding et al. discussed the influence of ECAP for Mg alloy ZE41 on the alloy's microstructure and mechanical properties in tensile tests at 320°C. It was shown that the equal channel angular pressing process refined the deposits and the grains. Therefore, the strength and ductility of the alloy would improve. The strength and ductility before the ECAP process were 160 kPa and 8%, respectively, while after six passes of the ECAP process, the values were 230 kPa and 20%, respectively. The study revealed that T-phase (Mg Zn_3 Re) particles spread at the boundaries of the grains and a few particles of the Zr-rich phase (Zn_2Zr_3) would spread inside the grains. The ECAP process was adequate to refine the size of particles and the grain. Grain sizes had decreased to 2 μm after six passes of the process. In the tensile test, it was observed that two kinds of twining would appear [12].

Y.K. Jing et al. used a three-dimensional rotary die for the equal channel angular pressing process (3D-RD ECAP) to study the influence of routes on the mechanical properties and microstructure of magnesium alloy AZ31. The researchers used four routes: $A^{'}$, B'_A, B'_C and C'. It was shown that all the routes hade influences on the microstructures. However, these influences were different for the microstructural uniformity and ductility of the samples. For example, grain sizes and tensile elongations had better improvement on routes $A^{'}$, B'_A than on routes B'_C and C' at ambient temperatures. The spread of hardness through the centers of the linear planes from various planes were regular with the symmetric microstructural edges. The conventional shear mode of ECAP was limited when the strain analysis was done on the cubic elements. The study revealed that using experimental and numerical for the uniformity of the deformation belonged to the alternative effect

of the tensile and compressive stresses at various places and it did not depend on the harmony of the cubic elements [13].

2.1.3 Types of Test

K. Bryla et al. revealed the effect of the number of ECAP passes on the microstructure and mechanical properties of magnesium alloy AZ31. The study discusses the effects after two and four passes of the ECAP process at temperatures of 423°K and 523°K using optical and transmission electron microscopy. The evaluation of the micro hardness test with the Vickers and compression test were performed. The refinement after the ECAP process was 1.5 µm at 423°K. Dynamic recrystallization would also occur. The researchers found that when the number of passes increased, the grains sizes would decrease which increase the mechanical properties. Homogeneous grains occurred after two and four passes. After two passes, the deformation caused bimodal grain structure. Coarse grains would form because of the action of the dynamic recrystallization procedure. These were demonstrated because the dislocations were rearranged in the shape of cells and formed the sub-grain borders [14].

G.D. Fan et al. discussed the influence of grain size on the cyclic micro plasticity of the equal channel angular pressing process for pure magnesium. The process was performed at a temperature of 250°C over four passes. To improve the microstructures A heat treatments were done. By performing tensile loading and unloading tests, the cyclic plastic deformation development was able to be measured for pure magnesium at various grain sizes in the micro strain region. The deformation was divided into two stages, the first of which would explain plastic deformation and its relationship to the dislocation movement at the basal plane that began with a small pressure. The coefficient of the strain hardening and stresses of the friction were small [15].

Y Ogushi et al. discussed another method of equal channel angular pressing that would improve the properties and increase grain refinement by disbanding different

phases with various alloying elements. In their method, improvements could be made to the properties of magnesium alloy AZ80 by combining the ECAP process with some heat treatment processes. A comparison between traditional ECAP and the new, improved method was made for a constant temperature T = 200°C and many passes until reaching the best grain size. In this study, two modes of work were performed: (1) ECAP followed by heat treatment for aging; and (2) solution heat treatment followed by the ECAP process and then heat treatment for aging. The results showed that the solution treatment led to occurrences of precipitation which would reduce grain sizes and improve mechanical properties [16].

G. Qiang et al. worked with pure magnesium and magnesium alloy ZM21 in these metals' important application and use in biomedical fields. Boundary conditions depended on work piece material properties and the process condition of the ECAP process during warm metal forming. In this condition, it was seen that a great improvement in grain refinement would occur which increased hardness and strength. During the strength tests, the study showed that tension strength was more important than compression strength. The ECAP process also showed high progress in metal plastic deformation while flowing. These grain size improvements would lead to increases in corrosion resistance. The degradability of some metals attracted the researchers' attention to use them in different fields and to conduct many studies to increase their efficiency [17].

E. Mostaed et al. discussed how magnesium alloys were widely used in ECAP process applications and research because of their properties in hot and warm deformation. The ECAP process was applied to magnesium alloy to increase its strength and improve its mechanical properties. In this study, ZK60 was used to demonstrate how the number of passes and how temperatures changes would influence microstructure and strength. Temperatures values of 523°K, 473°K and 423°K were used over four passes of pressing to compare the effects. The study showed that good refinement and strength would occur after the fourth pass at T = 423°K where corrosion resistance would increase and grain size would

decrease and there would be improvements in mechanical properties and ductility [18].

E. Mostaed et al. used ZM21 magnesium alloy to demonstrate the influence of decreasing temperatures on structure and ductility undergoing equal channel angular pressing by using two temperatures, namely T = 473°K and T = 423°K, in two steps of pressing. In each step, four passes were made. The results showed that useful refinement and grain sizes were achieved only in the first step, while no further decrease in grains size occurred in subsequent steps. The best refinement occur at T = 473°K and after pass four, when the grain size reached 700 nm. An analysis of the microstructure revealed that from the first pass, there was a clear decrease in grain size and increase in strength as well as the formation of another basal structure. The yield stress decreased to the half while elongation increase to the double and that was shown in the non-uniform yielding point which could be lessened in two ways: (1) by making basal plane weaker, and (2) by reducing the grain size [19].

In this field, it has been shown that the previous studies on magnesium alloy with equal channel angular pressing do not deal with the effects of velocity, lubrication, and die geometry on material structure and mechanical properties. Therefore, in this study, this alloy has been used to demonstrate the effect of temperature, number of passes, and punch velocity on microstructure, hardness and loads required when using a circular cross section punch and a suitable manufactured die with a 90-degree angle channel and 20-degree curvature angle with lubrication. Magnesium alloy AZ31 has been used as the work piece material in our investigation.

CHAPTER 3

FUNDAMENTALS OF THE ECAP PROCESS

3.1 Introduction

Severe plastic deformation (SPD) has garnered the attention of researchers because of how the process improves for the mechanical properties of magnesium alloys and increases their ductility and strength. Equal channel angular pressing (ECAP) is one of the most important SPD processes with many applications using magnesium alloys. Using this method, a very large shear strain can be applied to a billet by pressing it repeatedly with a die that has an angular channel. In this chapter, the fundamentals, procedures and main parameters of the ECAP process and its effects on magnesium alloys are explained [20].

3.2 Severe Plastic Deformation (SPD)

3.2.1 Definition

SPD processes are related to metal forming methods that use compression to achieve high strain rates without making any important changes to the dimensions and shape of a work piece in which coarse grains in the work piece are reduced in size to ultrafine grains ıf less than 1 micrometer. This method is applied with all metals and alloys that have low strength and ductility in order to improve their mechanical properties [6].

3.2.2 Advantages of Severe Plastic Deformation

These processes are capable of introducing:

1- Large plastic straining.
2- Efficiency to achieve microstructural refinement.
3- Increased super plasticity.
4- Improved ductility

In this process, the microstructures have grain sizes between 70 μm and 500 μm [21, 22].

3.2.3 Types of Severe Plastic Deformation Process

1- Equal channel angular pressing (ECAP)
2- High pressure torsion (HPT)
3- Accumulative roll bounding (ARB)
4- Multi-axial forging
5- Twist extrusion
6- Cyclic extrusion compression (CEC)
7- Parallel channel ECAP
8- Continuous process
9- Continuous repetitive corrugating
10- Incremental ECAP [6, 8]

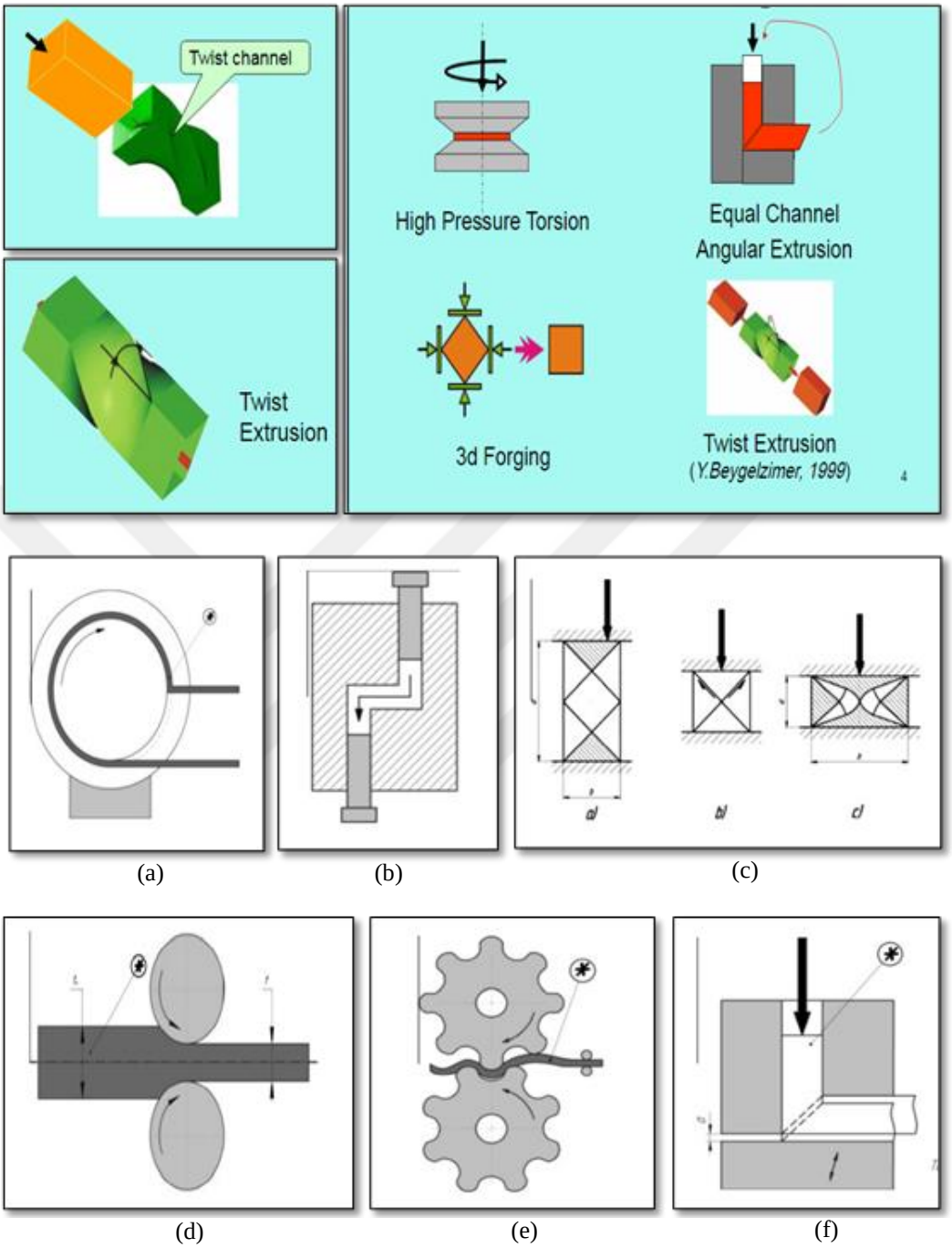

Figure 3.1: Some SPD techniques [23]: (a) Continuous processes (ECAP); (b) Parallel channel; (c) Multi axial forging; (d) Accumulative roll bonding; (e) Continuous repetitive corrugating; and (f) Incremental ECAP (I-ECAP)

3.3 Equal Channel Angular Pressing (ECAP)

The equal-channel angular pressing process is one of the most efficient severe plastic deformation (SPD) techniques used to produce bulk ultrafine-grained metals and improve the mechanical properties for some light metals by using a simple die of two channels with an inside channel angle and outside curvature angle with a lubricated billet being pressed under hydrostatic pressure to refine the grains without significant change to shape or dimensions [24].

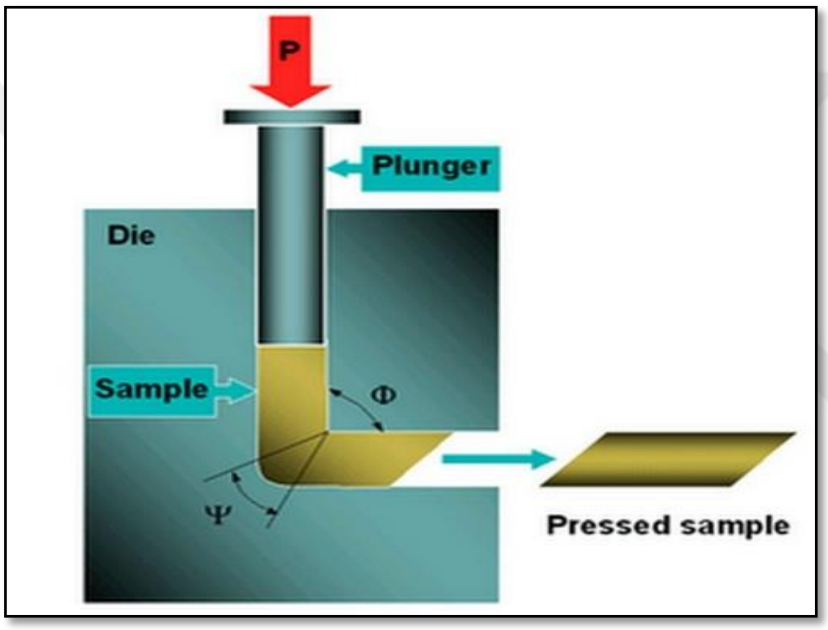

Figure 3.2: ECAP process die [25]

3.3.1 Equal Channel Angular Pressing (ECAP) Method

Equal channel angular pressing (ECAP) is a die containing a channel with a sharp angle near the center of the die. A billet is pressed inside the channel using a plunger or punch which has a pressure (P) applied to it. The cross-sectional dimensions remain unchanged during the process. The process can be repeated many times in order to decrease the grain size and improve ductility with no clear shape modification [6].

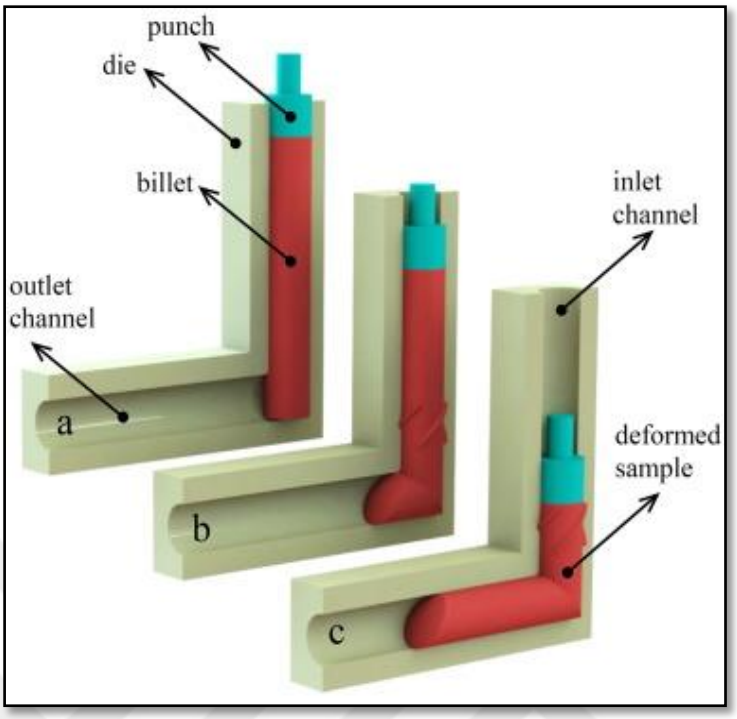

Figure 3.3: ECAP process [26]

3.3.2 Types of Angle Used in the ECAP Process

The ECAP die is a simple die but of greatest importance to die geometry are the angles between two constant cross-sectional channels. These angles can be 90° and greater. These angles control the grain size, the direction of the metal and the plastic deformation during the process. The two angles in this process are:

1- The outside angle called the curvature angle ψ; and
2- The inside angle called the channel angle Φ.

The angle of the arc of curvature is more important if it is below 90°. [27].

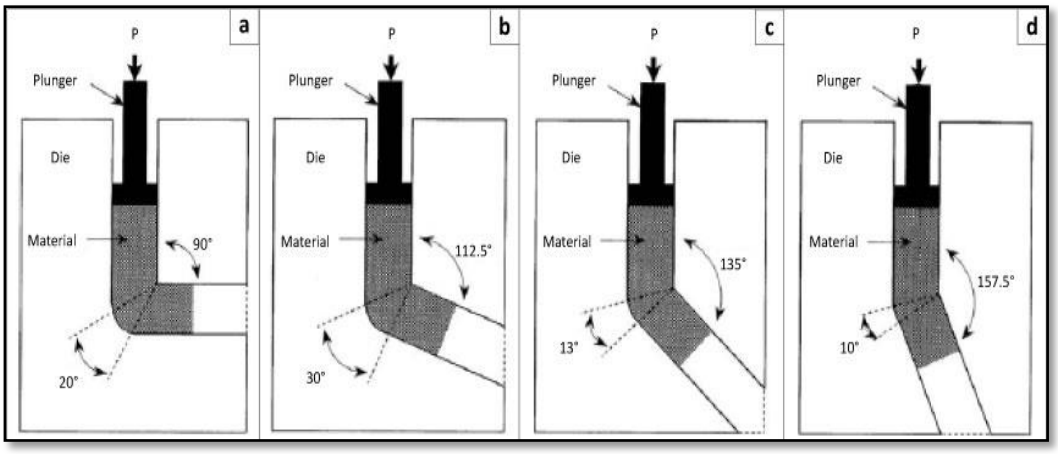

Figure 3.4: Angle types in the ECAP process [27]

3.3.3 Important Conceptions of ECAP

The process of equal channel angular pressing (ECAP), known also as equal channel angular extrusion (ECAE), has many important control parameters, such as:

1- Channel cross section
2- Corner angle
3- Processing route
4- Friction
5- Number of passes
6- Work piece dimensions
7- Process condition
8- Lubrication
9- Temperature [28]

Microstructures, micro hardness, grain size, super plasticity or ductility, and mechanical properties such as elongation and ultimate tensile strength are the main parameters that change after equal channel angular pressing [29].

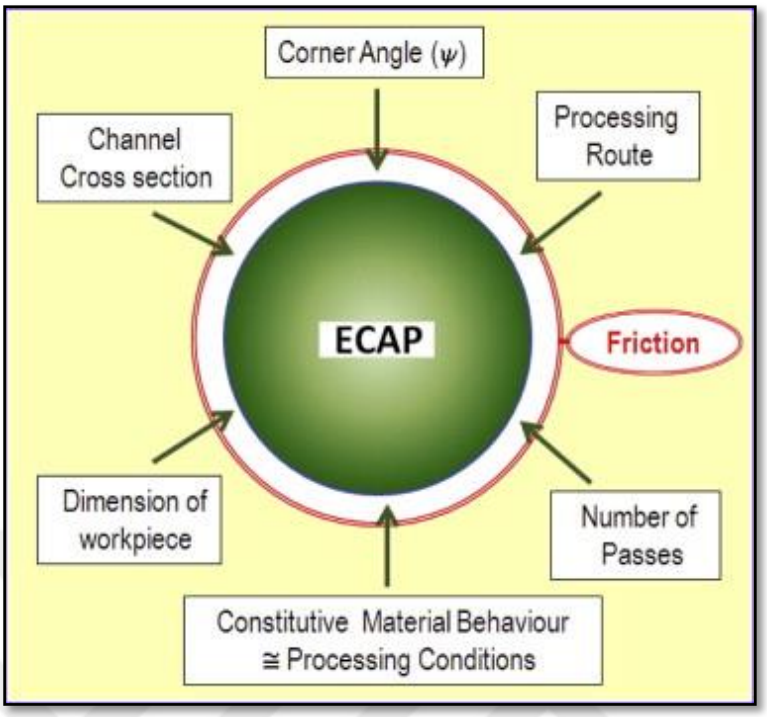

Figure 3.5: Parameters related to ECAP [30]

3.3.4 Die Geometry of ECAP

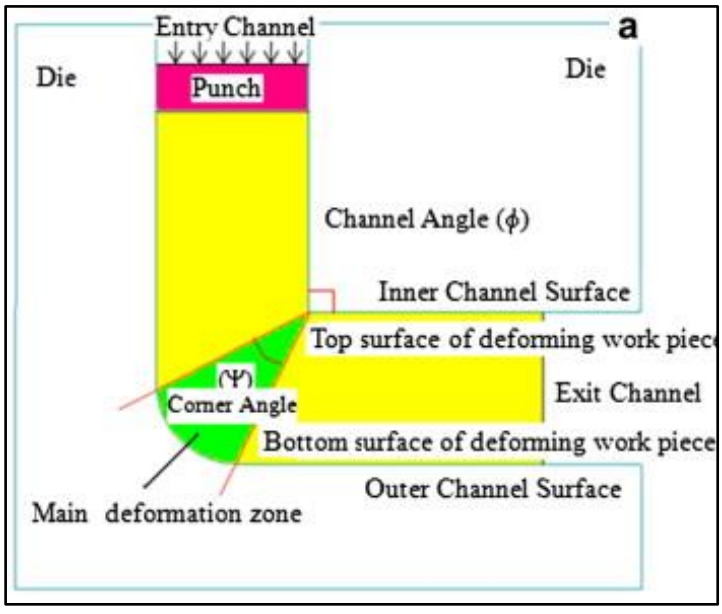

Figure 3.6: Details of ECAP dies [31]

3.3.5 Fundamental Parameters

The ECAP procedure is a metal flow process operating in simple shear with the important basic parameters:

1- Strain range imposed during every separate pass into the die
2- Slip systems operating during the pressing process
3- Shearing planes on the deformed pressed work piece [6, 32].

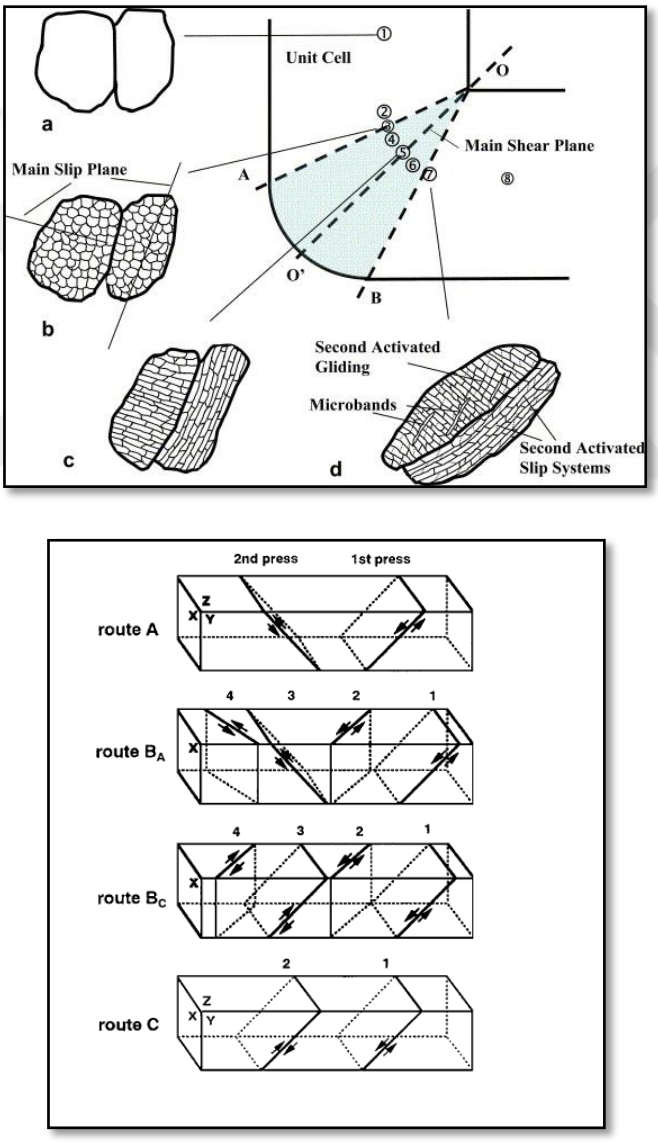

Figure 3.7: Slip systems in the ECAP process [33]

3.3.6 Factors Influencing the ECAP Process

A number of factors influence the workability and microstructure characteristics of the pressed billets during equal channel angular pressing. These factors can be classified according to the following criteria:

1- Experimental work condition related to die angles
2- Process conditions including velocity, punch pressure and temperature
3- The crystal structure of the undeformed work piece [34, 6]

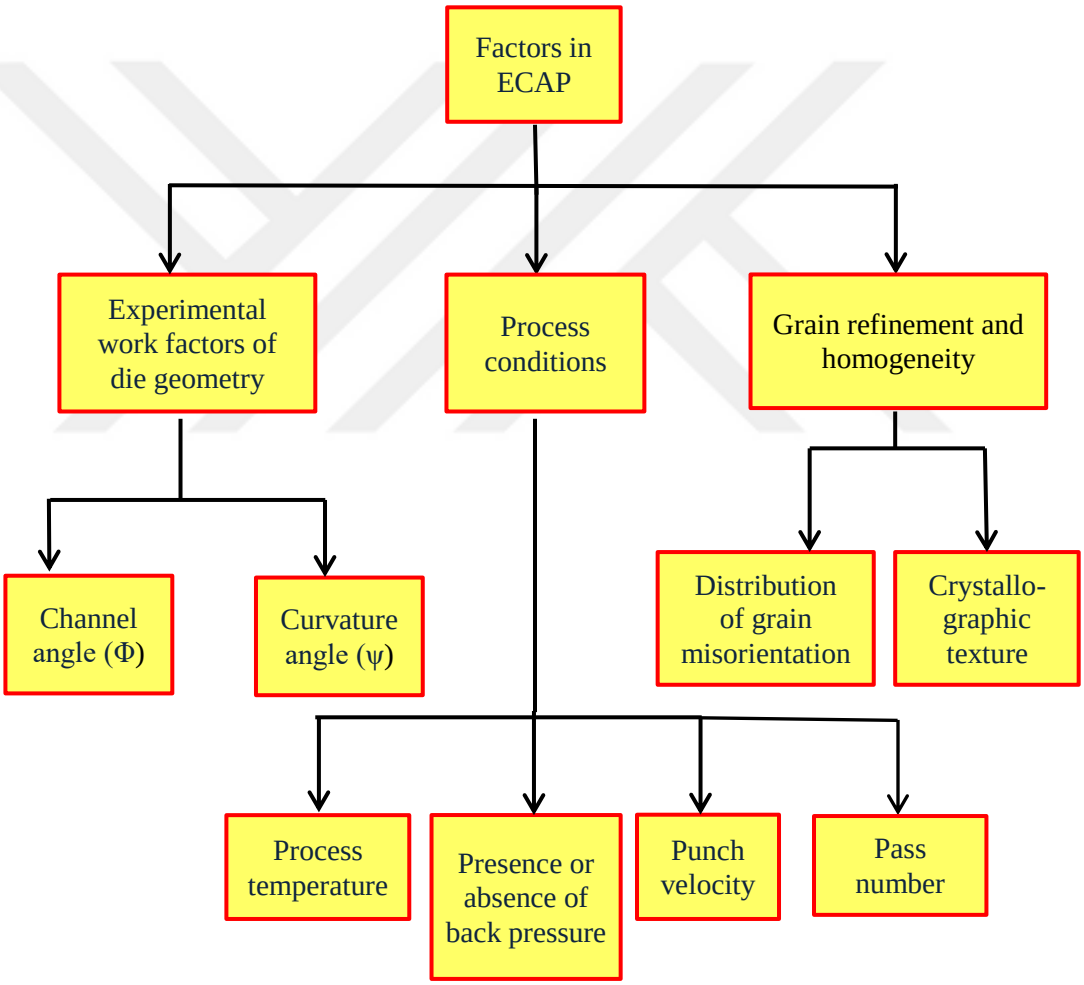

Figure 3.8: Experimental factors influencing ECAP [34-36]

3.3.7 Routes of the ECAP Process

In the ECAP process, the procedure follows four main routes which can result in various systems of slips due to the pressing work. These routes have the ability to make important changes to the microstructures and grain size. These routes can be classified as:

1- Route A – the work piece being pressed with no rotation
2- Route B_A – a 90-degree rotation of the work piece in an alternative orientation with sequences passes
3- Route B_C – a 90-degree, clockwise or counterclockwise rotation of the work piece through every pass
4- Route C – the billet is rotated 180° between different passes

Sometimes two routes can be combined without any further improvement in mechanical properties occurring [37, 38].

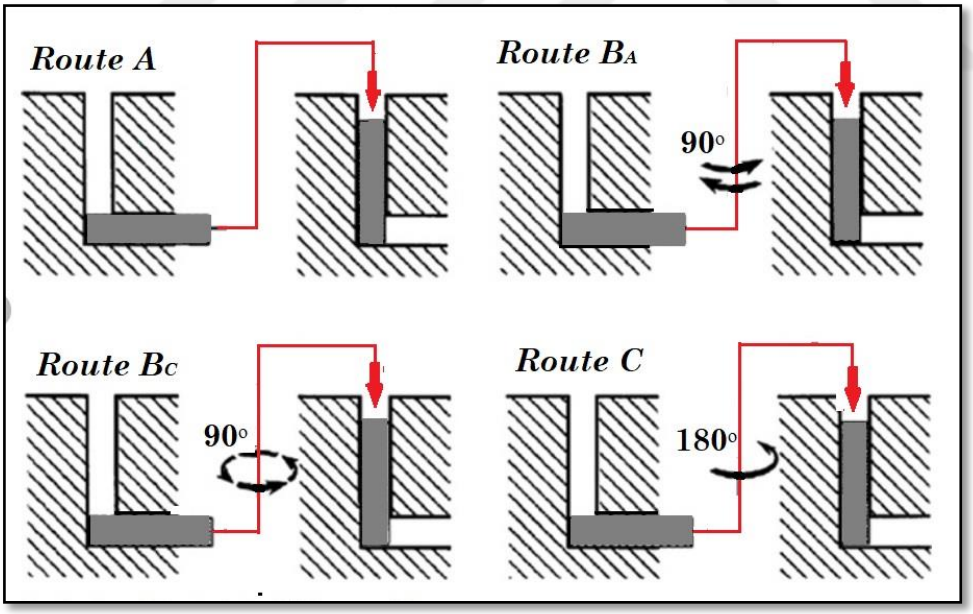

Figure 3.9: Four fundamental routes in the ECAP process [6]

3.3.8 Shear Zones in ECAP

In the ECAP process, there are many deformations between the layers of the material because the material passes through the angular channel movement and deforms to produce a new system arrangement of micro grains. The main differences between equal channel angular pressing and other extrusion processes are:

1- The billet dimensions and shape have no changes after ECAP, in contrast with traditional extrusion, where there are significant changes during extrusion.
2- The effective deformation is an accumulation of deformations per pressing in ECAP; however, it is a single press in conventional extrusion [37, 38].

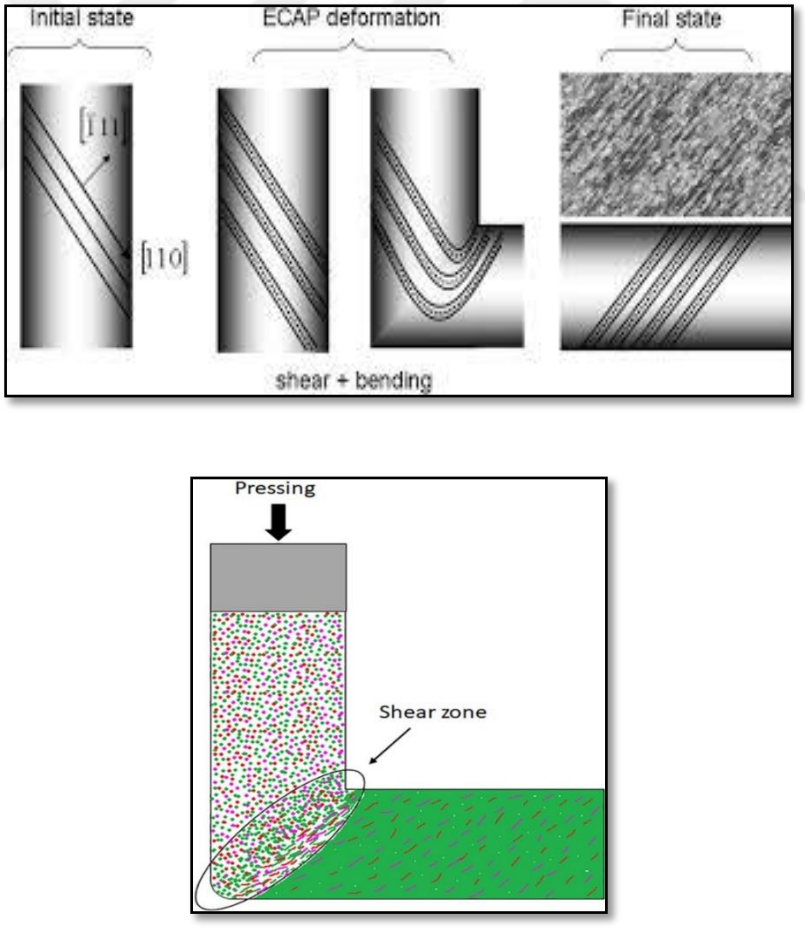

Figure 3.10: Shear and bending zones in the ECAP process [39]

3.3.9 Influence of Temperature on the ECAP Process

Generally in metal forming, three types of works can occur: (1) cold forming, where billets are not heated and used at room temperature; (2) warm forming, in which billets are heated to a temperature below recrystallization temperature; and (3) hot working, in which billet temperatures are brought to high values. At high temperatures, deformation and grain size normally increase, which leads to a reduction in strain hardening. Conversely, lower temperatures lead to reductions in grain sizes. In the ECAP process, high temperatures with multiple pressing over a larger number of passes through a specific bending angle leads to high strain with high refinement with no clear changes in the dimensions of the product [40-42].

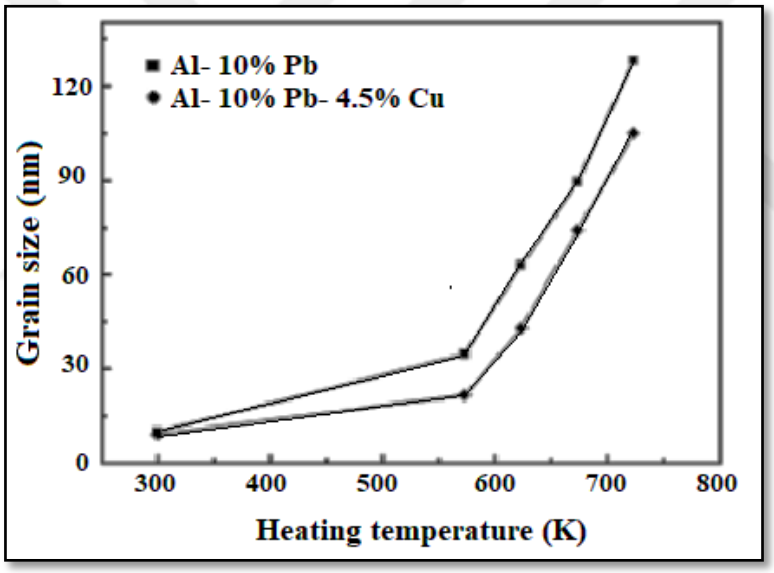

Figure 3.11: Effect of temperature on grain size after many passes [42]

3.4 Process Limitations and Features

3.4.1 Advantages of the ECAP Process

1- High deformation and strains with little to no change in dimensions.
2- Homogeneous and uniform grain structure.
3- Low or zero porosity on deformed work pieces.

4- Large numbers of billets can be produced in a limited time.
5- Superplasticity can be produced with ECAP.
6- Grain refinement and microstructure with ultrafine grains.
7- Composite materials can be produced with good mechanical properties.
8- Hardness improvement.
9- Increase in toughness and fatigue life [43-45].

3.4.2 Disadvantages of the ECAP Process

1- Defects in pressed samples.
2- Difficulties related to product removal from die.
3- Time consumption to extract products.
4- Low productivity.
5- Long duration of process.
6- Fractures after a number of passes.
7- Decrease in electrical conductivity.
8- Limitation on billet diameter to 20 mm.
9- Limited product shape and no ability to produce complicated products [46-49].

3.5 Magnesium and Its Alloys

Magnesium alloys are considered to be metallic materials that have many properties making them useful in medical devices, light weight parts, military items, automotive parts, aerospace items and energy-saving products. However, magnesium alloys have limited formability at low temperatures. Therefore, severe plastic deformation process with the ECAP process can be applied to improve the properties of magnesium alloys, such as strength and ductility [13]. These alloys generally have many applications in transportation and electronics as well as biomedical uses according to the alloys' superior characteristics, such as low density and good stiffness. Their crystal structure is a close packed hexagonal,

making them have low effective slip systems which reduce their formability and ductility, especially at low temperatures. Therefore, the ECAP process is used with magnesium alloys to improve the material by changing coarse grains to very fine grains and increasing the alloys' hardness [14] [17].

3.5.1 Effects of the ECAP Process on the Mechanical Properties of Magnesium

Mechanical properties can be controlled easily by contolling grain size. Thus, the ECAP process is used to decrease the grain size of magnesium alloys by repeating a number of passes [17].

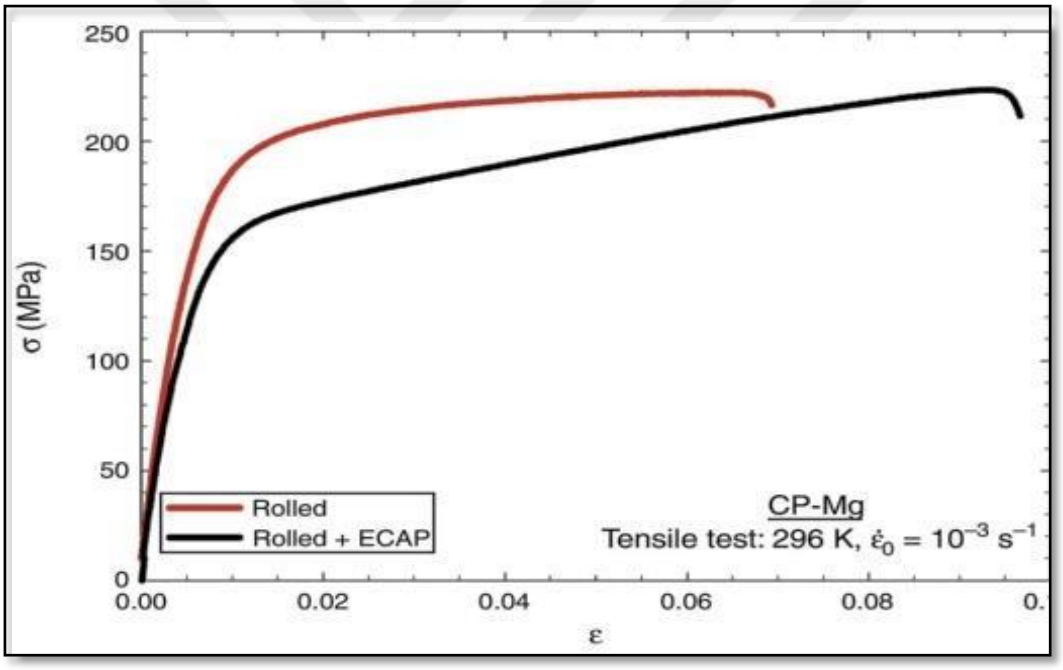

Figure 3.12: Stress-strain curves after ECAP for pure Mg [50]

3.5.2 Influences on Grain Structure

The modes of reducing coarse grains to very fine grains in equal channel angular pressing occur by fragmenting and breaking grains into smaller grains while pressing over many passes of the ECAP process. Sub-grain boundaries can be

produced due to shear forces during the first pass. Multiple passes lead to an increase in the misalignment of the boundaries. Therefore, low angle boundaries become high angle boundaries for the refined produced structure. This increases the dislocation and reduces the grain size [51].

During deformation processes, the original grains under subdivision and volume elements are produced during misorientation of their lattice. Misorientation ranges increase gradually when deformation and passes increase and the boundary spacing decreases. Cell size reduction occurs during very high values of strain [52].

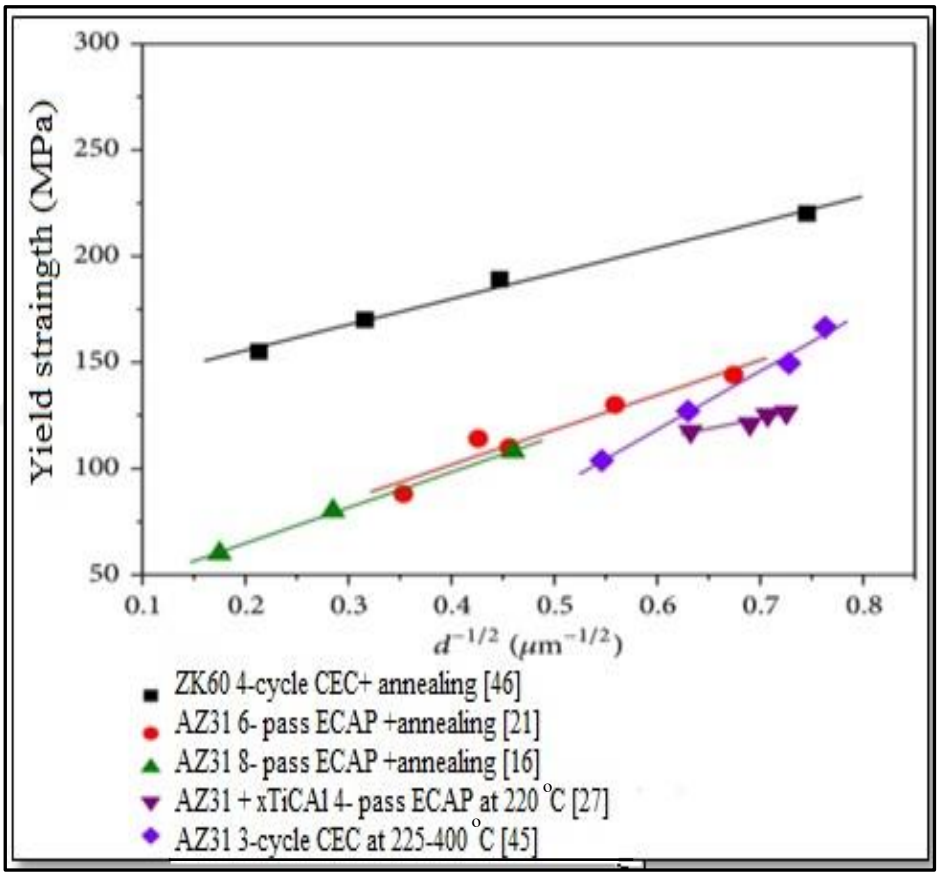

Figure 3.13: Grain size dependencies of yield strength of Mg alloy after SPD process and annealing [53]

The figure below explains the grain refinement mechanism of magnesium and its alloys in the ECAP processes.

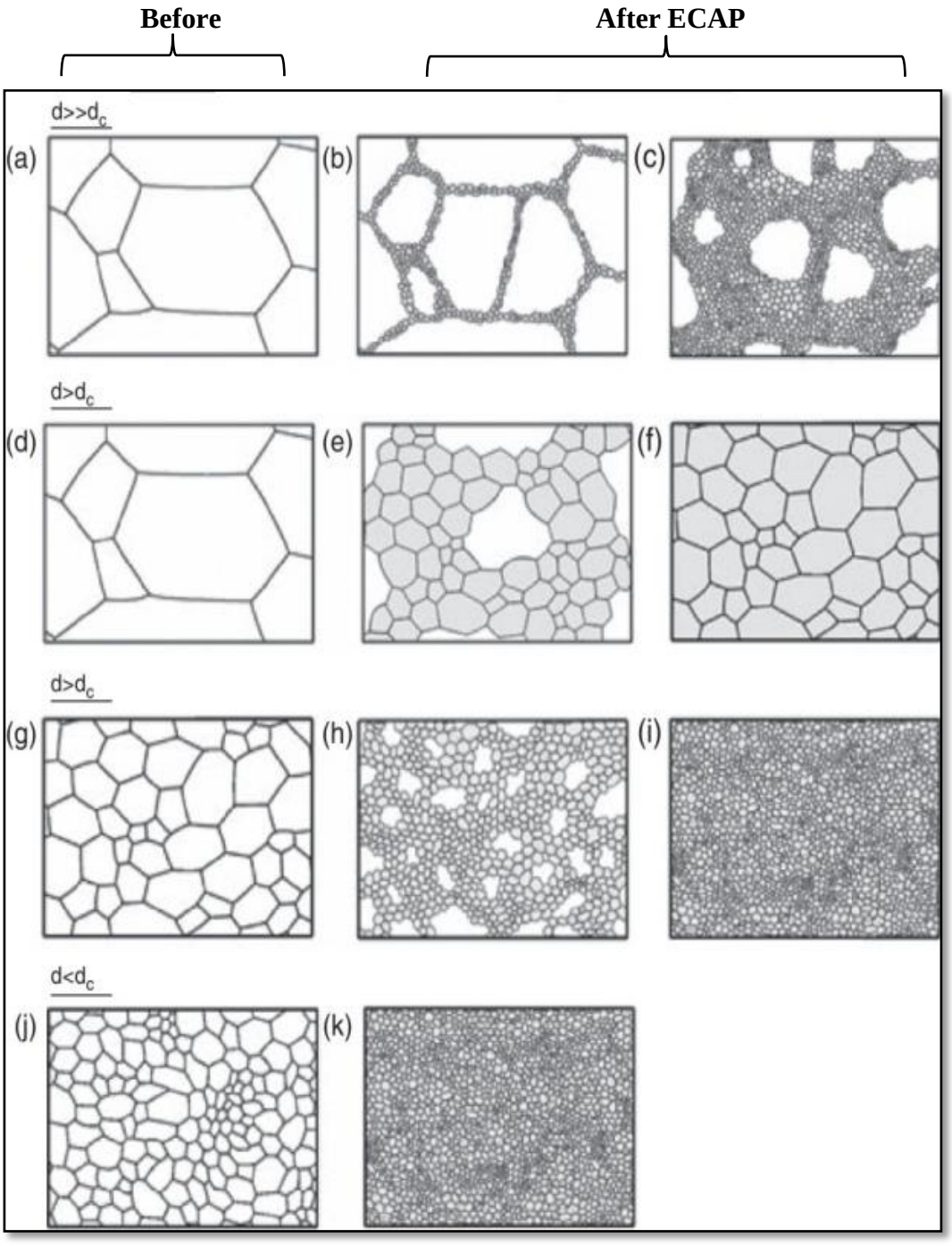

Figure 3.14: Illustration of the grain refinement mechanism for magnesium and its alloys with ECAP and different initial grain structures [54]

3.6 Analysis of the ECAP Process

In conventional extrusion,

$$\varepsilon_{tot} = \varepsilon_1 \qquad (3.1)$$

In equal channel angular pressing:

$$\varepsilon_{tot} = \varepsilon_1 + \varepsilon_2 + \ldots + \varepsilon_N \qquad (3.2)$$

where N is the number of passes and ε the strain.

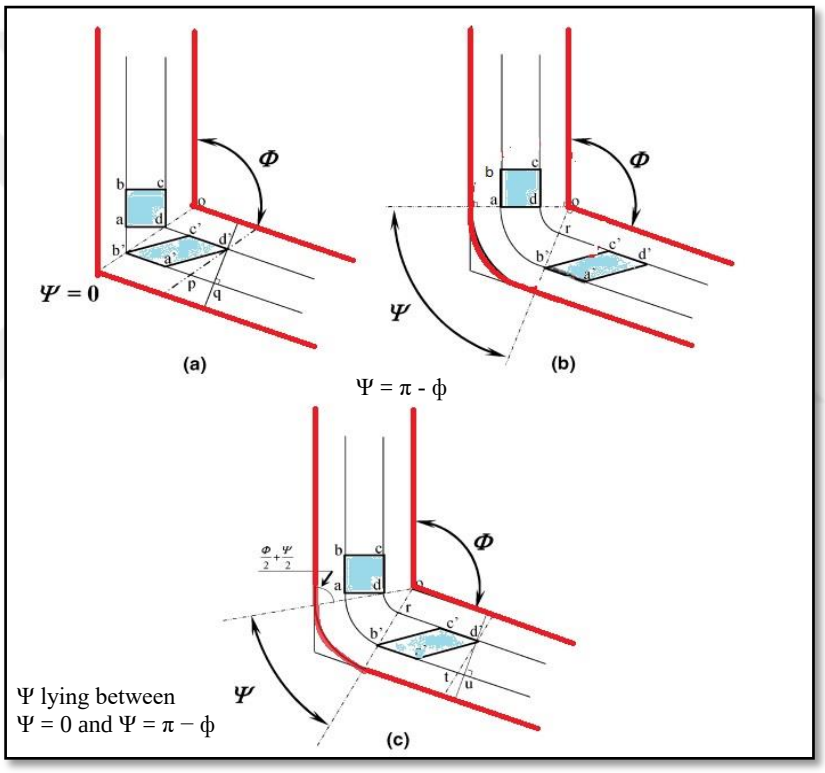

Figure 3.15: Angles of the ECAP process [6]

Shear strain through ECAP can be estimated as a relationship between the values of ψ and Φ for single passes under actual cases.

Shear strain (γ) is given by the case with $\psi = 0°$ as in Figure 3.13a; therefore, the equation becomes:

$$\gamma = 2\cot\left(\frac{\Phi}{2}\right) \qquad (3.3)$$

When using the same approximation as shown in Figure 3.13b, the equation becomes:

$$\gamma = \psi \tag{3.4}$$

where Φ is the angle of intersection of the two channels, and ψ is the angle subtended by the arc of curvature at the point of intersection.

In a similar fashion for Figure 3.13c, it leads to a universal solution [6]:

$$\gamma = 2\cot\left(\frac{\Phi}{2}+\frac{\psi}{2}\right)+\psi\,\mathrm{cosec}\left(\frac{\Phi}{2}+\frac{\psi}{2}\right) \tag{3.5}$$

when direct from inspection that the general solution in Equation 3.4 reduces to Equation 3.3 when ψ = 0° and to Equation 3.4 when [6, 48, 49]:

$$\psi = (\pi - \Phi) \tag{3.6}$$

Finally, for the equivalent strain after N passes, ƐN may be expressed in a general form with the relationship thus [55]:

$$\varepsilon_N = \frac{N}{\sqrt{3}}\left[2\cot\left(\frac{\phi}{2}+\frac{\Psi}{2}\right)+\Psi\,\mathrm{cosec}\left(\frac{\phi}{2}+\frac{\Psi}{2}\right)\right] \tag{3.7}$$

Equation 3.6 is consistent with an earlier estimate of the strain where a die was analyzed with ψ = 0. The channel angle Φ was taken as 2φ and the strain after N passes was estimated as [56, 57]:

$$\varepsilon_N = \frac{2N}{\sqrt{3}}\cot\varphi \tag{3.8}$$

The yield strength is:

$$\sigma_\circ = \sigma_1 + \frac{k}{\sqrt{D}} \tag{3.9}$$

where

$\sigma_\circ$ = yield strength (MPa)

σ_1 = frictional stress (MPa)

K = Hall Petch slope

D = diameter of grains (mm)

The hardness of the material [47, 58] is calculated thus:

$$H_{\circ} = H_1 + \frac{k}{\sqrt{D}} \quad (3.10)$$

where

$H_{\circ}$ = Hardness of material (HV)

H_1 = Constant

CHAPTER 4

SIMULATION OF THE ECAP PROCESS

4.1 Simulation Analysis Work Procedure

1- Selection of magnesium alloy AZ31 as the material used for the ECAP process.
2- Setting suitable boundaries conditions for this process.
3- Designing a suitable die for this process.
4- Using Q Form software for numerical analysis to find initial results.
5- Setting new mechanical tests for the products of the ECAP process.

4.2 Material and Method

The material used in this process is magnesium alloy, which has been used to explain the details of the Equal-Channel Angular Pressing (ECAP) process, which is one of the serve plastic deformation processes. The Q Form software is suitable for simulating forging and extrusion processes of metal forming and it can analyze and predict the results prior to any manufacturing of the die and any experimental work [59].

In this process, the billet is pressed through a die though two equal channels at a channel angle of 90°. The deformation zone is at the intersection of the channel, with a simple shear mechanism. The plastic strain that is applied to the work piece depends on the channel angle and its curvature angle. Only a small work piece can be processed using this method because of the high amount of friction and limitation force [60].

4.2.1 Magnesium and Its Alloys

Magnesium and its alloys are among a number of metals that are used widely in industrial applications because of its properties, which include:

1- High strength to weight ratio
2- Low weight
3- Stiffness
4- Good fatigue strength
5- High damping capacity
6- Non-magnetism
7- Good thermal and electrical conductivity [61]

4.2.2 Material Selection

The alloy used in this study is magnesium alloy AZ31. The table below shows the chemical composition of this material.

Table 4.1: Standard chemical composition of magnesium alloy AZ31 [62]

Mg%	Al%	Mn%	Zn%	Fe%	Ca%	Si%	Ni%	Cu%
95.89	3.1	0.25	0.73	0.005	0.0014	0.02	0.005	0.0001

Table 4.2: Chemical composition of magnesium samples in the laboratory

Mg%	Al%	Mn%	Zn%	Cu%	Ca%	Si%	Ag%
95.78	2.245	0.286	1.664	0.001	0.001	0.02	0.002

4.3 Sample Dimensions

An approximately 20-millimeter diameter, 50-millimeter long cylindrical sample of magnesium can be used for practical experiments:

Table 4.3: Billet dimensions

Billet Dimensions	
Diameter (mm)	19.5
Height (mm)	50

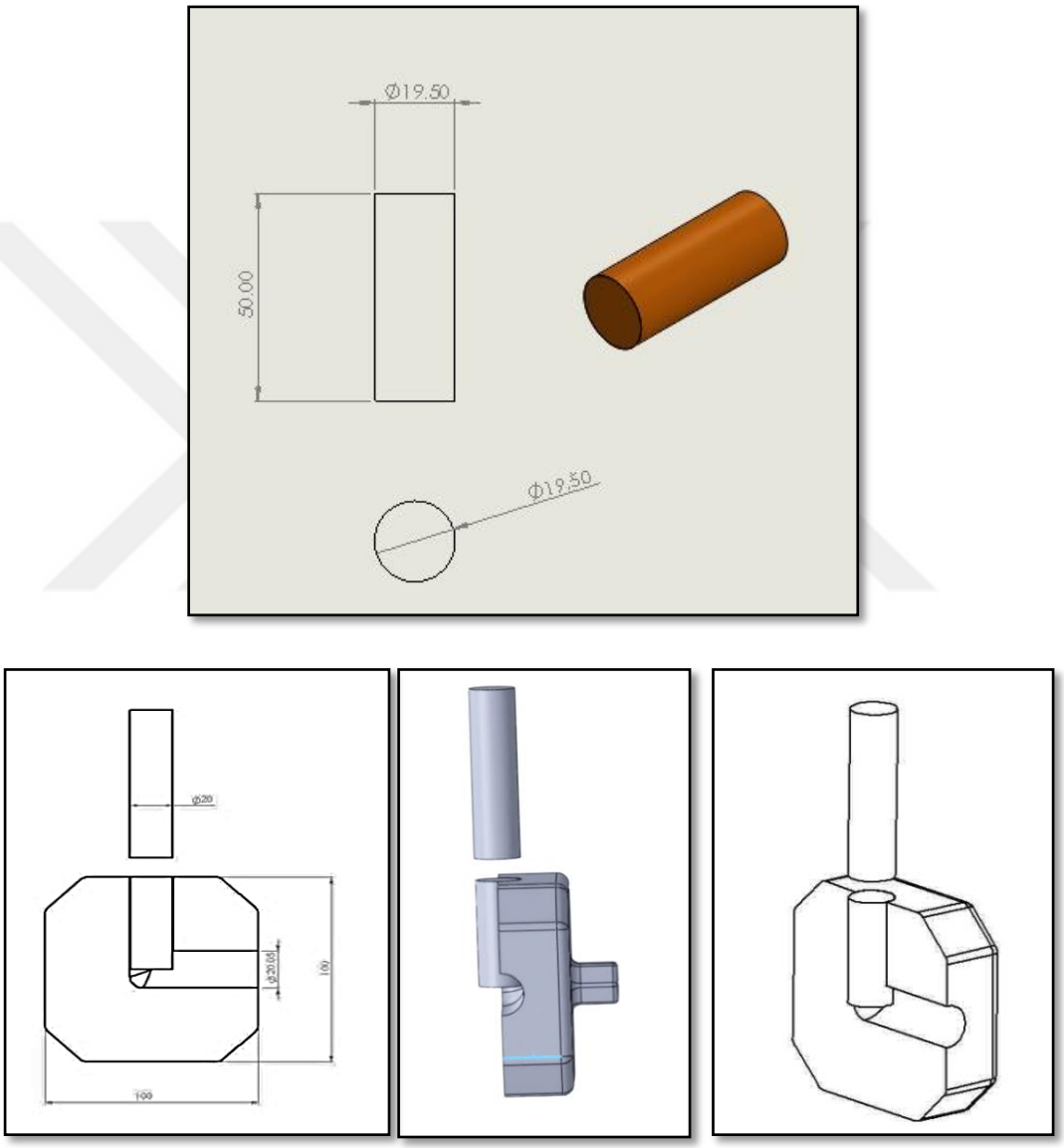

Figure 4.1: Sample with its dimensions

4.4 Die Design

The figure below shows the die geometry used in the QForm simulation software of the ECAP process with curvature angle ψ = 20° and channel angle Φ = 90°. The radius of the channel angle r = 0 mm, which means a sharp angle in the first analysis showing defects and errors in the simulation. Then the radius value changes to r = 0.5 mm for more curvature and smooth and uniform deformation. The punch has a cross-section diameter of 20 mm and a length of 70 mm. The material of the die and punch is tool steel.

The die is fixed in a manner that can be used by two sides in order to make different passes by rotating the die which changes the direction of pressing.

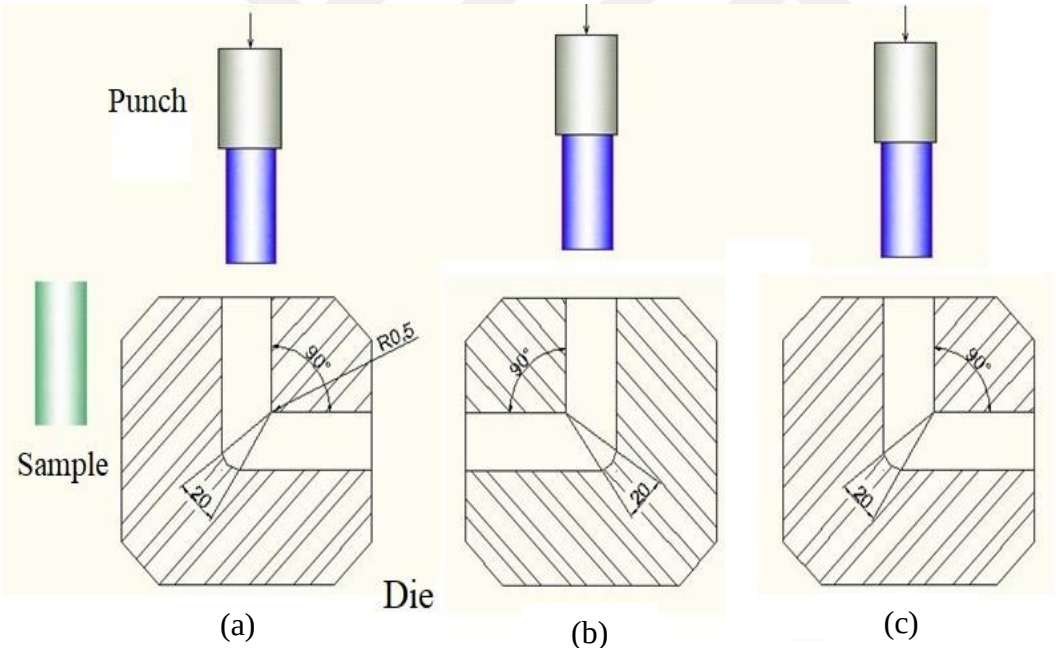

Figure 4.2: Die geometry at different passes (a) Pass 1 (b) Pass 2 (c) Pass 3

The die dimensions and shape are shown in the following figure:

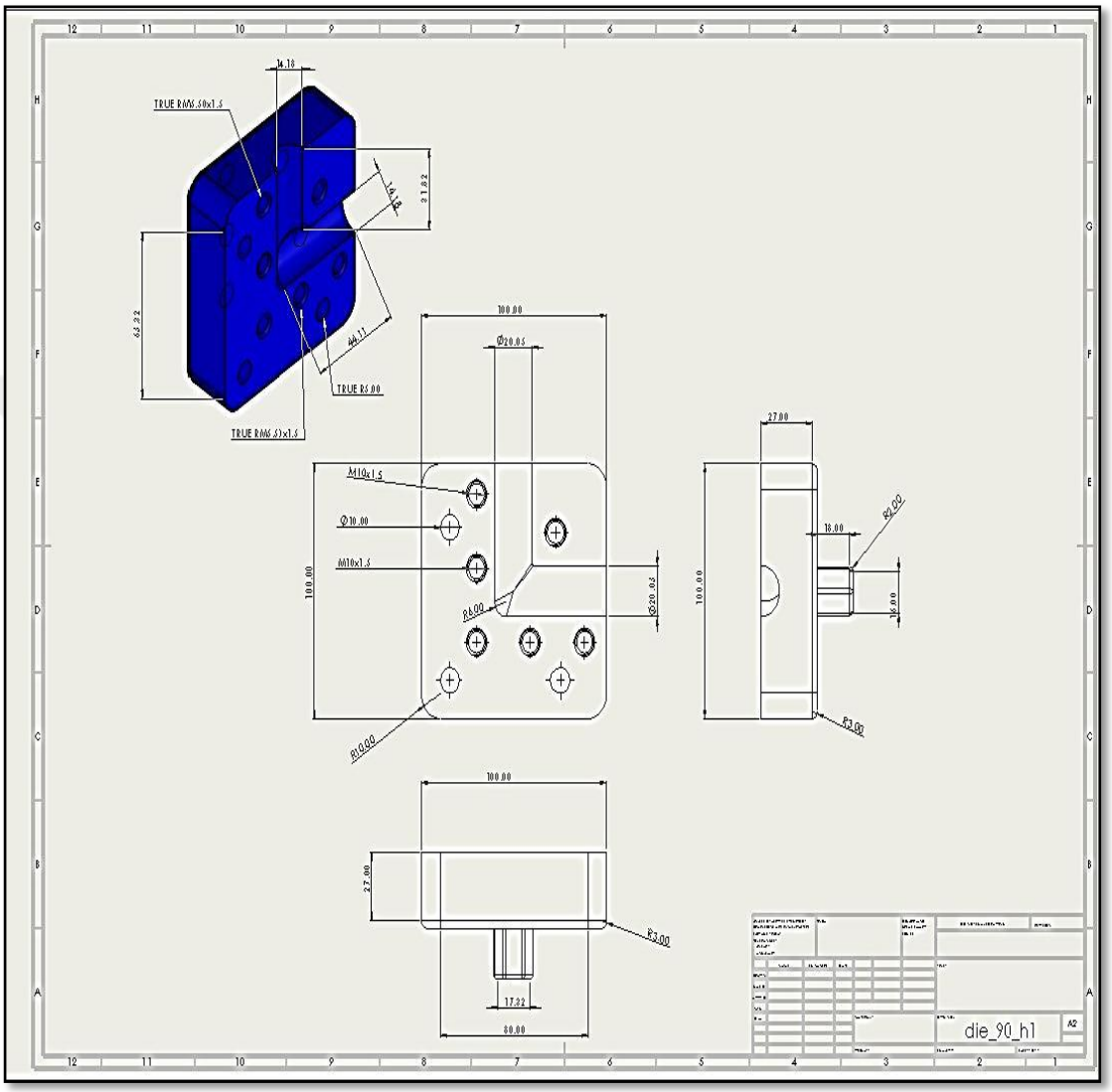

Figure 4.3: Details of the ECAP die design

4.5 The Boundary Condition

The boundary condition includes:

1- Input parameters:

- Temperature

- Velocity
- Number of passes

2- Output parameters:

- Load
- Hardness
- Grain size
- Microstructure

Table 4.4: Boundary condition of the process

Temperature	Velocity	No. of passes		
275°C	14 mm/s	1	2	3
275°C	27 mm/s	1	2	3
300°C	14 mm/s	1	2	3
300°C	27 mm/s	1	2	3

The pressure is constant through the use of a hydrostatic press with a maximum pressure of 50 tons with mineral lubrication and a 2D symmetric analysis to simplify the results of the analysis. The temperature is kept constant at T1 = 275℃ and the velocity changes between V1 and V2 over three passes with each velocity. Then, the second temperature of T2 = 300℃ is used under the same conditions of velocity and number of passes.

4.6 Simulation Analysis

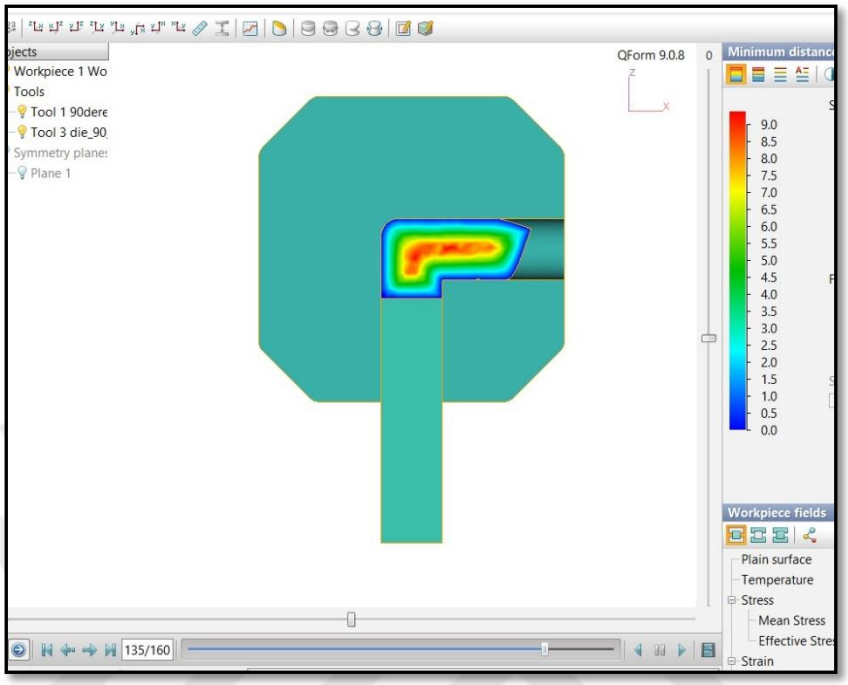

Figure 4.4: Billet prior to deformation at the first pass in the ECAP die

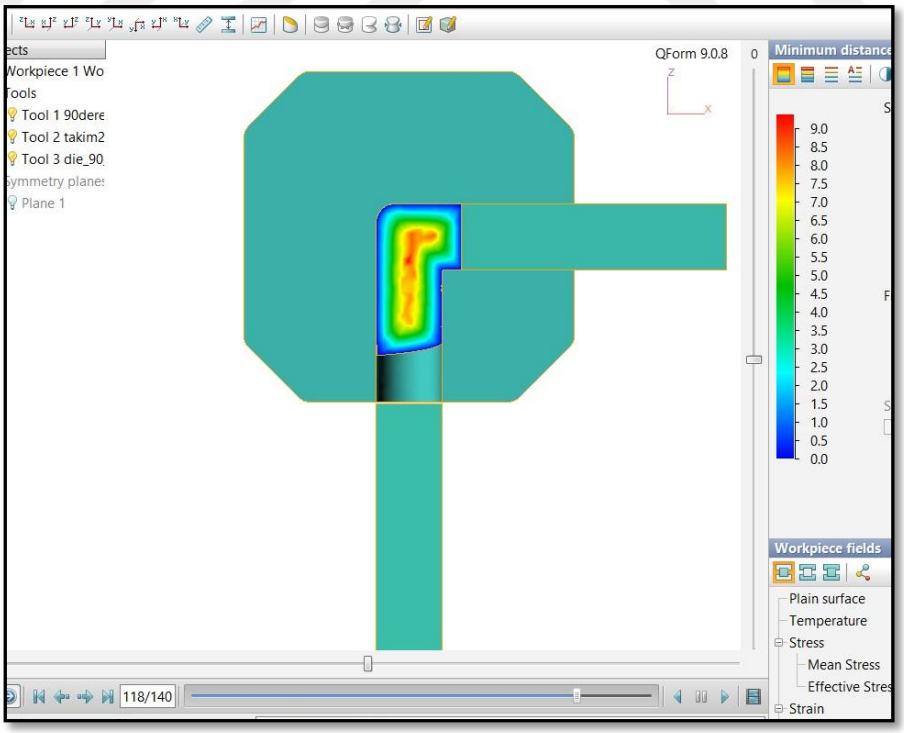

Figure 4.5: The billet during deformation in the ECAP die with QForm analysis

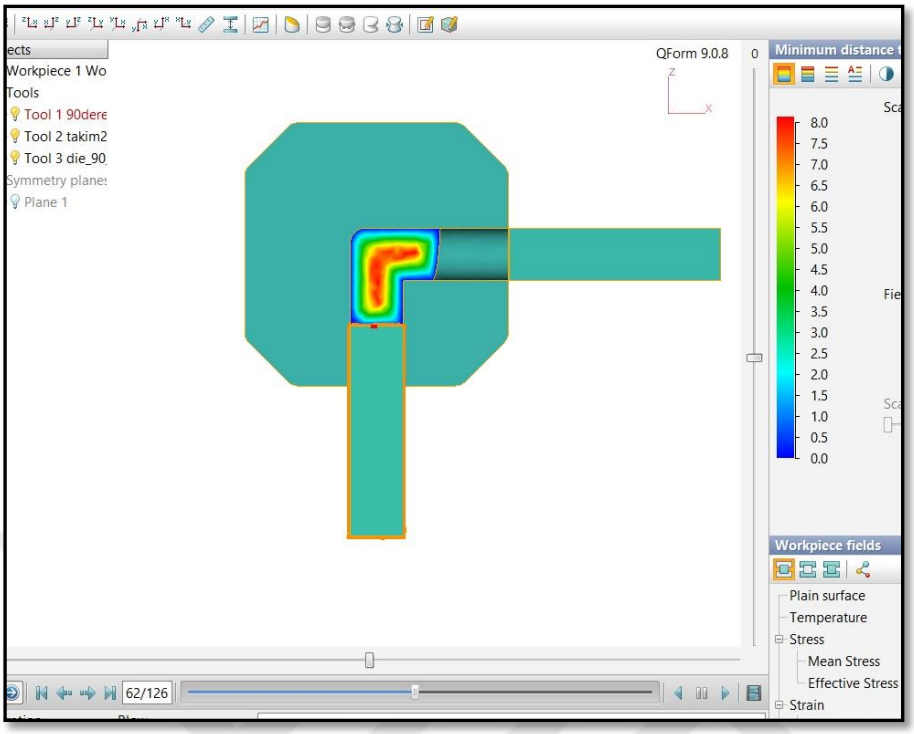

Figure 4.6: Billet prior to deformation at the second pass

Figure 4.7: The QForm home page

CHAPTER 5

EXPERIMENTAL WORK

In the experimental work, all equipment related to the ECAP process was manufactured to produce magnesium samples. Included in the process is preparation of the press machine and fixing the supported die, and items such as the die and punch, jacket heater and thermostat controller. The ECAP die is set with in a hot working and lubricated condition.

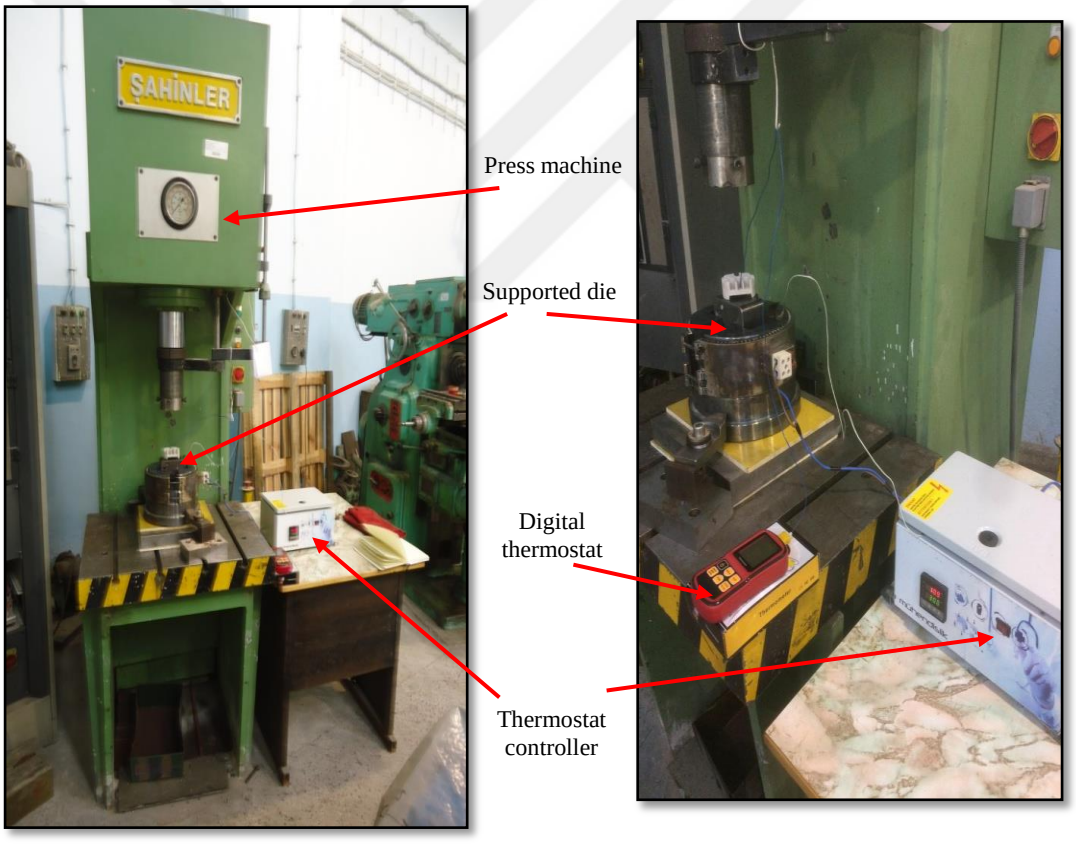

Figure 5.1: The experimental equipment

5.1 Experimental Work Equipment

5.1.1 Punches

The final shapes of the punch used in experimental work are shown below:

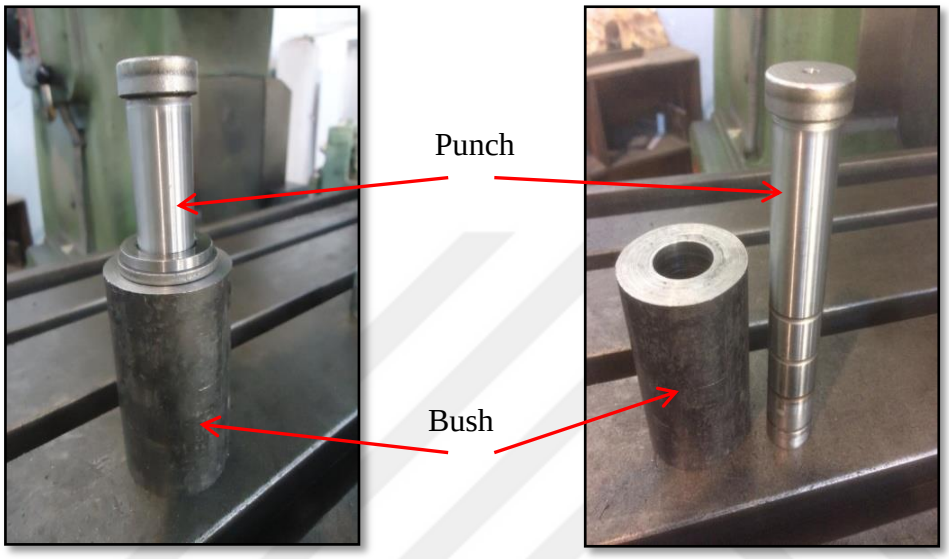

Figure 5.2: Initial punch shape

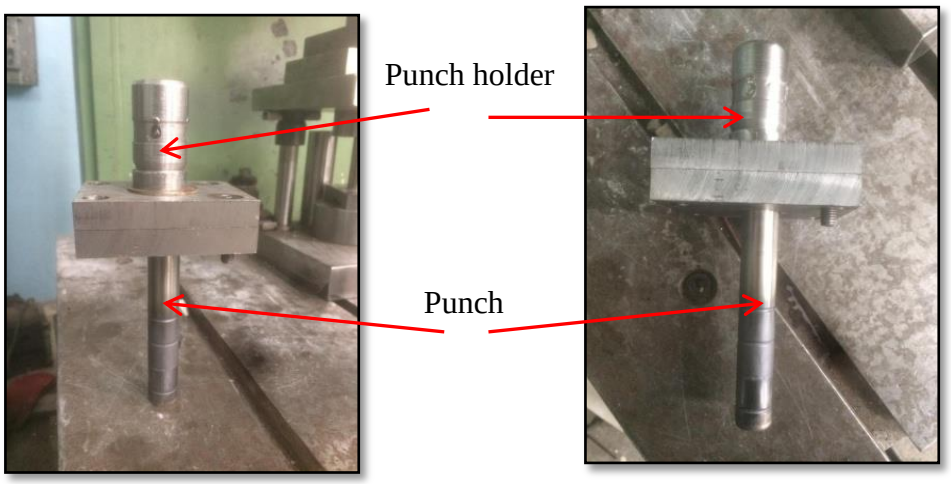

Figure 5.3: Final punch shape

5.1.2 Die in the ECAP Process

The die, containing angles Φ = 90° and ψ = 20°, used in the process is shown in the figure below.

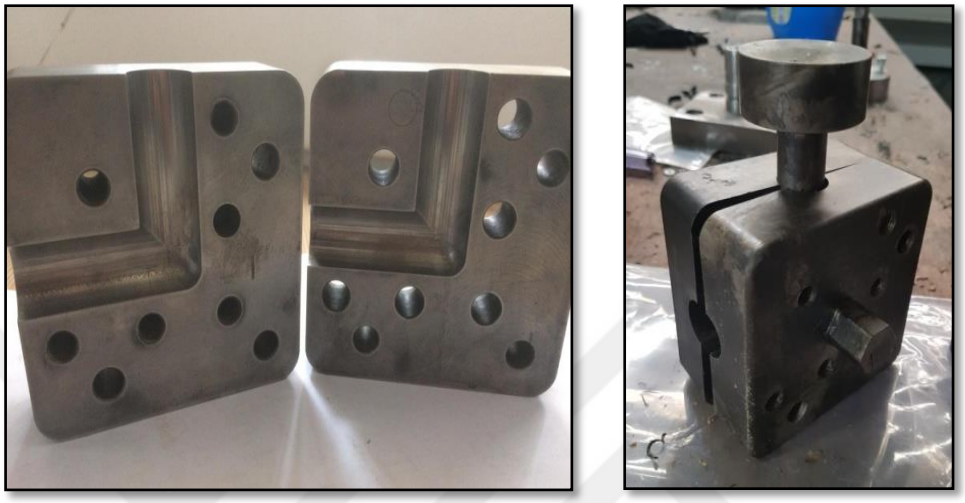

Figure 5.4: The die for the process

5.1.3 Jacket Heater

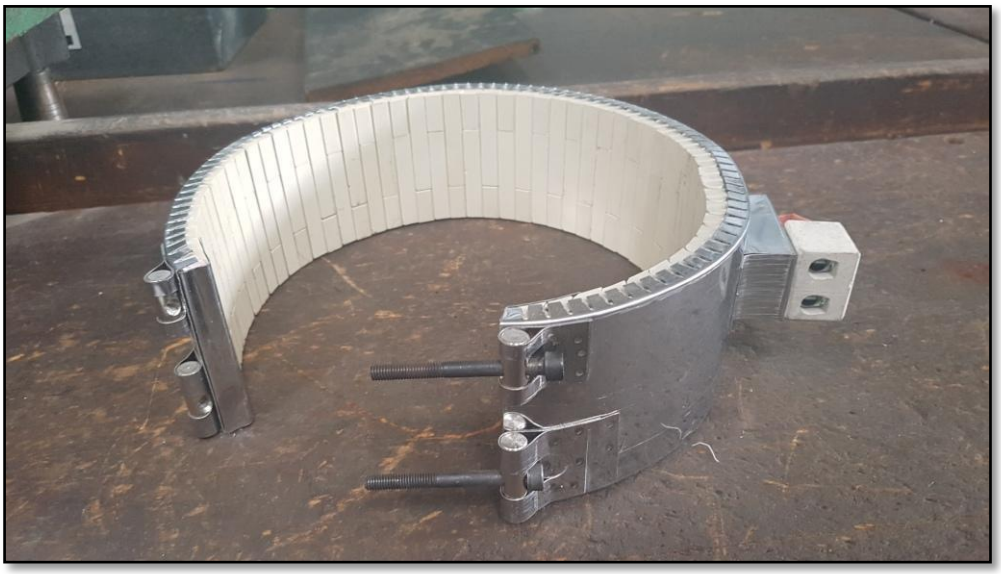

Figure 5.5: Jacket heater for die heating

5.1.4 Supporting Part for Die

The part when the die is being setting is called the supported die, which is set at the same time as the heating jacket from outside, as shown in the figure below.

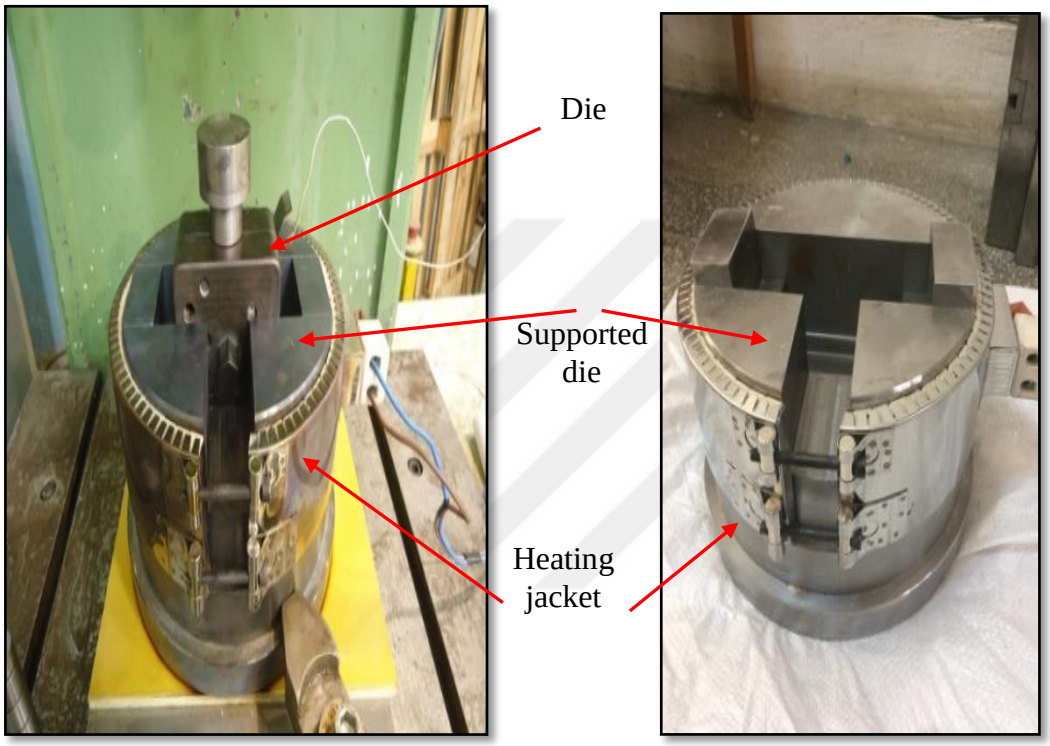

Figure 5.6: Supported die and heating jacket

5.1.5 Heating Measurements

Many devices were used to complete the experimental work, and the ECAP process should achieved at hot working; therefore, a digital thermometer and a thermostat controller, as well as insulation material were used.

Figure 5.7: Heating measurements

A digital thermometer is a device that measures the temperature of the sample until it increases to the required temperature.

The thermostat controller is used to control the temperature of the heating jacket around the supported die.

Insulation material is used to reduce any heating loss from the heating jacket.

5.2 Experimental Work

In the experimental work, it is necessary to maintain a constant temperature inside the die. For this case, the heater jacket was insulated to maintain the temperature and reduce the time to reach the actual temperature and change the punch to its final shape, as shown in the figures.

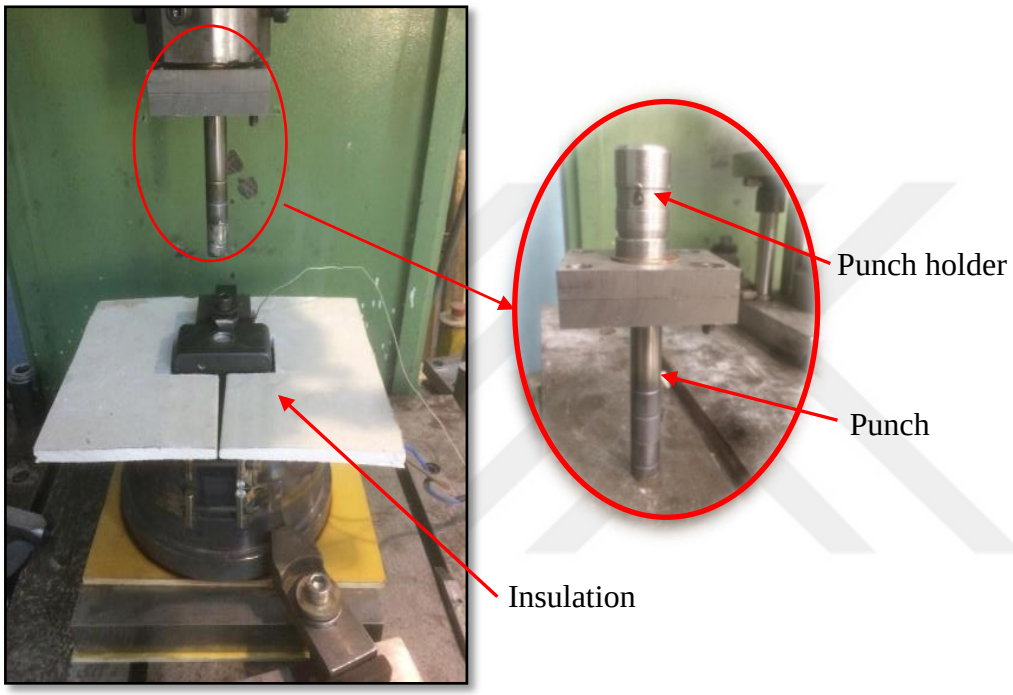

Figure 5.8: Insulation metal and the new punch holder

5.2.1 Boundary Condition of the Experimental Work

The boundary condition (temperature, velocity and the number of passes) for the experimental work was as shown in Table 5.1.

Table 5.1: Boundary conditions

Temperature	Velocity	No. of passes		
275°C	14 mm/s	1	2	3
275°C	27 mm/s	1	2	3
300°C	14 mm/s	1	2	3
300°C	27 mm/s	1	2	3

T = 300°C T = 275°C

Figure 5.9: Temperatures of the samples

V1 = 14 mm/s V2 = 27 mm/s

Figure 5.10: Velocity control of the punch

5.2.2 Magnesium Alloy AZ31 Billets

Figure 5.11: Magnesium alloy AZ31 work piece materials

5.2.3 Steps of the Experimental Work

The following figures show the steps to producing the magnesium samples through the ECAP process.

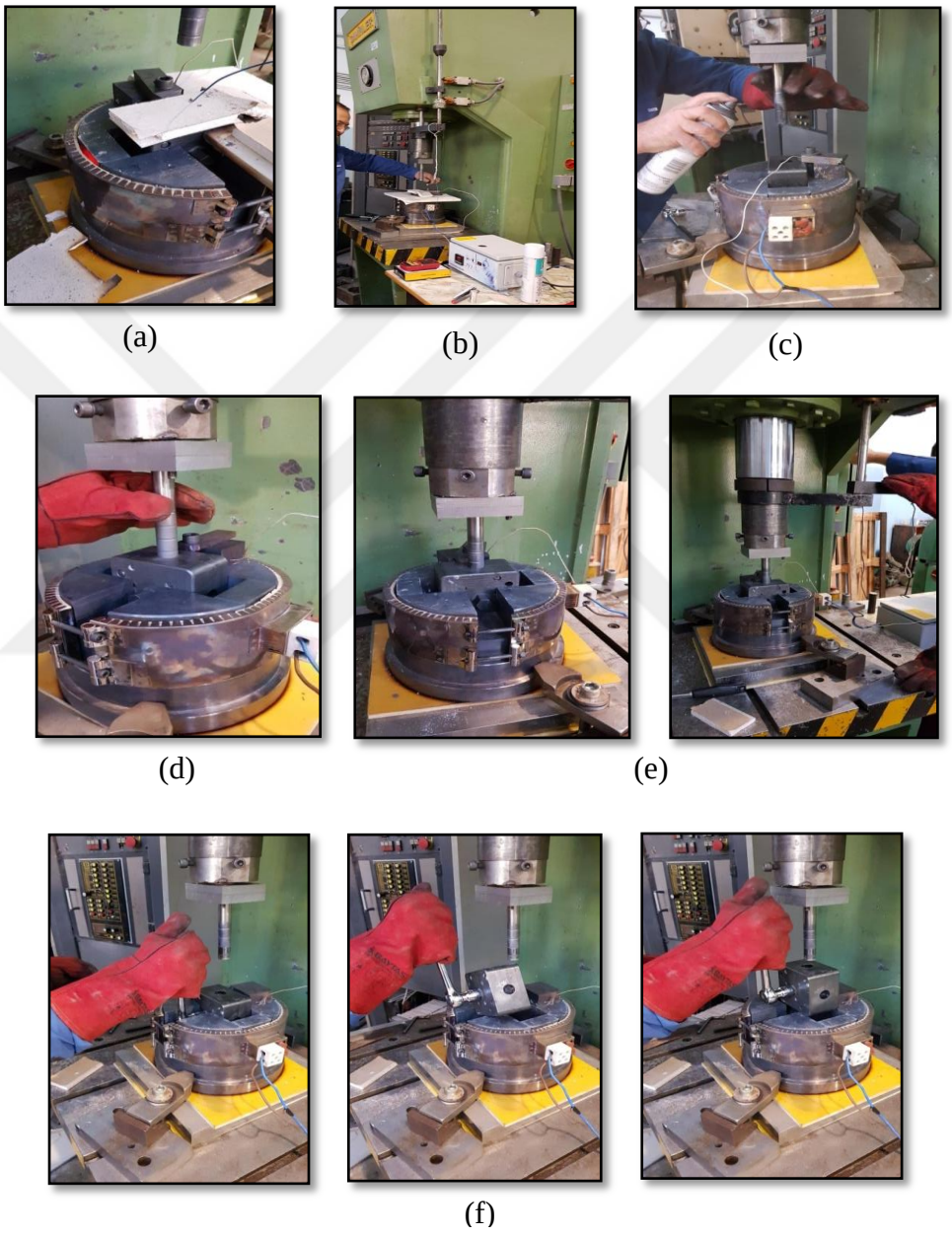

Figure 5.12: Experimental work: (a) Heating the die; (b) Checking the temperature; (c) Lubricating the punch (d) Checking the punch (e) Operating the press machine; (f) Rotating the die 90° to make another pass

5.2.4 Die Opening

After finishing the operation, the die is opened to remove the product, as shown in the following pictures.

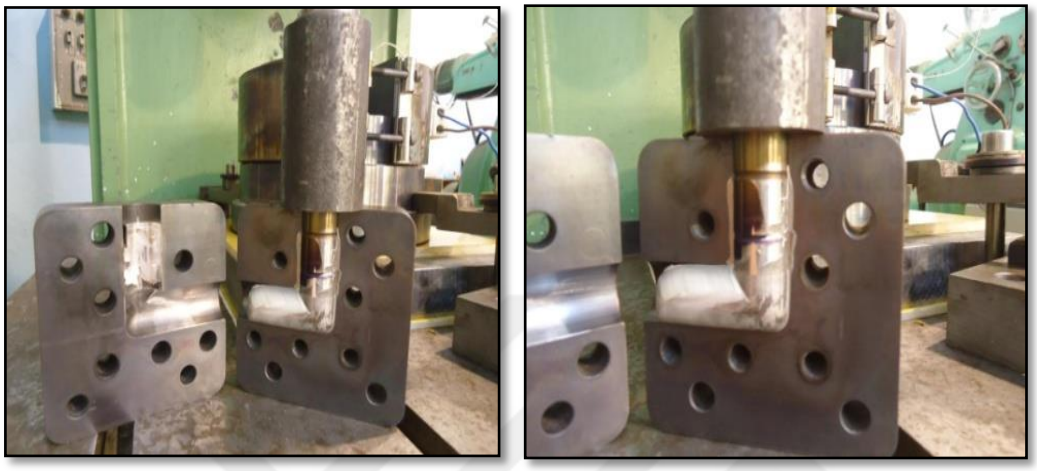

(a)

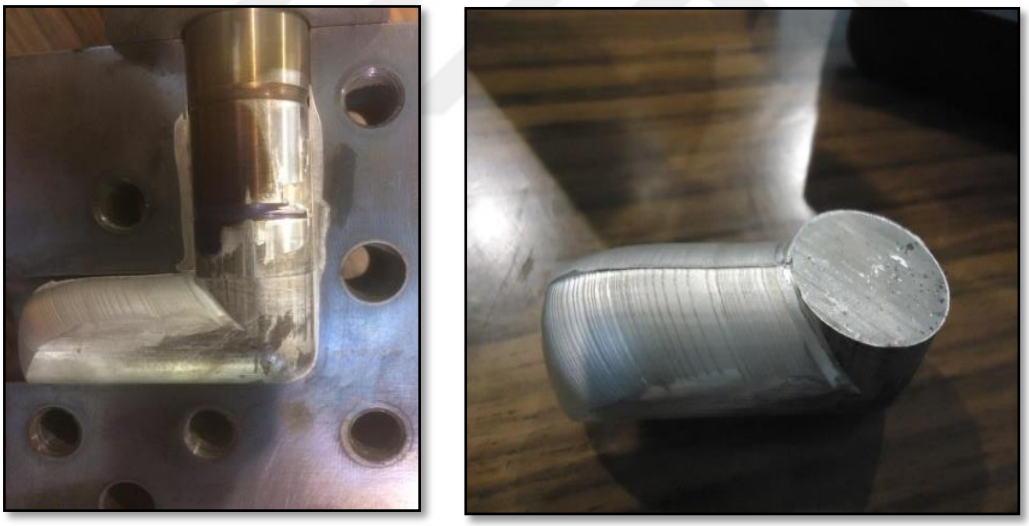

(b)

Figure 5.13: Die opening: (a) Opening the die; (b) Product after the ECAP process

5.2.5 Products of Magnesium Alloy

In the experimental work, samples of magnesium alloy were produced with different boundary conditions that depend on the boundary condition of the process, as shown in the figure below

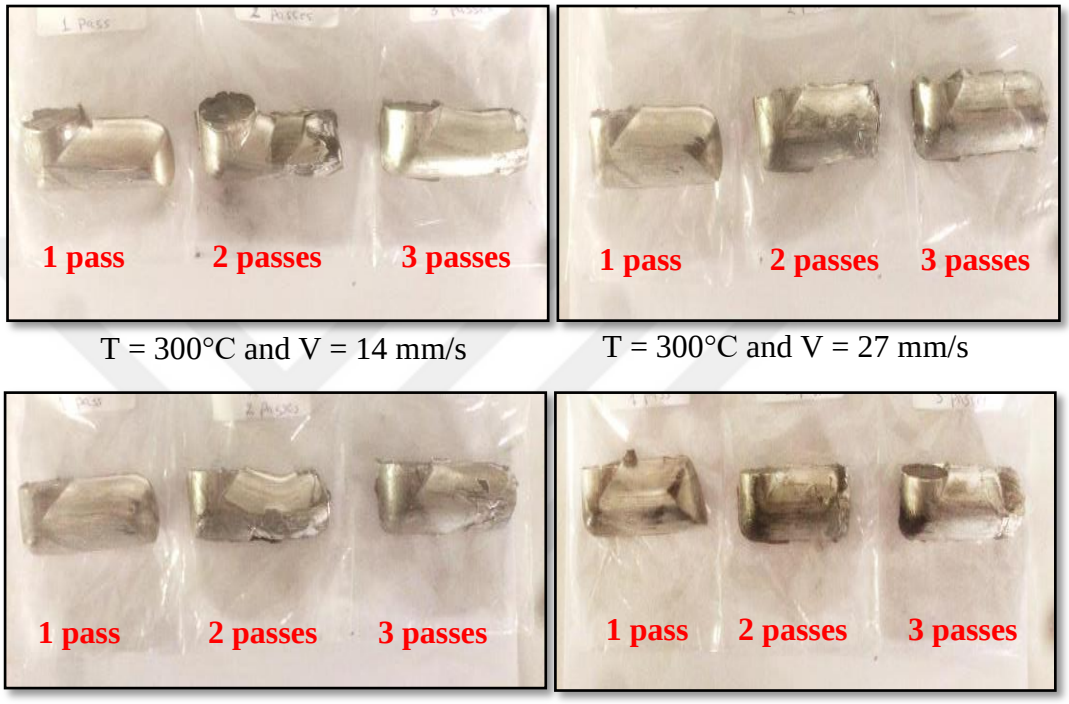

T = 300°C and V = 14 mm/s

T = 300°C and V = 27 mm/s

T = 275°C and V = 14 mm/s

T = 275°C and V = 27 mm/s

Figure 5.14: Products of the ECAP process under different conditions

5.3 Process and Product Defects

Figure 5.15: Product defects: (a) wrinkles; (b) flakes; (c) non-uniform shape; (d) cracks (e) flashes; (f) sloping ends (g) incomplete process; (h) curvature

5.4 Preparing Samples for Testing

There are many tests that should be done on the samples, but first, the samples have to be prepared taking the following steps:

5.4.1 Samples Cutting

The samples are cut using a sawing machine, as shown in the figures below.

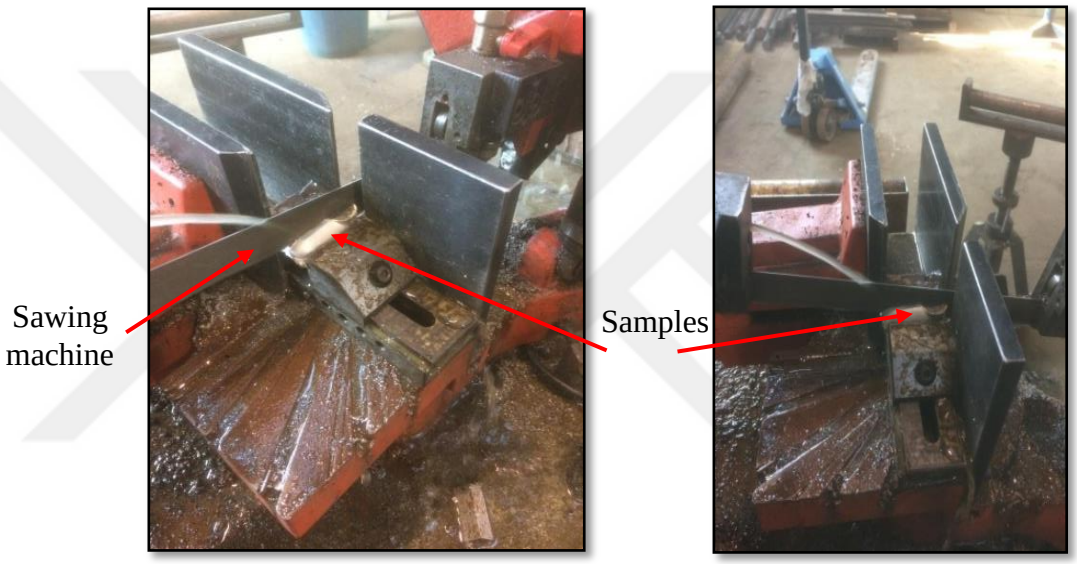

Figure 5.16: Cutting the samples

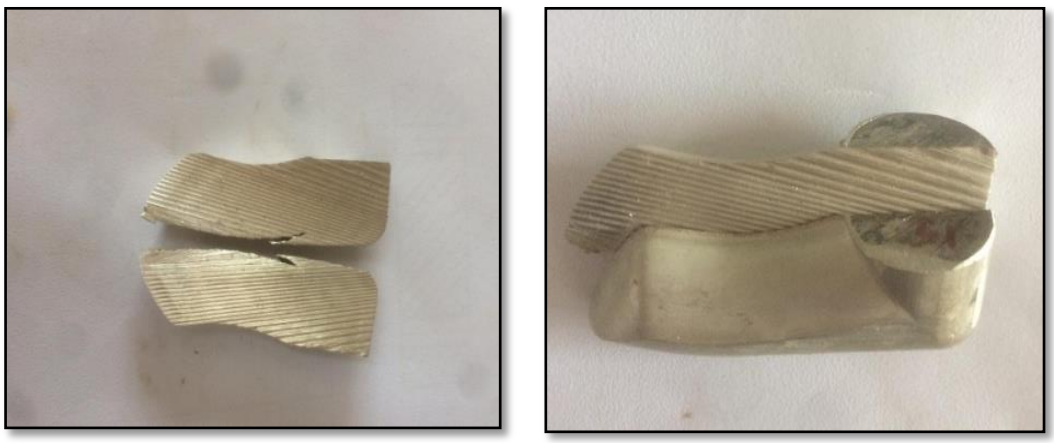

Figure 5.17: Samples after cutting

5.4.2 Samples Molding

The second step is the molding of the sample using an epoxy material, as shown below.

Figure 5.18: Sample molding: (a) Samples before molding; (b) Samples after molding

5.4.3 Samples Grinding

Three types of grinding paper were used for grinding the samples, as shown below:

320 600 1200

Figure 5.19: Grinding process

5.4.4 Samples Polishing

Many degrees of polishing were applied to the samples, such as 6 µm, 3 µm and 1 µm, to prepare the samples for the microstructure test [63].

6 µm 3 µm 1 µm

Figure 5.20: Polishing process

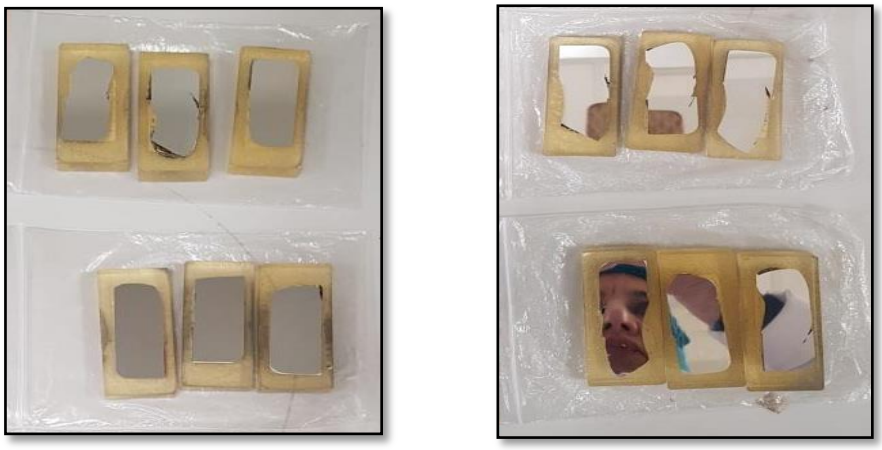

Figure 5.21: Samples after polishing

5.4.5 Samples Etching

The chemical materials and their percentage amounts are shown below.

1- Alcohol ethanol 96%, 150 mL
2- Acetic acid, 10 mL
3- Distilled water, 10 mL
4- Picric acid powder, 4.26 g [64]

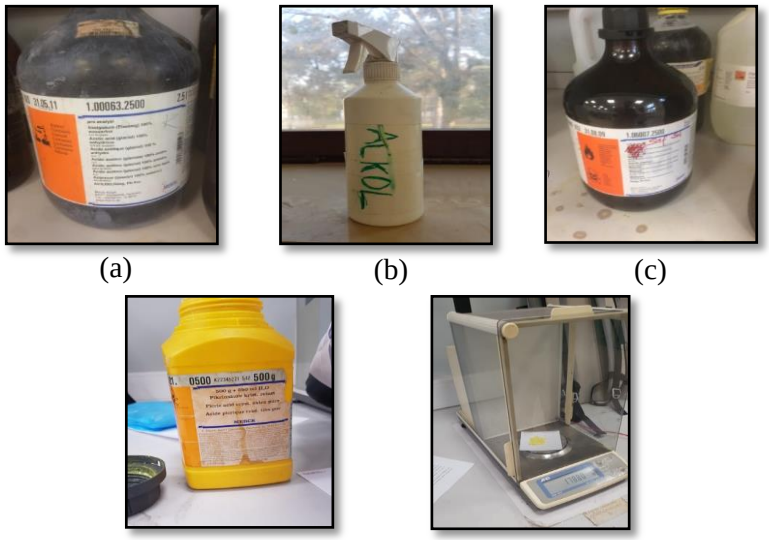

(a) (b) (c)

(d)

Figure 5.22: Chemical composition for the etching: (a) acetic acid; (b) alcohol (ethanol); (c) distilled water; and (d) picric acid powder [65].

5.5 Tests

5.5.1 Microstructure Test

According to the deformation system, the samples are divided into four areas, as shown in the figure below.

Figure 5.23: Microstructure of the sample

5.5.2 Hardness Test

The hardness measurements for the samples were taken with a Vickers hardness device, as shown in the figures below, which takes loads of about 200 grams for 10 seconds.

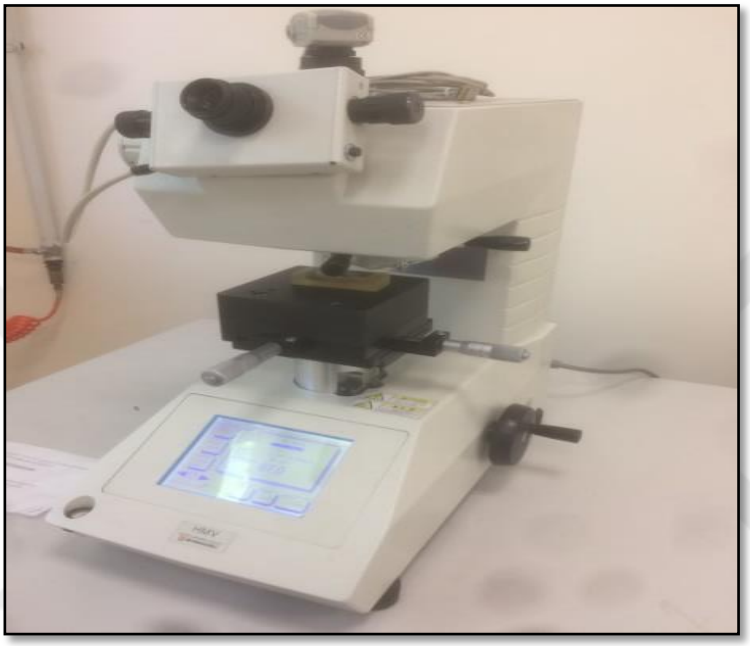

Figure 5.24: Vickers hardness device

The hardness readings for the ECAP samples are taken from four regions, as shown in Figure 5.25.

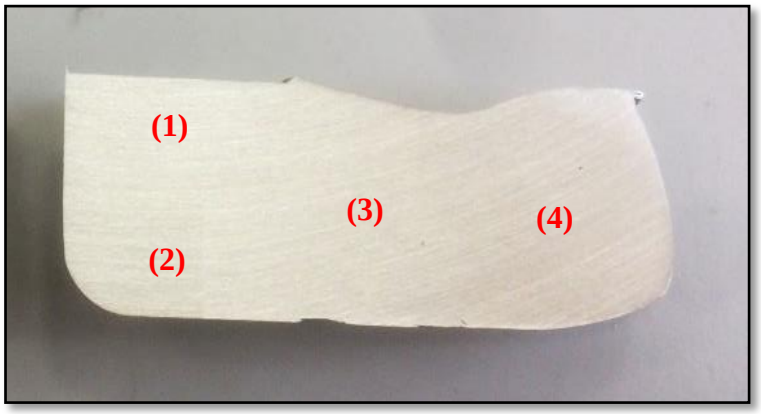

Figure 5.25: Four hardness regions in the samples

5.5.3 Grain Size Test

The ImageJ program is used to measure the grain size from the microstructure figures.

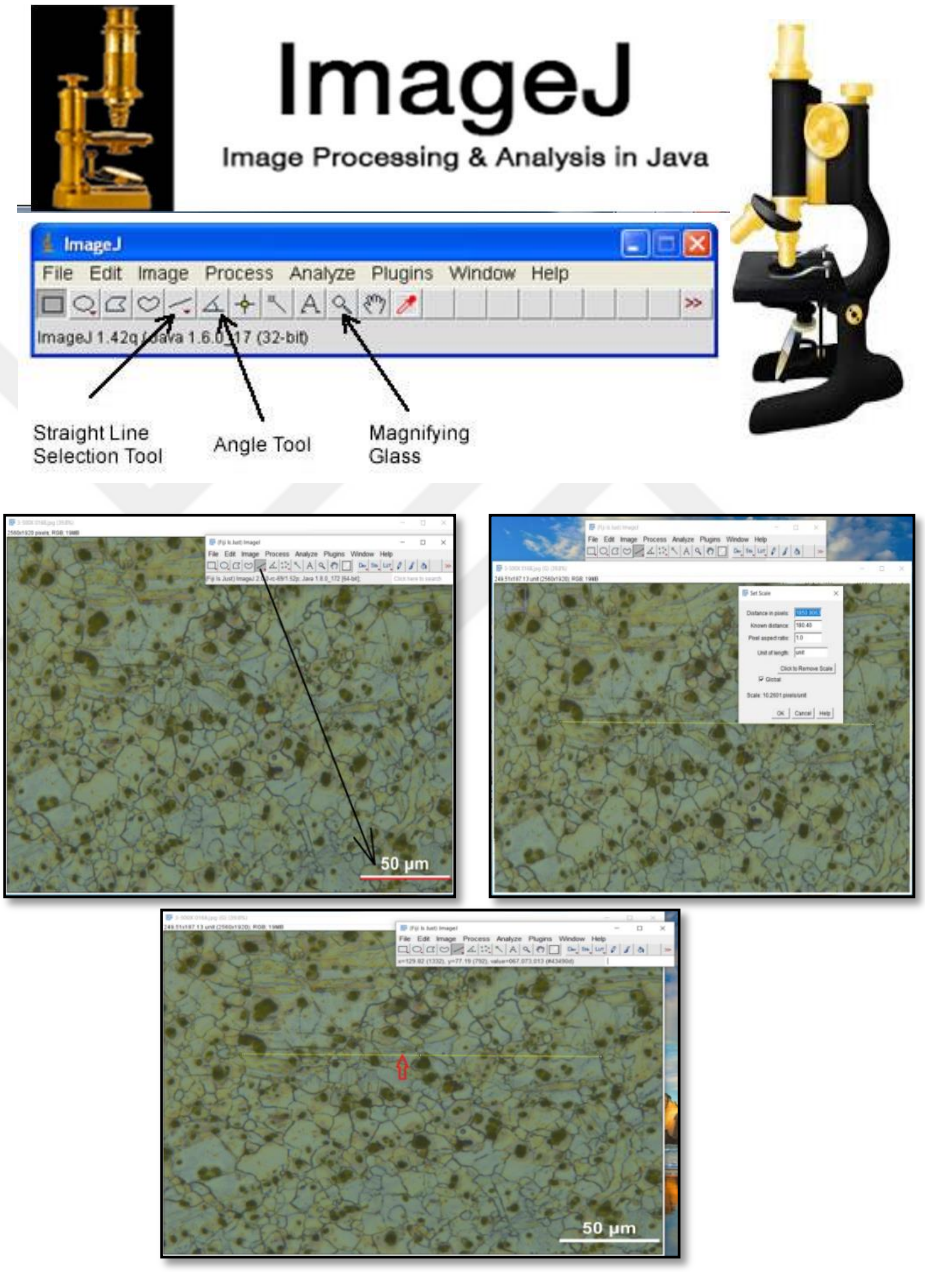

Figure 5.26: Steps of grain size measurement with ImageJ

CHAPTER 6

RESULTS AND DISCUSSION

6.1 Simulation Results from QForm

6.1.1 Stress Distribution

6.1.1.1 Mean Stress

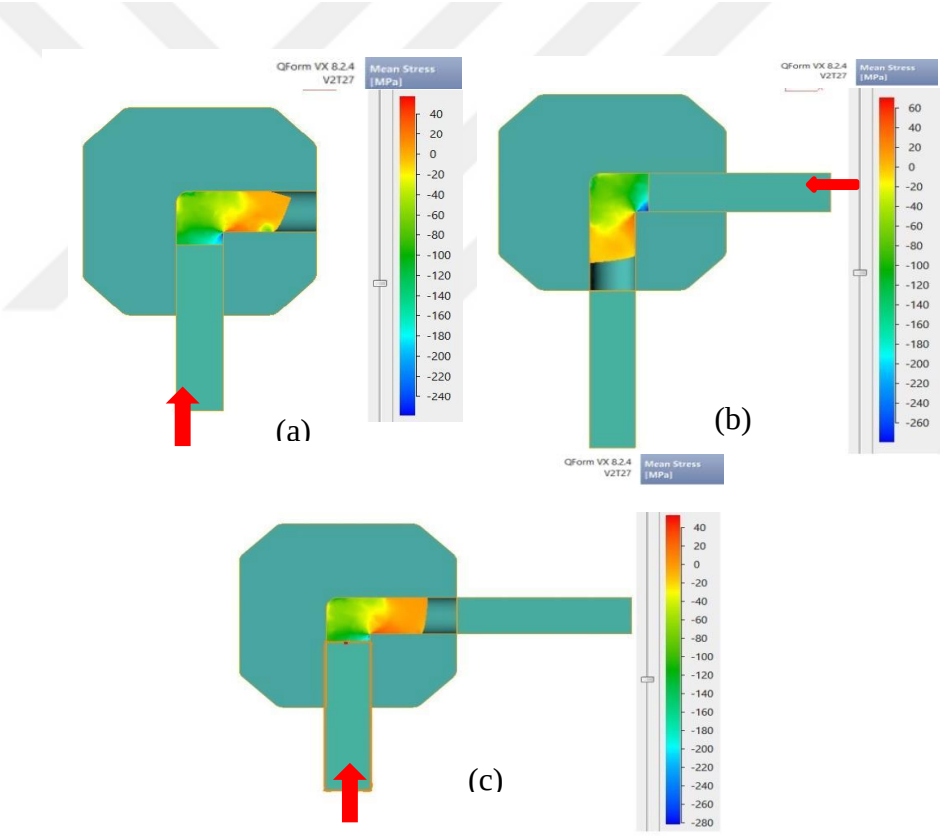

Figure 6.1: Mean stress distribution for work piece at die temperature T = 275°C, velocity V1 = 14 mm/s after (a) 1 pass, (b) 2 passes and (c) 3 passes

The stress distribution in Figure 6.1 shows that maximum stress is at the corner of angle ϕ because of the shear in the metal layer occurring in this edge. The minimum stress is in the contact area between the punch and the work piece.

6.1.1.2 Effective Stress Distribution

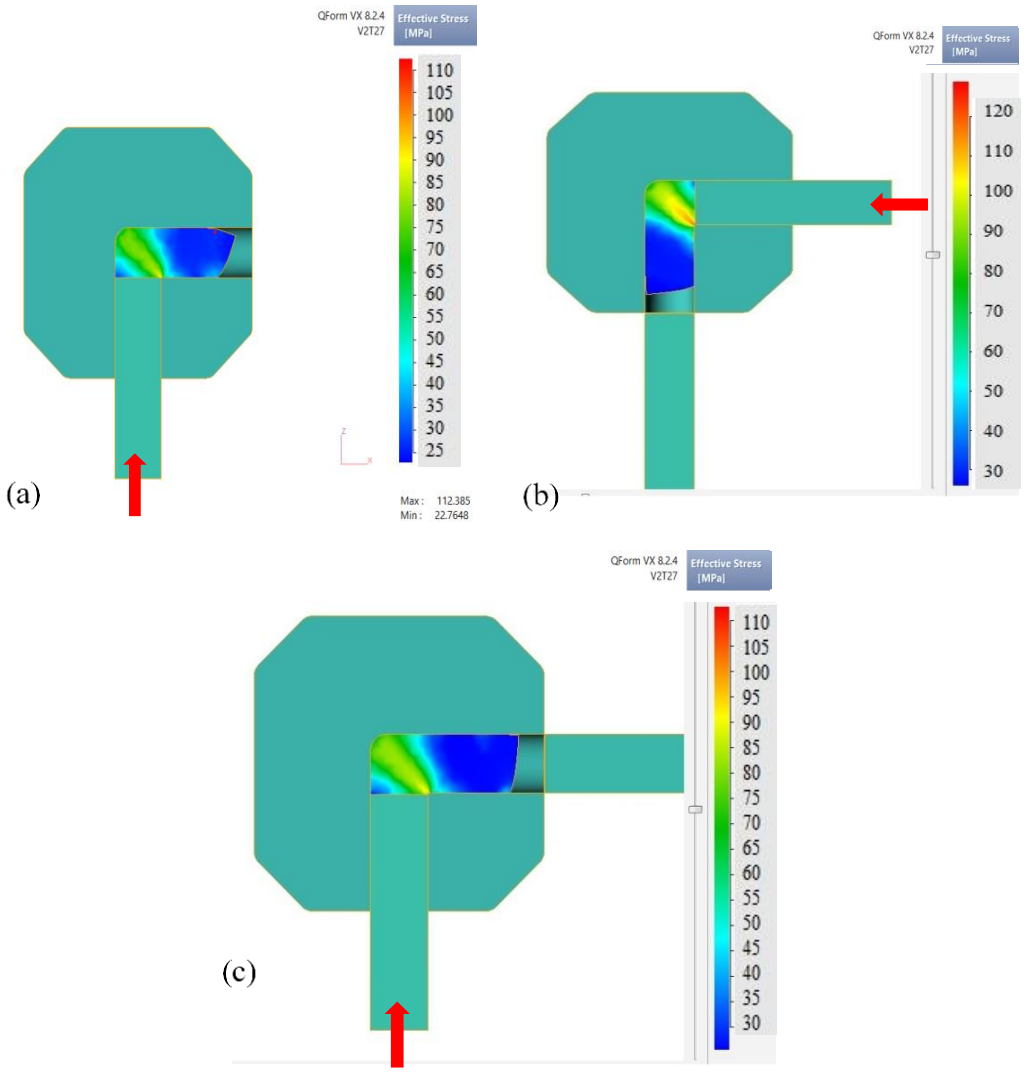

Figure 6.2: Effective stress distribution for work piece at die temperature T = 275°C, velocity V1 = 14 mm/s after (a) 1 pass, (b) 2 passes and (c) 3 passes

The effective stress distribution in Figure 6.2 shows the maximum stress at the corner of angle ϕ and curvature angle ψ because of the movement of the metal layer occurring in this area. The minimum effective stress is in the area far from the corners of the channel at the end of the work piece deformation.

1- At Constant Velocity

Table 6.1: Stresses at V1 = 14mm/s

Work piece temperature (°C)	Number of Passes	Maximum temperature (°C)	Minimum temperature (°C)	Mean stress (MPa)	Effective stress (MPa)
275	1	275.98	270.66	262.71	103.38
	2	217.82	210.19	382.53	128.86
	3	275.81	271.5	322	112.53
300	1	300.27	295.101	201.638	83.742
	2	296.30	291.45	286.27	104.07
	3	301.43	295.72	255.98	86.67

Table 6.2: Stresses at V2 = 27 mm/s

Work piece temperature (°C)	Number of Passes	Maximum temperature (°C)	Minimum temperature (°C)	Mean stress (MPa)	Effective stress (MPa)
275	1	277.84	271.67	351.28	104.70
	2	270.102	216.402	391.118	134.93
	3	277.50	272.034	291.037	120.548
300	1	302.068	295.726	240.829	92.362
	2	294.484	234.71	368.78	126.058
	3	301.668	296.257	230.736	93.428

2- At Constant Temperature

Table 6.3: Stresses at T1 = 275°C

Press velocity (mm/s)	Number of passes	Mean stress (MPa)	Effective stress (MPa)
14	1	262.71	103.38
	2	382.53	128.86
	3	322	112.53
27	1	351.28	104.70
	2	391.12	134.93
	3	291.04	120.55

Table 6.4: Stresses at T2 = 300°C

Press velocity (mm/s)	Number of passes	Mean stress (MPa)	Effective stress (MPa)
14	1	201.638	2.715
	2	286.27	3.382
	3	255.98	4.36
27	1	240.829	2.618
	2	368.78	3.025
	3	230.736	3.937

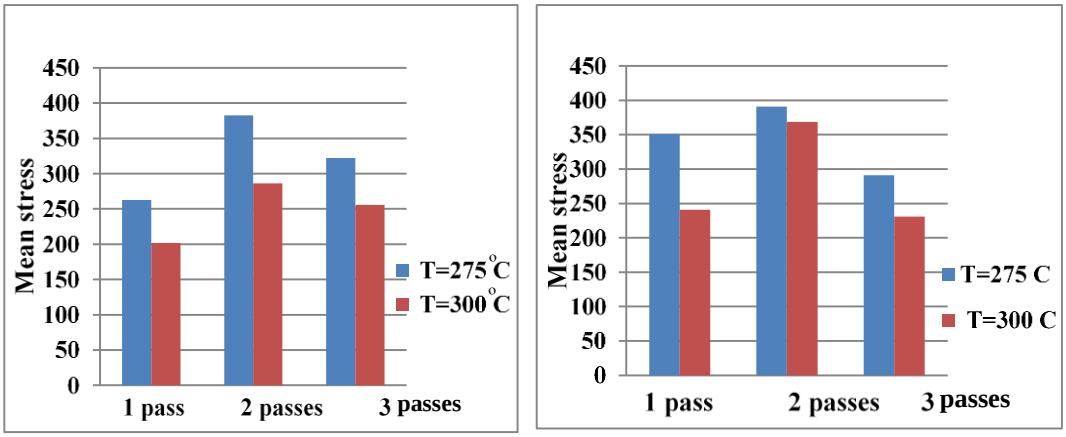

(a) (b)

Figure 6.3: Mean stress with different temperatures and constant velocities
(a) V1 = 14 mm/s (b) V2 = 27 mm/s

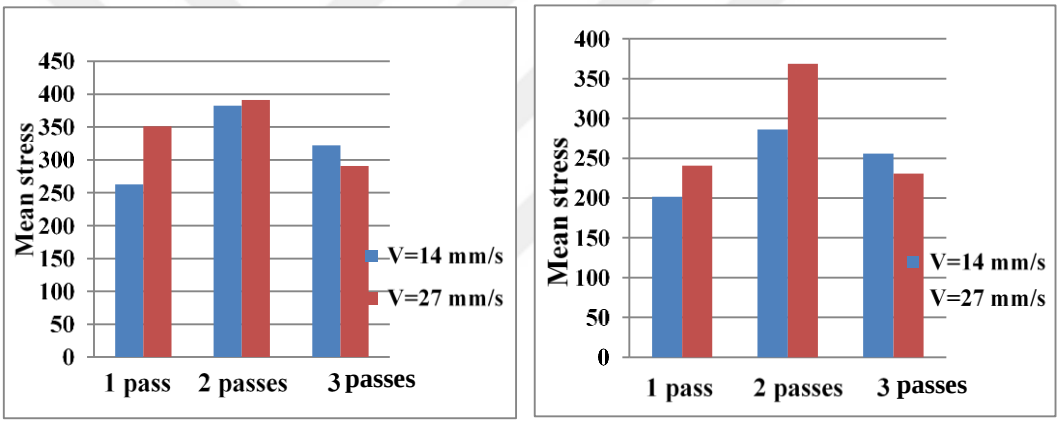

(a) (b)

Figure 6.4: Mean stress with different velocities at constant temperatures
(a) T1 = 275°C and (b) T2 = 300°C

Figure 6.3 shows that increasing the temperature would lead to a decrease in the mean stresses at constant velocity because of increasing ductility.

Figure 6.4 shows how increasing the velocity while keeping the temperature constant would lead to increases in stresses after pass 1 and pass 2 due to the friction force increasing. For pass 3, increasing the velocity would decrease the stress because of the increase in ductility.

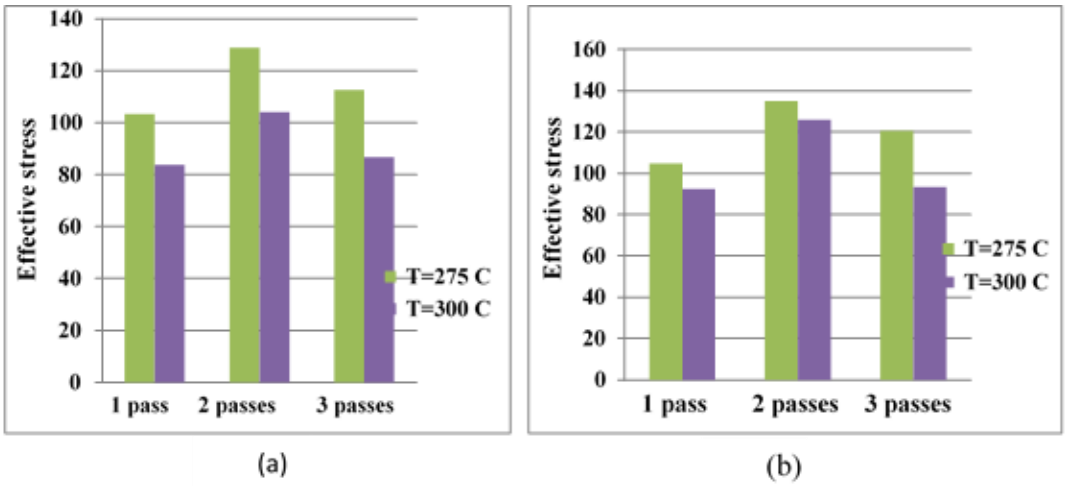

Figure 6.5: Effective stress with different temperatures at constant velocities (a) V1 = 14 mm/s and (b) V2 = 27 mm/s

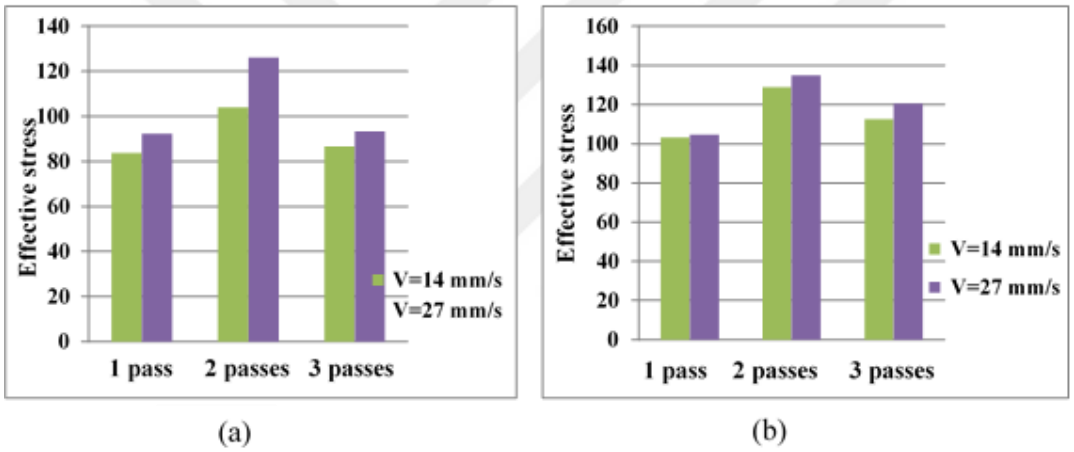

Figure 6.6: Effective stress with different velocities at constant temperatures (a) T1 = 275°C and (b) T2 = 300°C

Figure 6.5 show that increasing temperature lead to decrease effective stresses at constant velocity because of increasing in ductility higher friction forces.

Figure 6.6 shows how increasing velocity while temperature remained constant would increase the stresses after pass 1 and pass 2 due to friction force increasing. For pass 3, increasing the velocity would decrease the stress because of the increase in ductility.

6.1.2 Plastic Strain Distribution

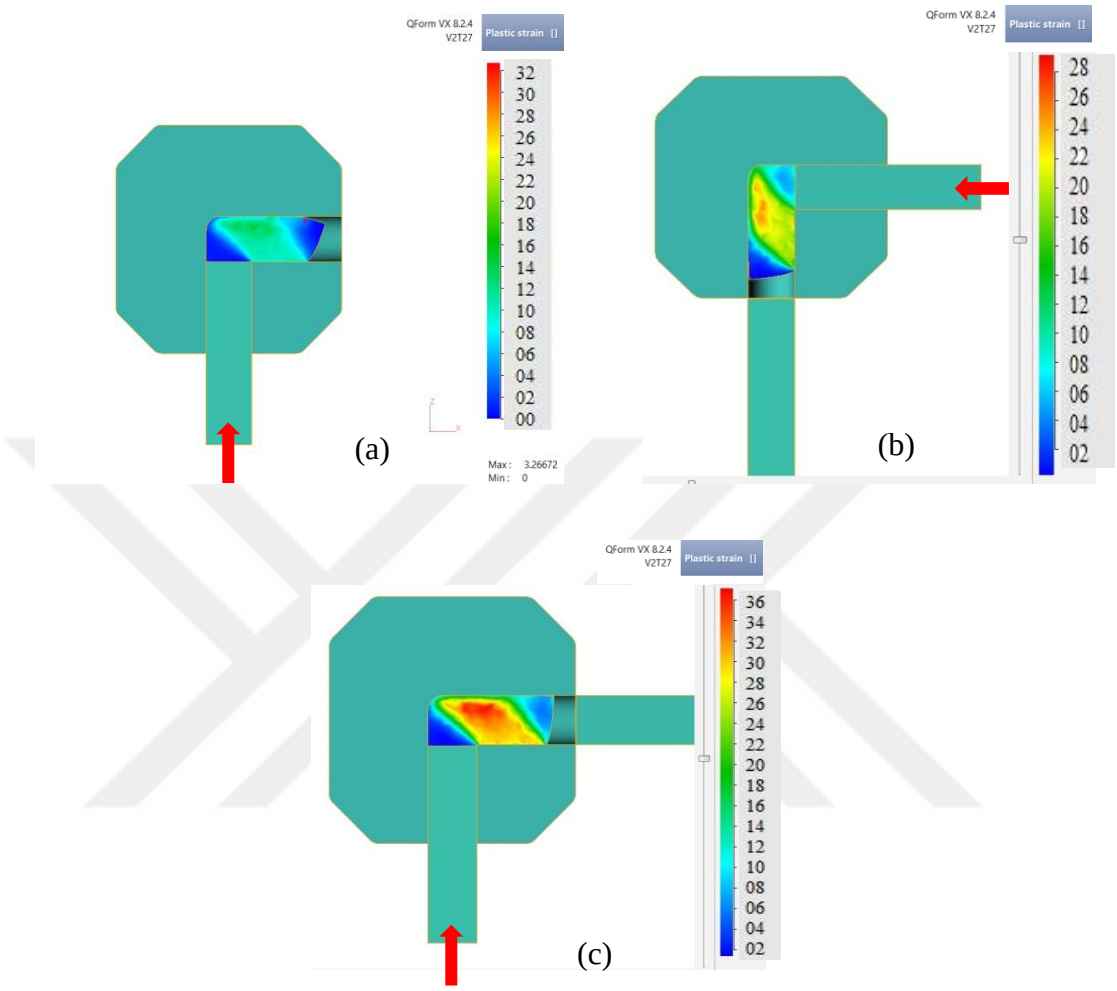

Figure 6.7: Plastic strain distribution for work piece at die temperature T = 275°C and velocity V1 = 14mm/s after (a) 1 pass, (b) 2 passes and (c) 3 passes

In Figure 6.7, the plastic strain distribution shows maximum strain at the center of the work piece because of the high plastic deformation of the metal in this area. The minimum plastic strain is at the end of the work piece after each pass and the maximum plastic strain occurs after the third pass.

1- At Constant Velocity

Table 6.5: Plastic strain at velocity V1 = 14mm/s

Work piece temperature (°C)	Number of passes	Maximum temperature (°C)	Minimum temperature (°C)	Plastic strain
275	1	275.98	270.66	2.521
	2	217.82	210.19	2.908
	3	275.81	271.5	3.72
300	1	300.27	295.101	2.715
	2	296.30	291.45	3.382
	3	301.43	295.72	4.36

Table 6.6: plastic stain at velocity V2 = 27mm/s

Work piece temperature (°C)	Number of passes	Maximum temperature (°C)	Minimum temperature (°C)	Plastic strain
275	1	277.84	271.67	2.254
	2	270.102	216.402	3.207
	3	277.50	272.034	4.159
300	1	302.068	295.726	2.618
	2	294.484	234.71	3.025
	3	301.668	296.257	3.937

2- At constant temperature

Table 6.7: Plastic strain at T1 = 275°C

Press velocity (mm/s)	Number of passes	Plastic strain
14	1	2.521
	2	2.908
	3	3.72
27	1	2.254
	2	3.207
	3	4.159

Table 6.8: Plastic strain at T2 = 300°C

Press velocity (mm/s)	Number of passes	Plastic strain
14	1	2.715
	2	3.382
	3	4.36
27	1	2.618
	2	3.025
	3	3.937

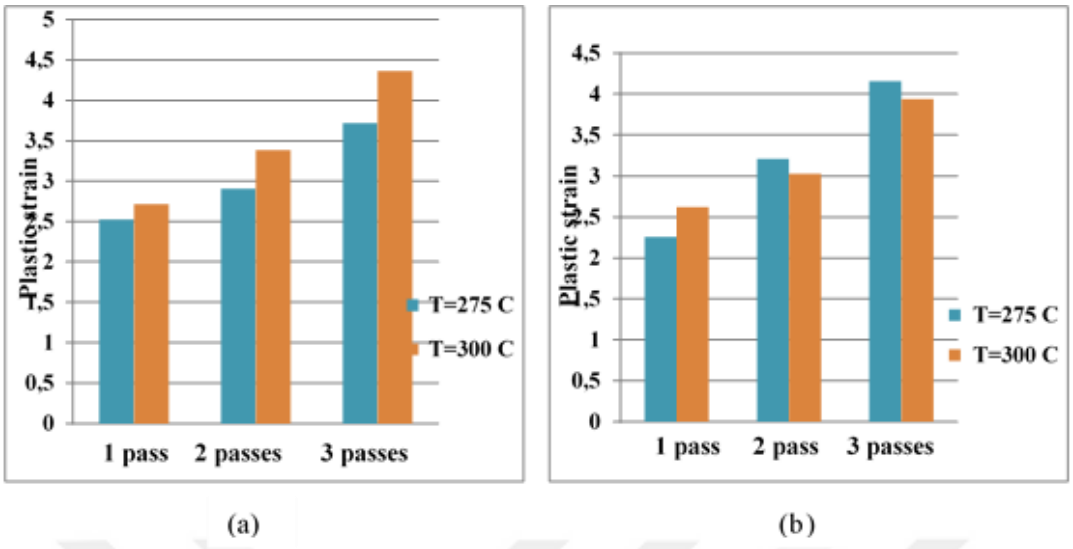

Figure 6.8: Plastic strain with different temperatures and constant velocities: (a) V1 = 14 mm/s and (b) V2 = 27 mm/s

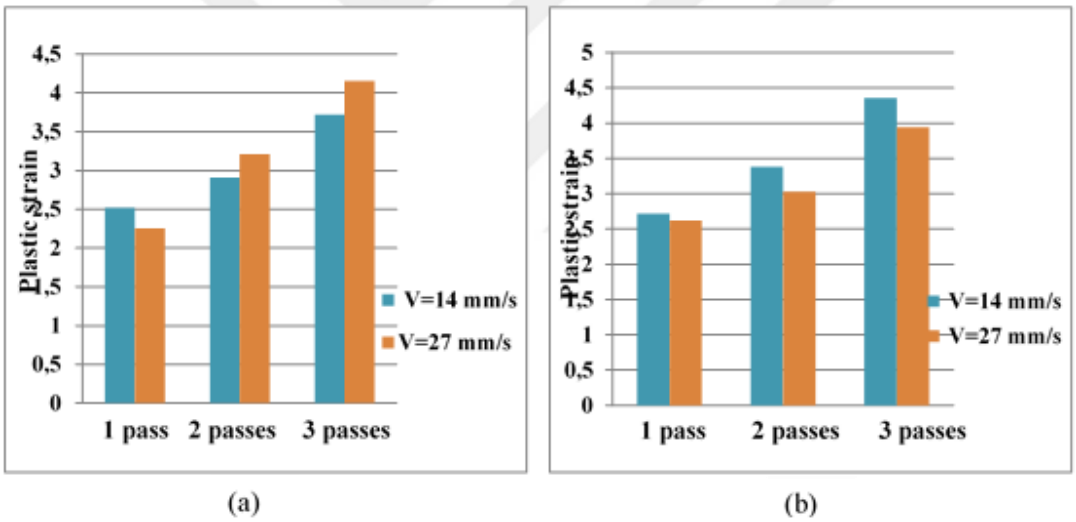

Figure 6.9: Plastic strain with different velocities at constant temperatures: (a) T1 = 275°C and (b) T2 = 300°C

Figure 6.8 shows that that increasing temperature would lead to increasing the plastic strain when the velocity was constant because of the higher friction forces.

Figure 6.9 shows how increasing the velocity but keeping the temperature constant would result in an increase to the plastic strain due to an increase in the dislocation of material layers. This occurs in all passes.

6.1.3 Grain Size Distribution

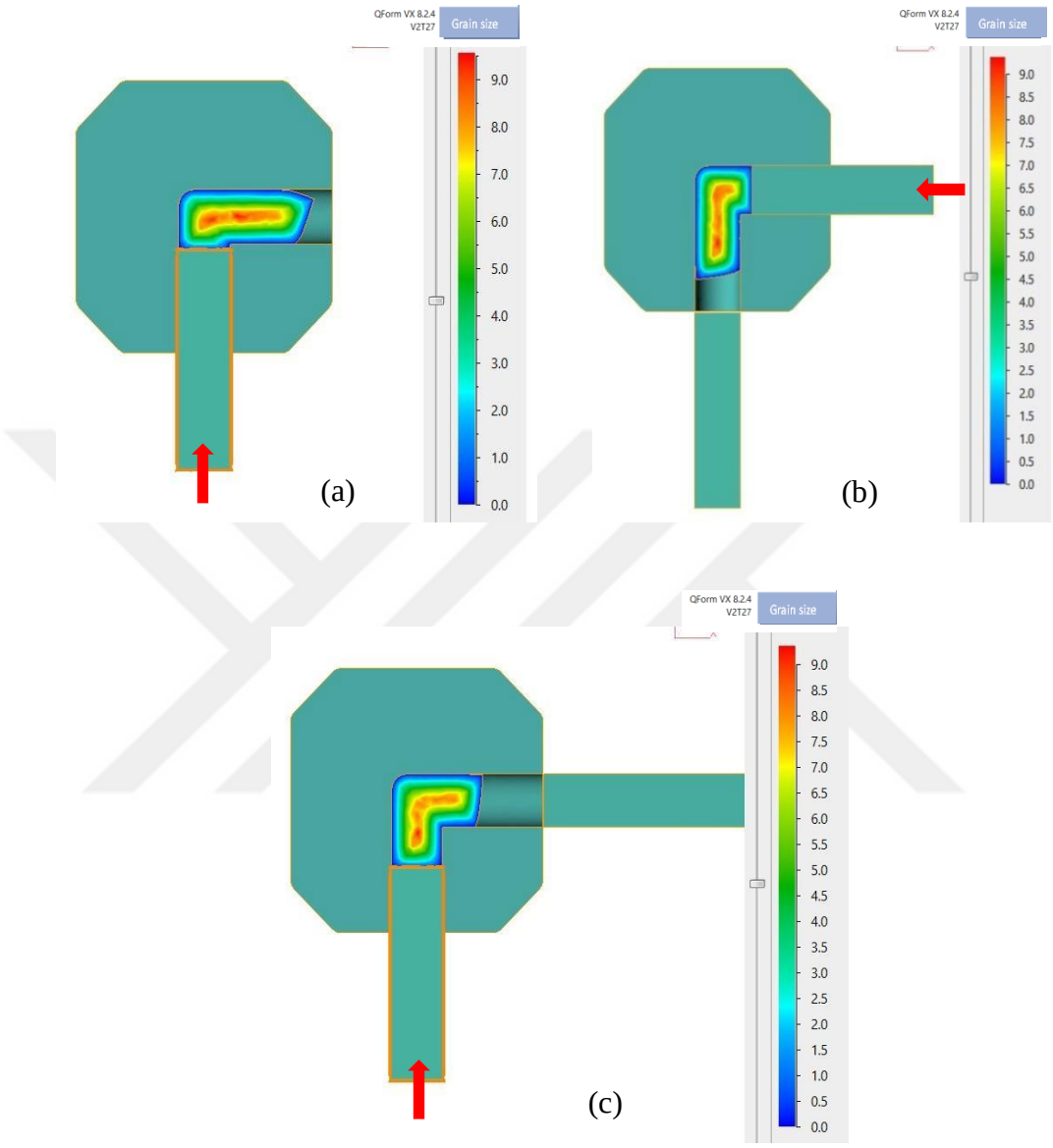

Figure 6.10: Grain size distribution for work piece at die temperature T = 275°C, V1 = 14mm/s through (a) 1 pass, (b) 2 passes and (c) 3 passes

This figure shows the minimum grain size in the outer surface of the work piece due to the change in shape and maximum deformation with dislocations occurring more in the corner of the channel than in the center of the work piece.

Table 6.9: Simulation results of grain sizes with different temperatures and velocities

T1 = 275°C	**1 pass**	**2 passes**	**3 passes**
V1 = 14 mm/s	6.543 µm	3.790 µm	2.853 µm
V2 = 27 mm/s	6.366 µm	3.513 µm	1.946 µm
T2 = 300°C	**1 pass**	**2 passes**	**3 passes**
V1 = 14 mm/s	6.530 µm	2.876 µm	1.880 µm
V2 = 27 mm/s	5.655 µm	2.352 µm	1.480 µm

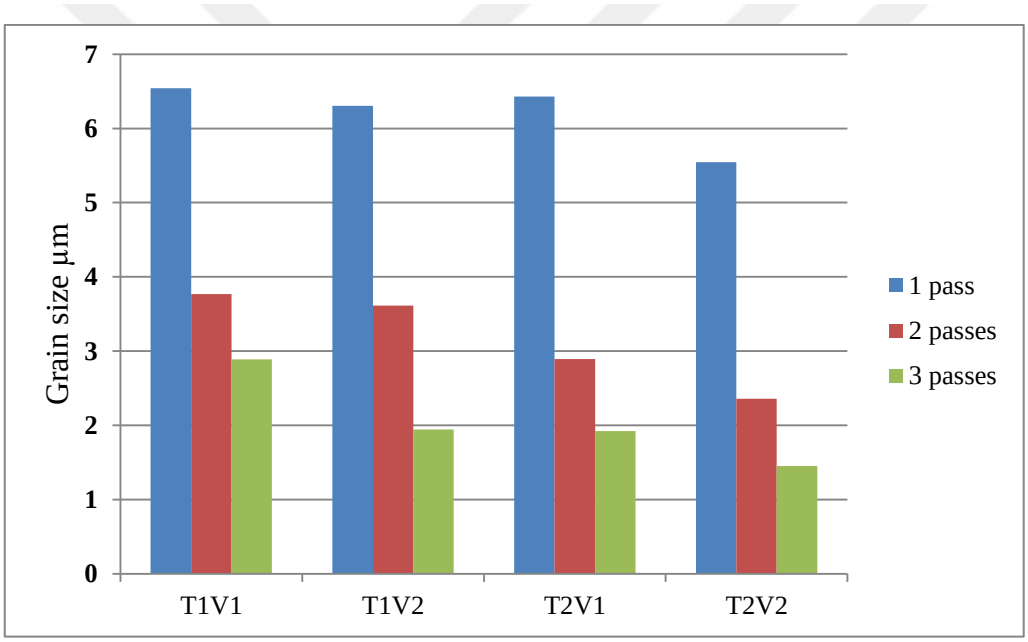

Figure 6.11: Diagram of grain sizes with different temperatures and velocities

Grain sizes decrease when the temperature increased. The finest grain size would occur at T = 300°C, while the highest value was recorded at T = 275°C.

For velocity increasing but temperature being constant, the grain size decreased and acquired the best refinement at V = 27 mm/s during pass 3 after three occurrences of pressing.

6.1.4 Temperature Distribution

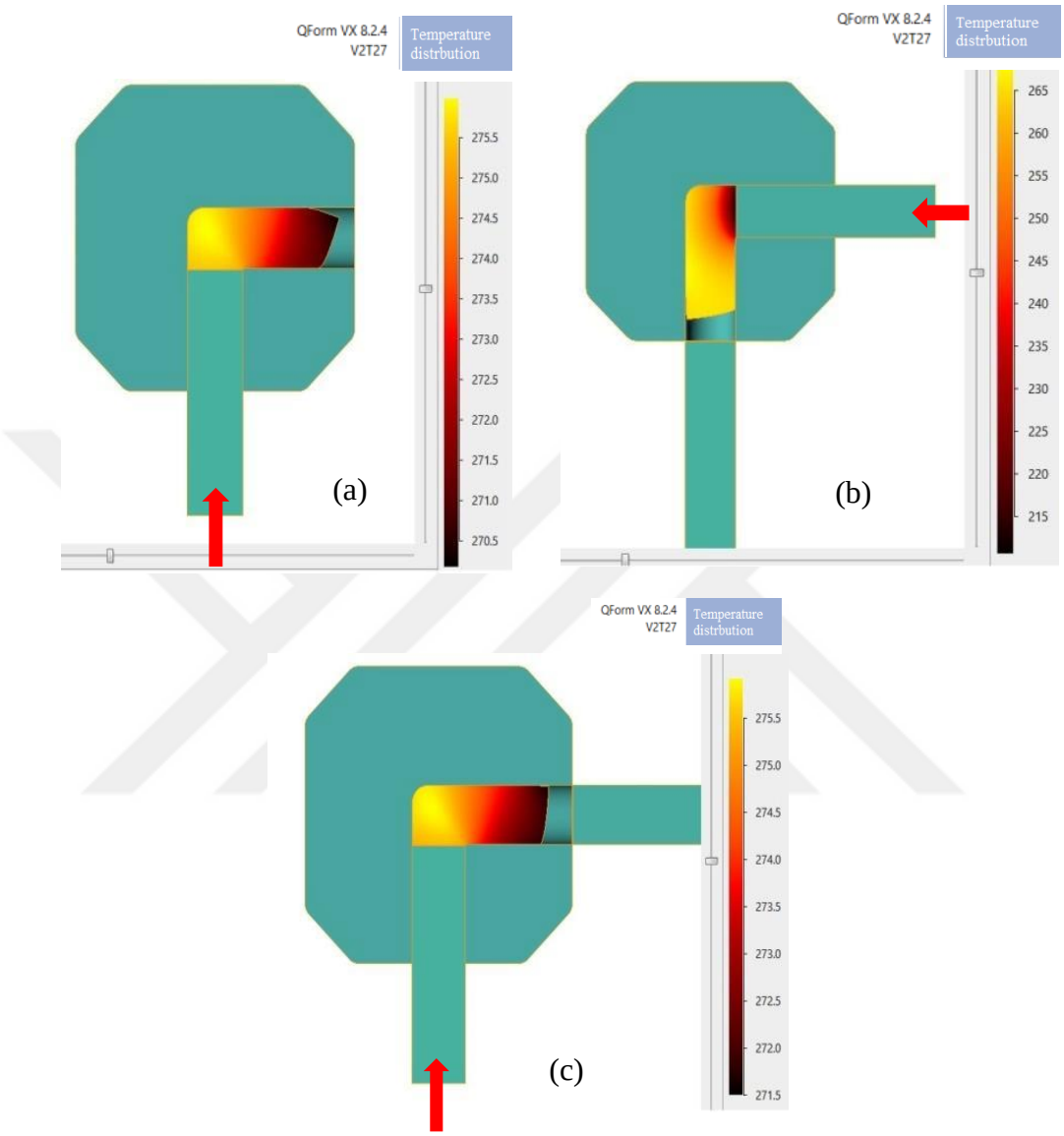

Figure 6.12**:** Temperature distribution for work piece at die temperature T = 275°C, velocity V1 = 14mm/s over (a) 1 pass, (b) 2 passes and (c) 3 passes

This figure shows the maximum temperature occurring in the work piece while passing through the channel angle with shape changes due to the shear zone and highest deformation occurring in those regions. The minimum temperature would occur at the end of the process where the friction force is at a minimum.

6.1.5 Loads and Times in Simulation Results

Table 6.10: Simulation results of loads and times at T1 = 275°C

Case 1 T1 = 275°C and V1 = 14 mm/s			
L (MN)	t (s)	Number of passes	Cases
1,290	4.2	1	1 pass
1,410	4.3	1	2 passes
1,085	3.95	2	
1,487	4.85	1	3 passes
1,073	4.15	2	
967	3.87	3	
Case 2 T1 = 275°C and V2 = 27 mm/s			
L (MN)	t (s)	Number of passes	Cases
1,088	2.87	1	1 pass
1,083	3.25	1	2 passes
973	2.29	2	
990	4.65	1	3 passes
880	4.58	2	
859	3.82	3	

Table 6.11: Simulation results of loads and times at T2 = 300°C

Case 3 T2 = 300°C and V1 = 14 mm/s			
L (MN)	t (s)	Number of passes	Cases
1,274	4.1	1	1 pass
1,435	6.25	1	2 passes
984	4.7	2	
986	13.2	1	3 passes
798	11.7	2	
695	5.3	3	
Case 4 T2 = 300°C and V2 = 27 mm/s			
L (MN)	t (s)	Number of passes	Cases
1,225	2.7	1	1 pass
1,223	4.75	1	2 passes
940	3.35	2	
1,289	4.65	1	3 passes
987	3.7	2	
785	2.35	3	

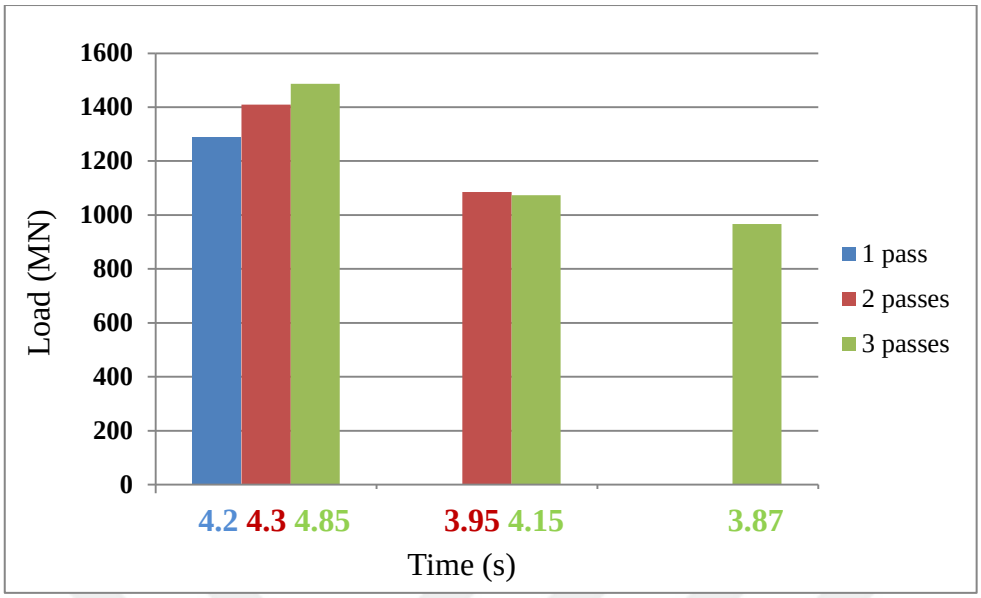

Figure 6.13: Loads and times with different numbers of passes with temperature T1 = 275ºC and velocity V1 = 14 mm/s (Case 1)

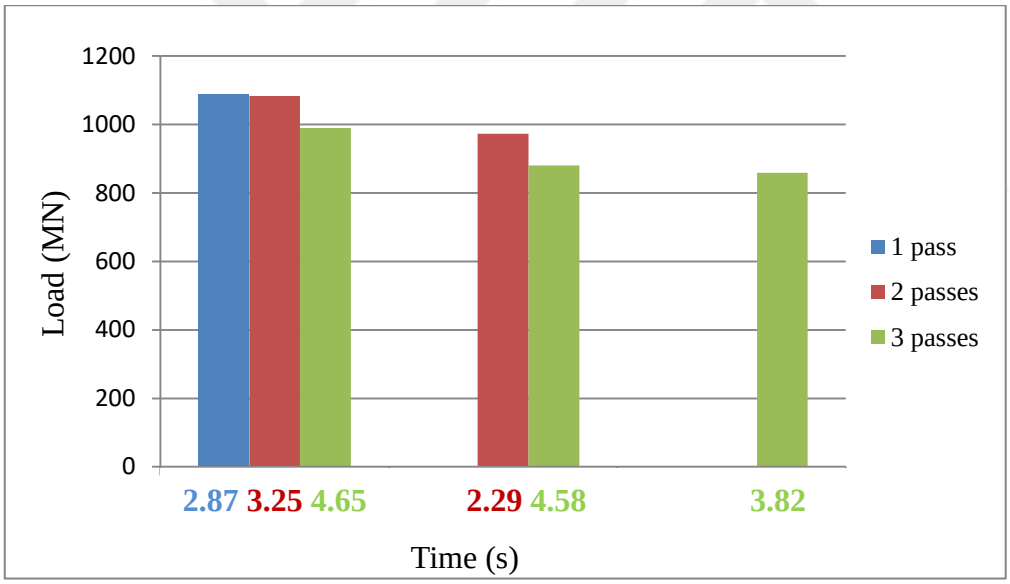

Figure 6.14: Loads and times with different numbers of passes with T1 = 275°C and velocity V2 = 27 mm/s (Case 2)

Figures 6.13 and 6.14 show how, with an increase of velocity with temperature (T1 = 275°C) being constant, the loads and times would decrease. This was due to the dislocation between the material layers when the velocity increased. Moreover, the dislocations, loads and times would decrease with an increase in the number passes.

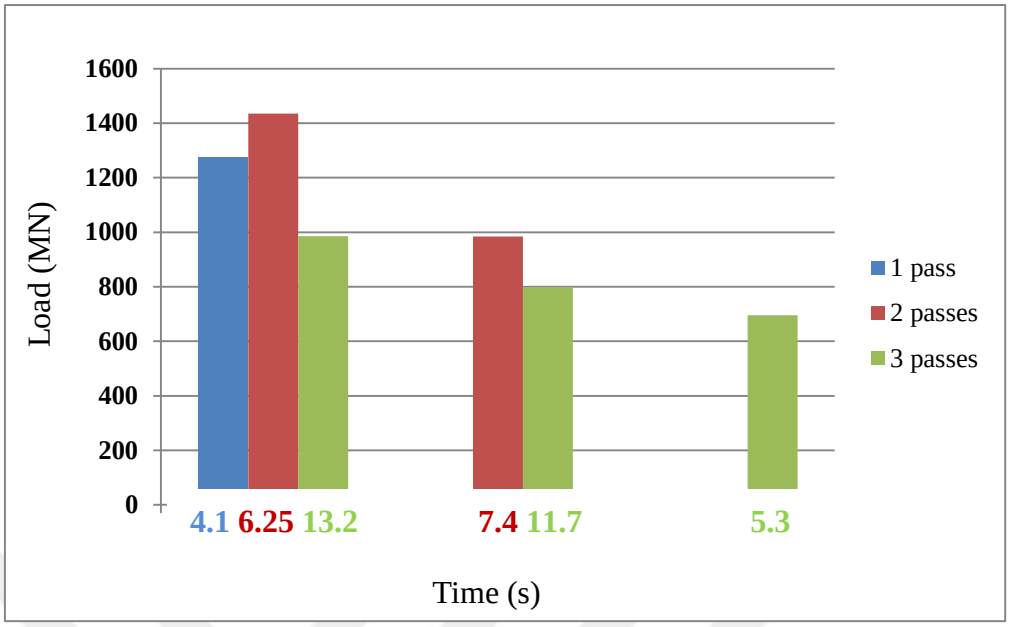

Figure 6.15: Loads and times with different numbers of passes, temperature T2 = 300°C and velocity V1 = 14 mm/s (Case 3)

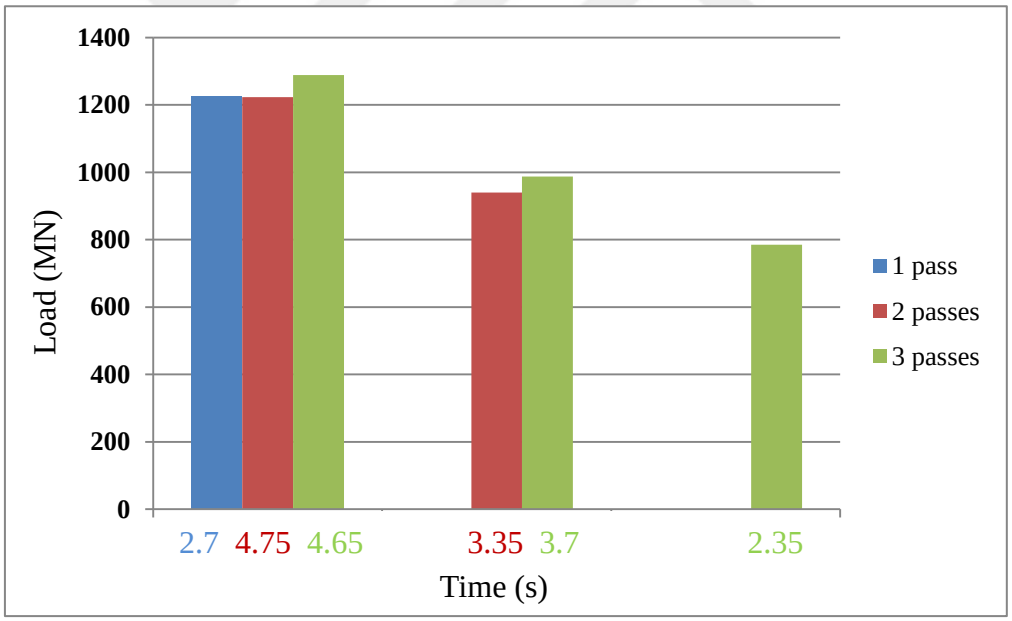

Figure 6.16: Loads and times with different numbers of passes, temperature T2 = 300°C and V2 = 27 mm/s (Case 4)

Figures 6.15 and 6.16 show when increasing the velocity but maintaining the temperature at T2 = 300°C, the loads and times decreased due to dislocation between the material layers when increasing velocity. Moreover, dislocation, loads and times would decrease with an increase in the number of passes.

6.1.6 Hardness

Table 6.12: Simulation results for hardness values

No. of passes	Average region 1	Average region 2	Average region 3	Average region 4	Average
Sample at T1 = 275°C, V1 = 14 mm/s					
1 pass	89.5	86.3	86.0	82.2	86
2 passes	92.4	88.6	94.1	89.6	91.15
3 passes	93.9	91.8	94.9	89.8	92.6
Sample at T1 = 275°C, V2 = 27 mm/s					
1 pass	99.4	96.3	93.1	89.7	94.625
2 passes	98.7	97.0	91.3	92.3	95.375
3 passes	100.9	98.0	95.8	94.3	97
Sample at T2 = 300°C, V1 = 14 mm/s					
1 pass	87.4	88.9	87.5	90.2	88.5
2 passes	95.4	93.9	95.2	96.0	95.125
3 passes	97.3	98.0	98.5	94.3	97
Sample at T2 = 300°C, V2 = 27 mm/s					
1 pass	88.5	87.3	85.5	83.9	86.3
2 passes	91.3	93.3	91.8	92.3	92.175
3 passes	95.2	94.1	96.1	94.5	94.975

The figures below show the relationships of hardness values, different velocities and a constant temperature.

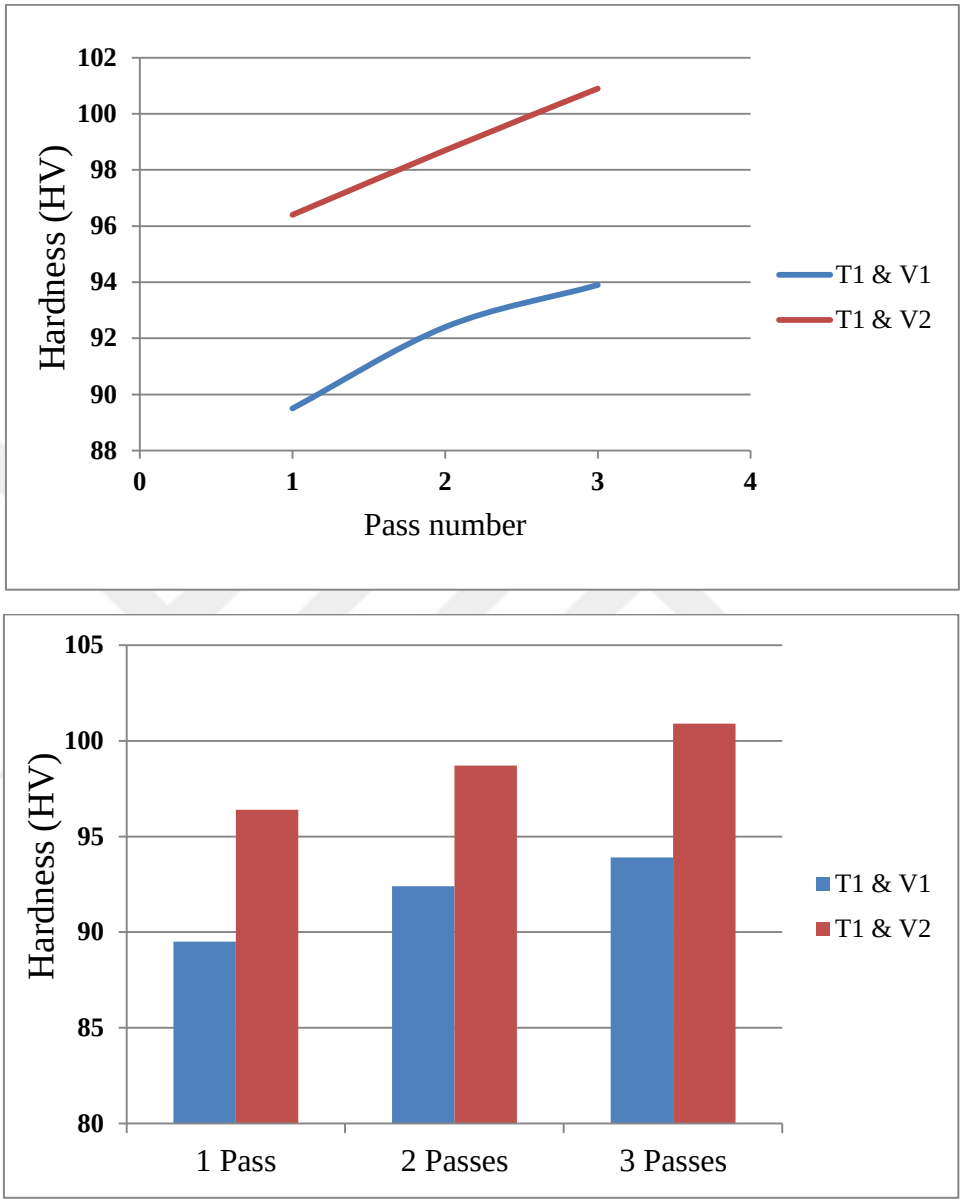

Figure 6.17: Hardness with different velocities V1, V2 and constant temperature T1

This figure shows how with a constant temperature (T1 = 275°C), the hardness values increased when the velocity increased. This was due to the grain size decreasing and an increase in the number of passes.

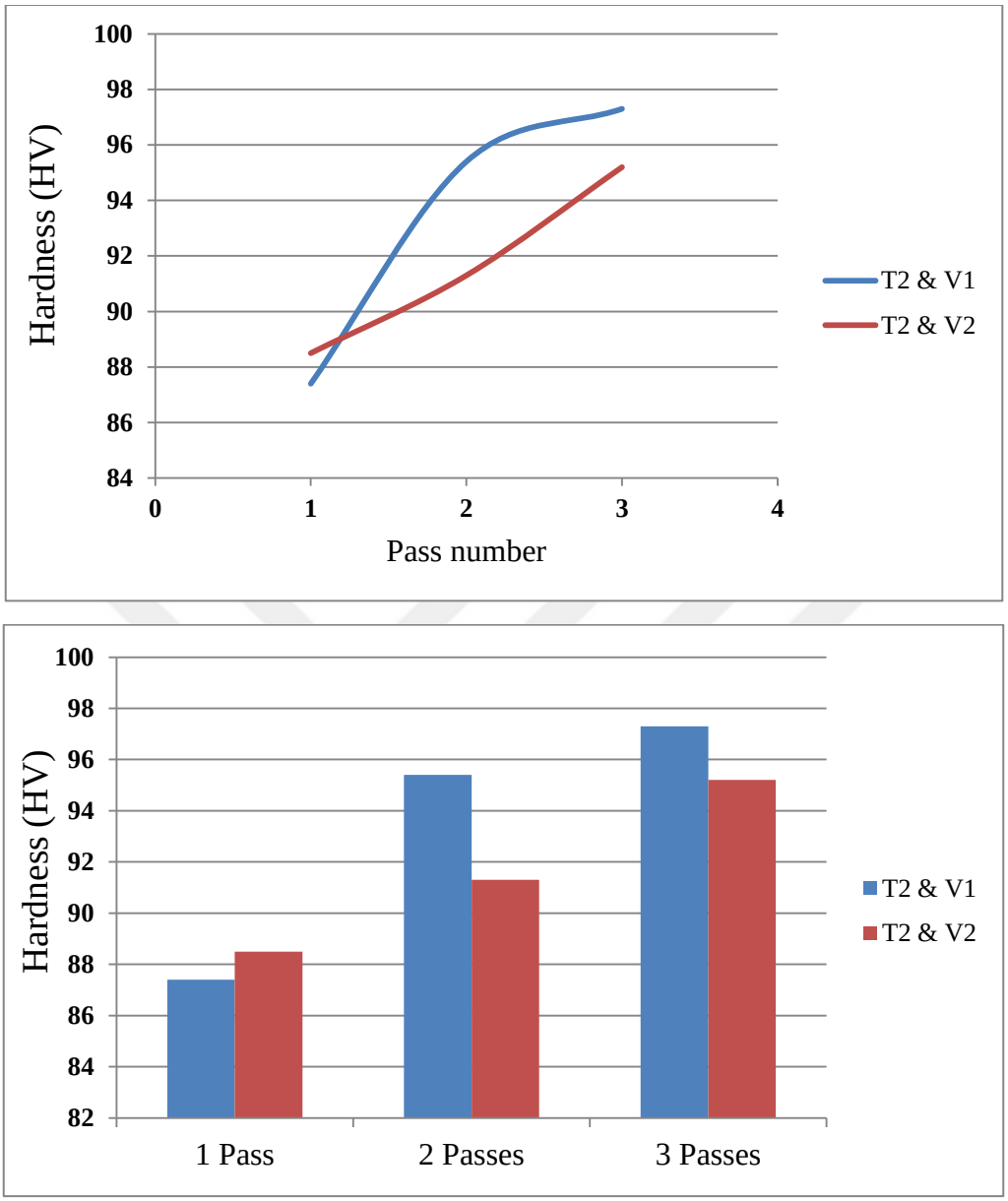

Figure 6.18: Hardness with different velocities V1, V2 and constant temperature T2

This figure shows that at a constant temperature (T2 = 300°C), the hardness values would increase when the velocity decreased. This would occur due to the grain size decreasing at low velocity; however, at the higher velocity, grain growth would occur. Moreover, grain growth would increase with an increase in the number of passes.

The figures below show the relationship between hardness values and different temperatures and a constant velocity.

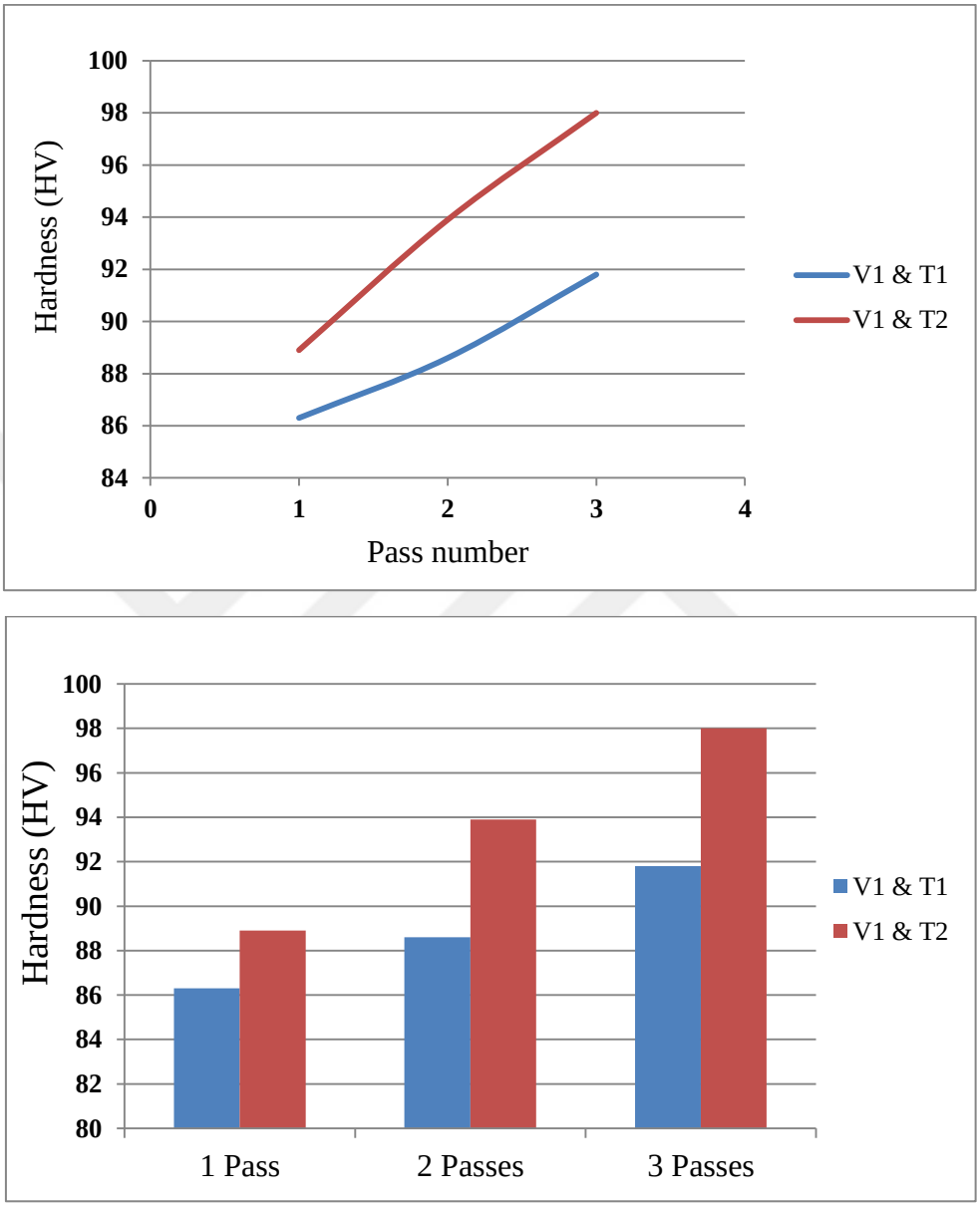

Figure 6.19: Hardness with different temperatures T1 and T2 and constant velocity V1 = 14 mm/s

Figure 6.19 shows how at constant velocity V1, the hardness values would increase when the temperature increased. This was due to the grain size decreasing and an increase in the number of passes.

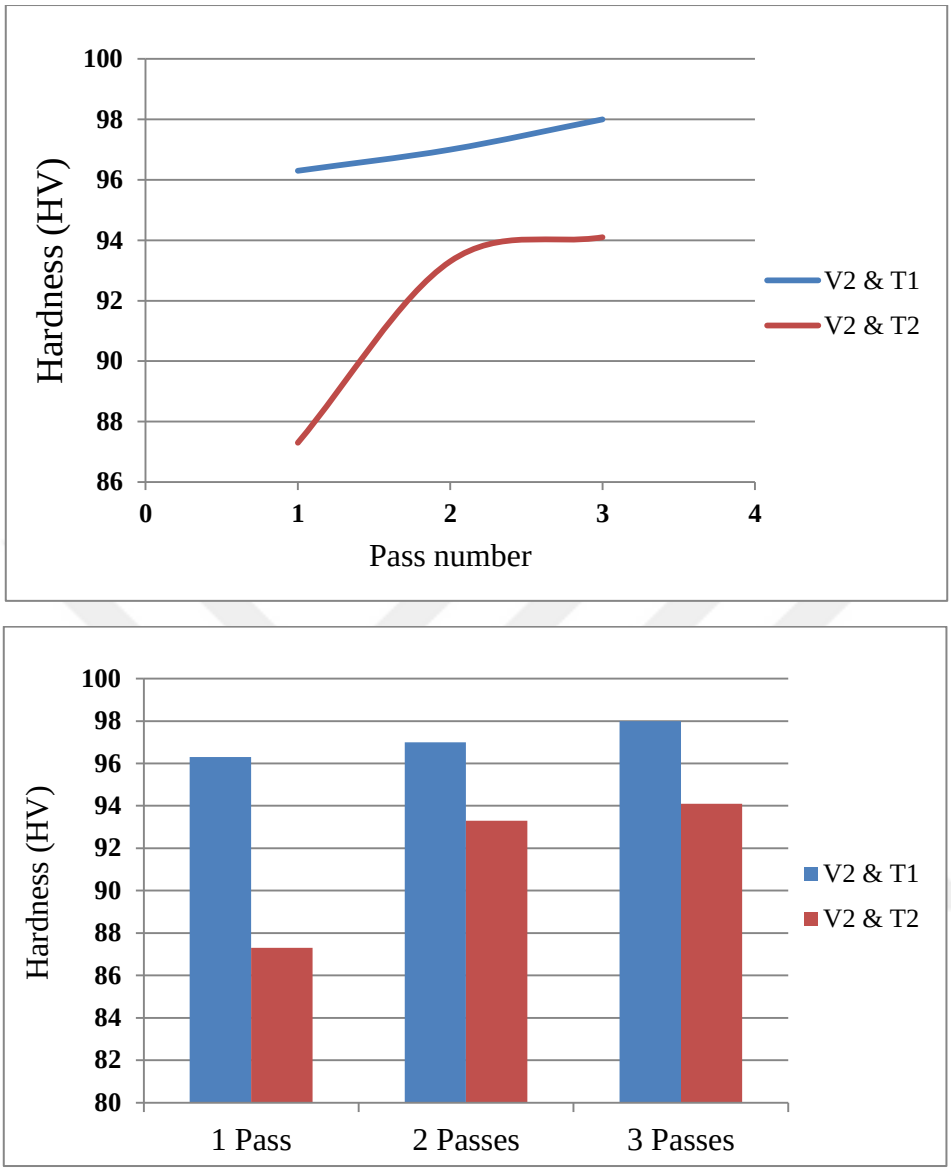

Figure 6.20: Hardness with different temperatures T1 and T2 and constant velocity V2 = 27 mm/s

Figure 6.20 shows how at constant velocity V2, the hardness values would increase when the temperature decreased. This was due to grain growth occurring at the higher temperature when the hardness was decreasing. Moreover, the hardness values would increase with an increase in the number the passes.

6.2 Experimental Results

Many tests were performed in the experimental work of the ECAP process. The results of this experimental work are presented below.

6.2.1 Grain Size

To measure the grain size of the sample for the ECAP process, ImageJ software was used. The microstructures below were taken at T2 = 300°C and different velocities (V1 = 14 mm/s, V2 = 27 mm/s) in Area 2 at 500× magnification.

T2 = 300°C and V1 = 14 mm/s

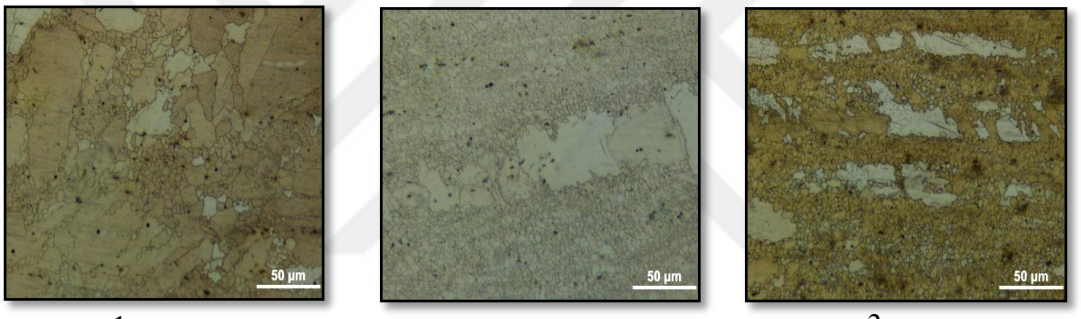

1 pass — *Grain size = 5.53 µm*

2 passes — *Grain size = 3.791 µm*

3 passes — *Grain size = 2.923 µm*

T2 = 300°C and V2 = 27 mm/s

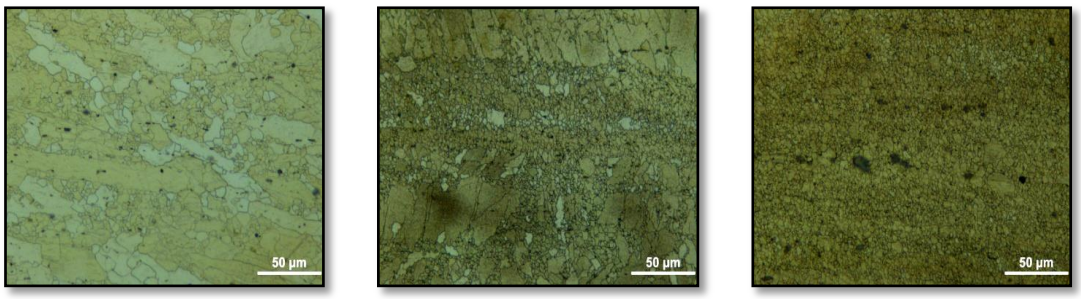

1 pass — *Grain size = 5.375 µm*

2 passes — *Grain size = 2.86 µm*

3 passes — *Grain size = 2.453 µm*

Figure 6.21: Grain sizes of the samples in area 2 with difference velocities

Increasing the velocity from V1 to V2 led a decrease in grain size while the temperature was constant.

Table 6.13: Grain sizes at temperature T2 = 300°C and different velocities

T2 = 300°C	1 pass	2 passes	3 passes
Grain sizes at V1	5.53 µm	3.791 µm	2.923 µm
Grain sizes at V2	5.375 µm	2.86 µm	2.453 µm

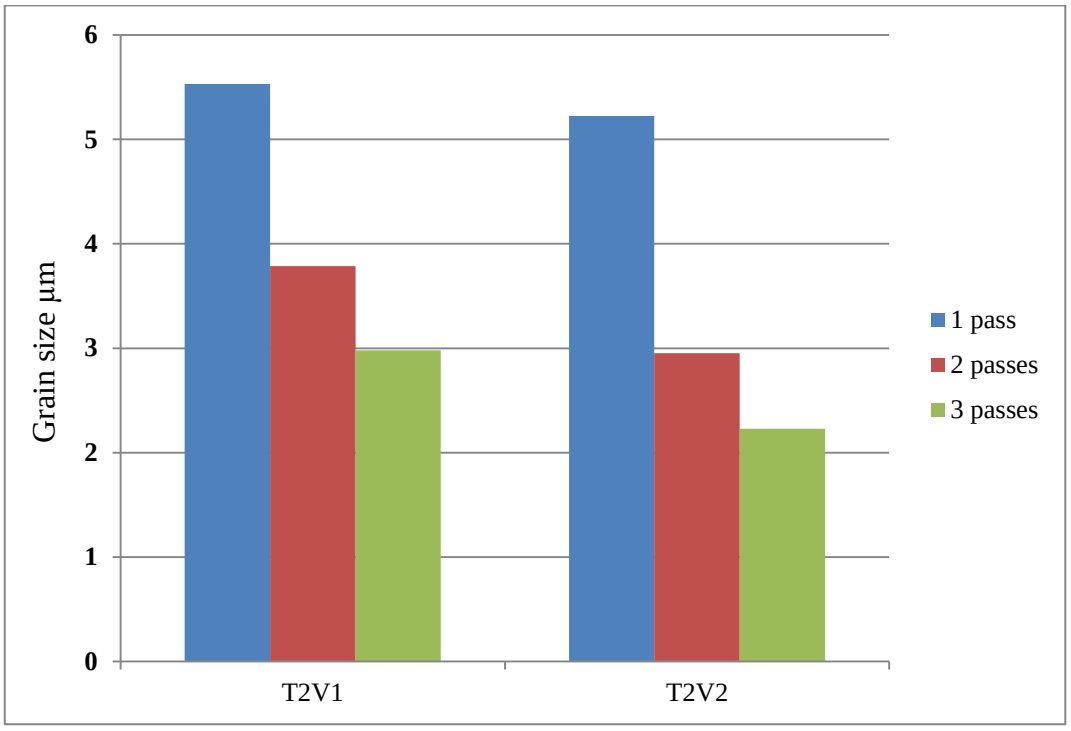

Figure 6.22: Grain sizes at constant temperature T2 = 300°C and different velocities through three passes

Grain sizes at temperature T2 and velocity V2 decreased more than at the same temperature but the for lower velocity V1, the grain size was larger than that of maximum velocity V2.

The microstructures below were taken at V1 = 14 mm/s and temperatures T1 = 275°C and T2 = 300°C.

T2 = 275°C and V1 = 14 mm/s

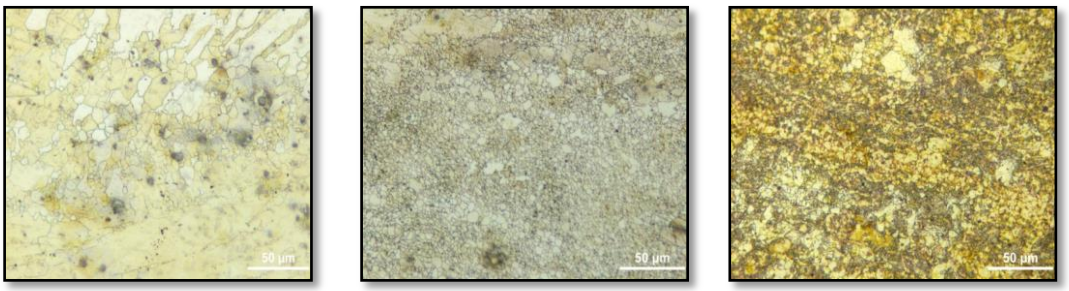

1 Pass — *Grain size = 5.398 µm*

2 Passes — *Grain size = 3.643 µm*

3 Passes — *Grain size = 2.846 µm*

T2 = 300°C and V1 = 14 mm/s

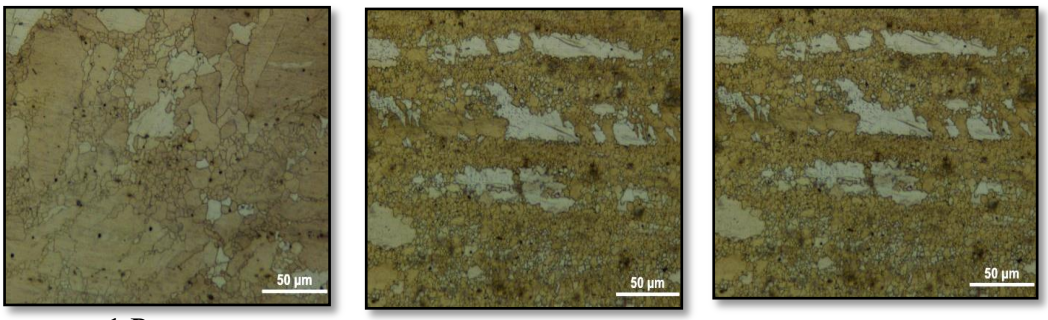

1 Pass — *Grain size = 5.53 µm*

2 Passes — *Grain size = 2.79 µm*

3 Passes — *Grain size = 1.923 µm*

Figure 6.23: Grain sizes of the samples in area 2 with different temperatures

When changing the temperature, a small difference in grain size could be observed between T1 and T2 at the same velocity V1.

Table 6.14: Grain sizes at velocity V1 = 14 mm/s and different temperatures

At V1 = 14 mm/s	**1 pass**	**2 passes**	**3 passes**
Grain sizes at T1	6.543 µm	3.768 µm	2.89 µm
Grain sizes at T2	5.53 µm	2.79 µm	1.923 µm

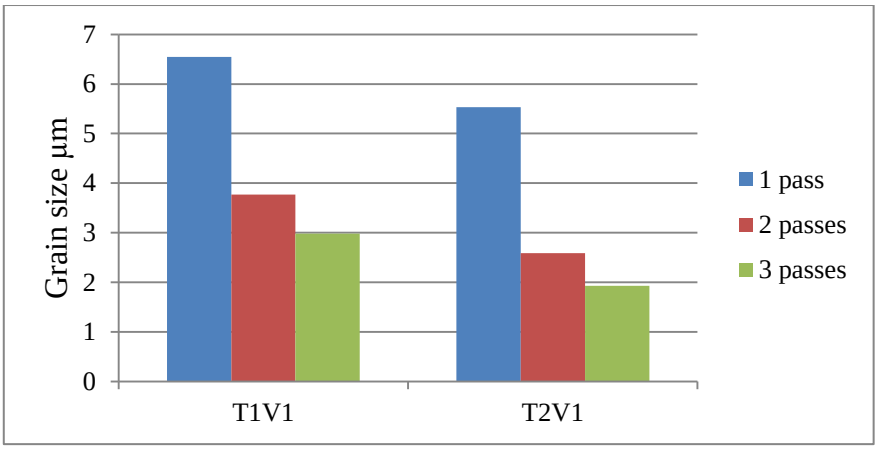

Figure 6.24: Grain sizes at constant velocity V1 = 14 mm/s and different temperatures through three passes

Table 6.15: Grain size values (µm)

T1 = 275°C	**1 pass**	**2 passes**	**3 passes**
V1 = 14 mm/s	6.543	3.768	2.89
V2 = 27 mm/s	6.275	3.615	1.953
T2 = 300°C	**1 pass**	**2 passes**	**3 passes**
V1 = 14 mm/s	6.53	2.891	1.923
V2 = 27 mm/s	5.675	2.36	1.453

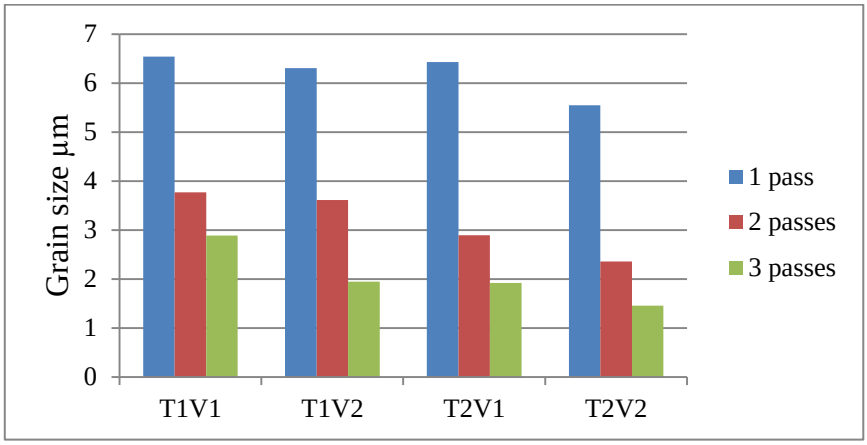

Figure 6.25: Grain sizes at different velocities and temperatures

With increases in the temperature (T2) and velocity (V2), grain sizes decreasing with an increasing number of passes were observed.

6.2.2 Microstructure

Area 1 at 200× magnification

Area 2 at 200× magnification

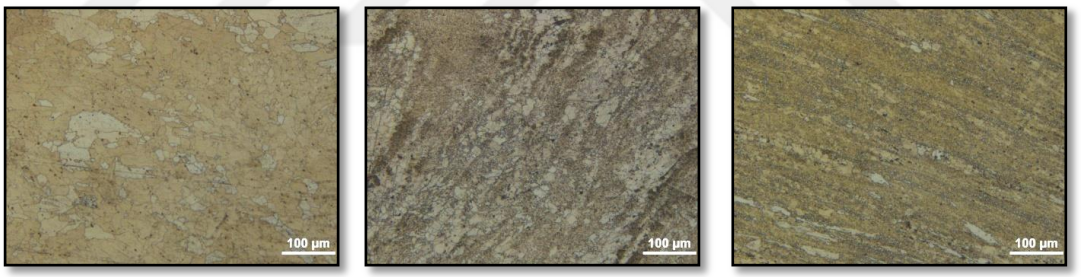

Area 3 at 200× magnification

1 pass 2 passes 3 passes

Area 4 at 200× magnification

Figure 6.26: Microstructures at T2 = 300°C and V = 14 mm/s

The microstructures below were taken at T2 = 300°C and velocitiesV1 = 14 mm/s and V2 = 27 mm/s in the same area.

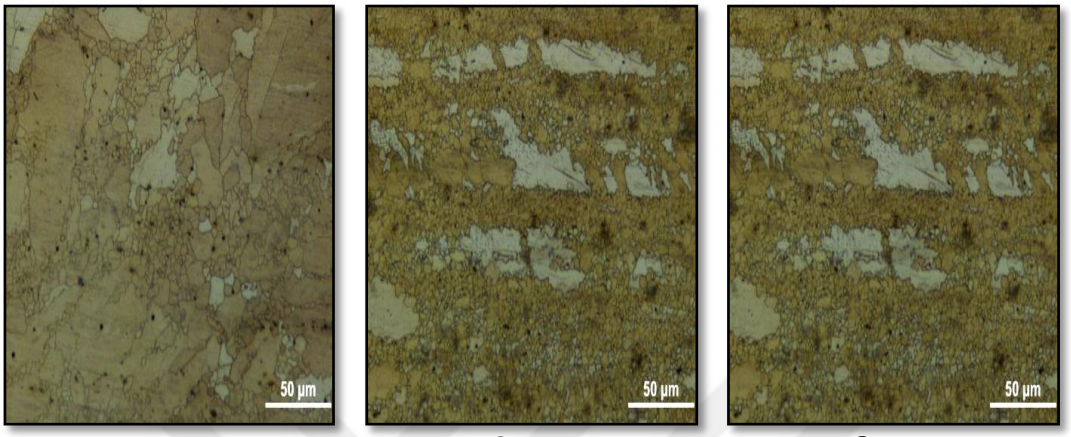

1 pass 2 passes 3 passes

Microstructure at T2 and V1 in Area 2 at 500× magnification

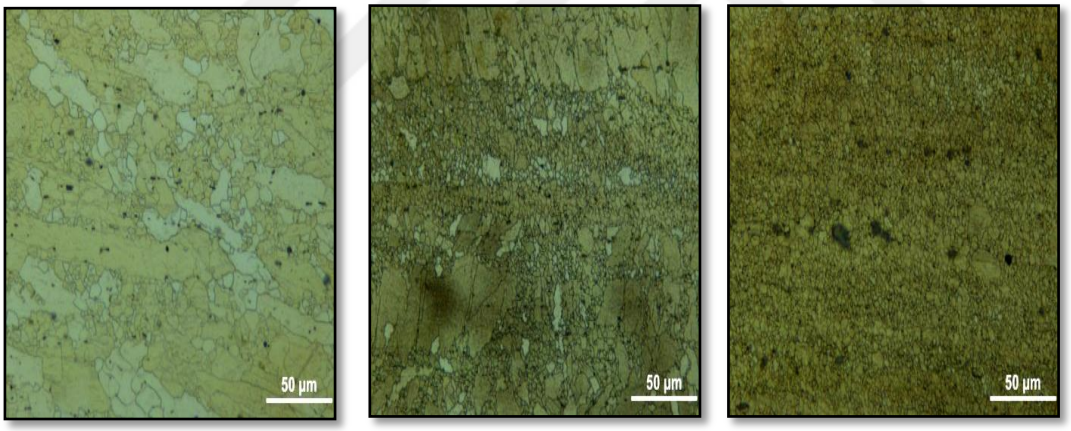

1 pass 2 passes 3 passes

Microstructures at T2 and V2 in Area 2 at 500× magnification

Figure 6.27: Microstructures of the sample in Area 2

When changing the velocity, a difference could be observed in grain size between V1 and V2 constant temperature T2.

The microstructures below were taken at temperatures T1 = 275°C and T2 = 300°C and constant velocity V1 = 14 mm/s in the same area.

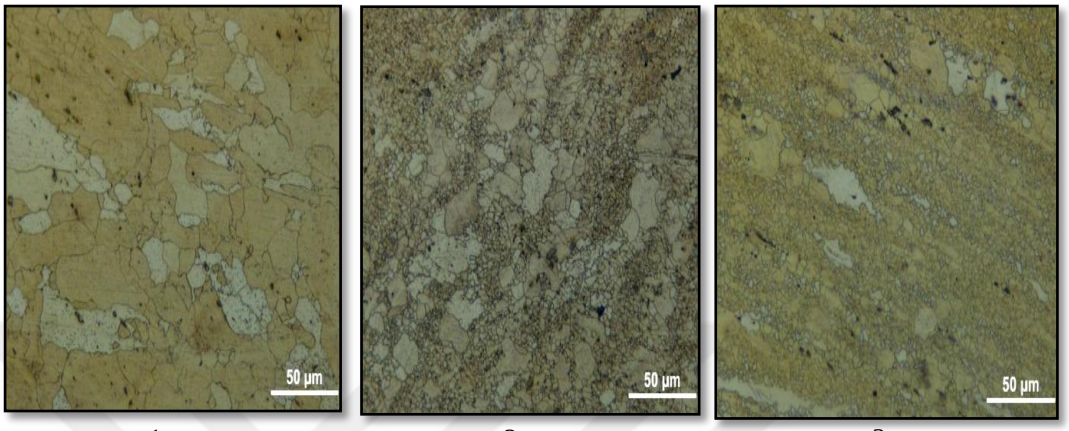

1 pass 2 passes 3 passes

Microstructures at T1 and V1 in Area 3 at 500× magnification

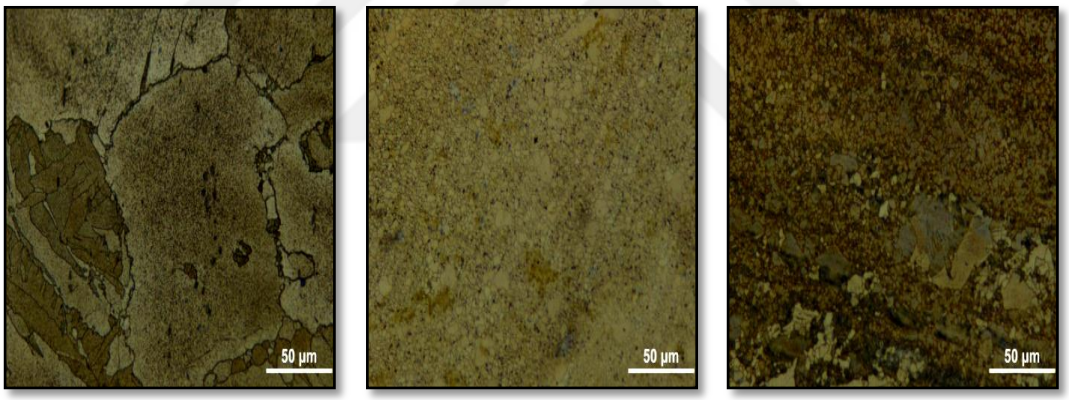

1 pass 2 passes 3 passes

Microstructures at T2 and V1 in Area 3 at 500×

Figure 6.28: Microstructures of the sample in Area 3

The difference in temperature in the ECAP process with the same velocity gave different grain sizes in the microstructures.

6.2.3 Hardness

The table below shows the hardness measurements from the Vickers Hardness tester (HV) for different temperatures and velocities.

Table 6.16: Hardness measurements for the samples

No. of passes	Average in Area 1	Average in Area 2	Average in Area 3	Average in Area 4	Average
Sample at T1 = 275°C, V1 = 14 mm/s					
1 pass	86.1	83.4	83.2	76.1	82.2
2 passes	88.1	80.9	92.9	85.6	86.875
3 passes	89.9	94.1	91.2	86.4	90.4
Sample at T1 = 275°C, V2 = 27 mm/s					
1 pass	98.4	92.4	89.1	83.6	90.875
2 passes	84.9	96.9	81.3	82.3	91.35
3 passes	89.8	92.8	93.8	93.3	92.425
Sample at T2 = 300°C, V1 = 14 mm/s					
1 pass	81.4	88.9	87.1	92.9	87.575
2 passes	89.4	91.6	105	101	89.75
3 passes	92	96.9	96.3	86.9	93.025
Sample at T2 = 300°C, V2 = 27 mm/s					
1 pass	82.7	82.9	83.5	79.3	82.1
2 passes	79.4	93.6	89.7	87	87.425
3 passes	81.1	101	103	89.8	93.725

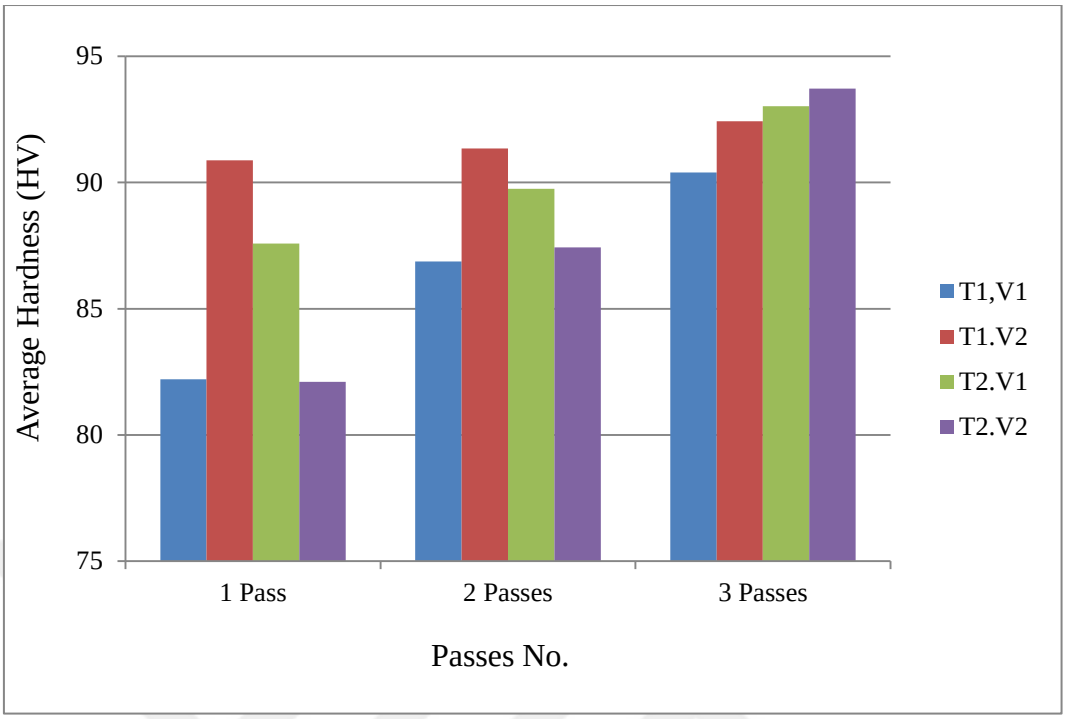

Figure 6.29: Hardness for different velocities and temperatures through three passes

When increasing the temperature, the hardness would increase during pass 3 in all the processes.

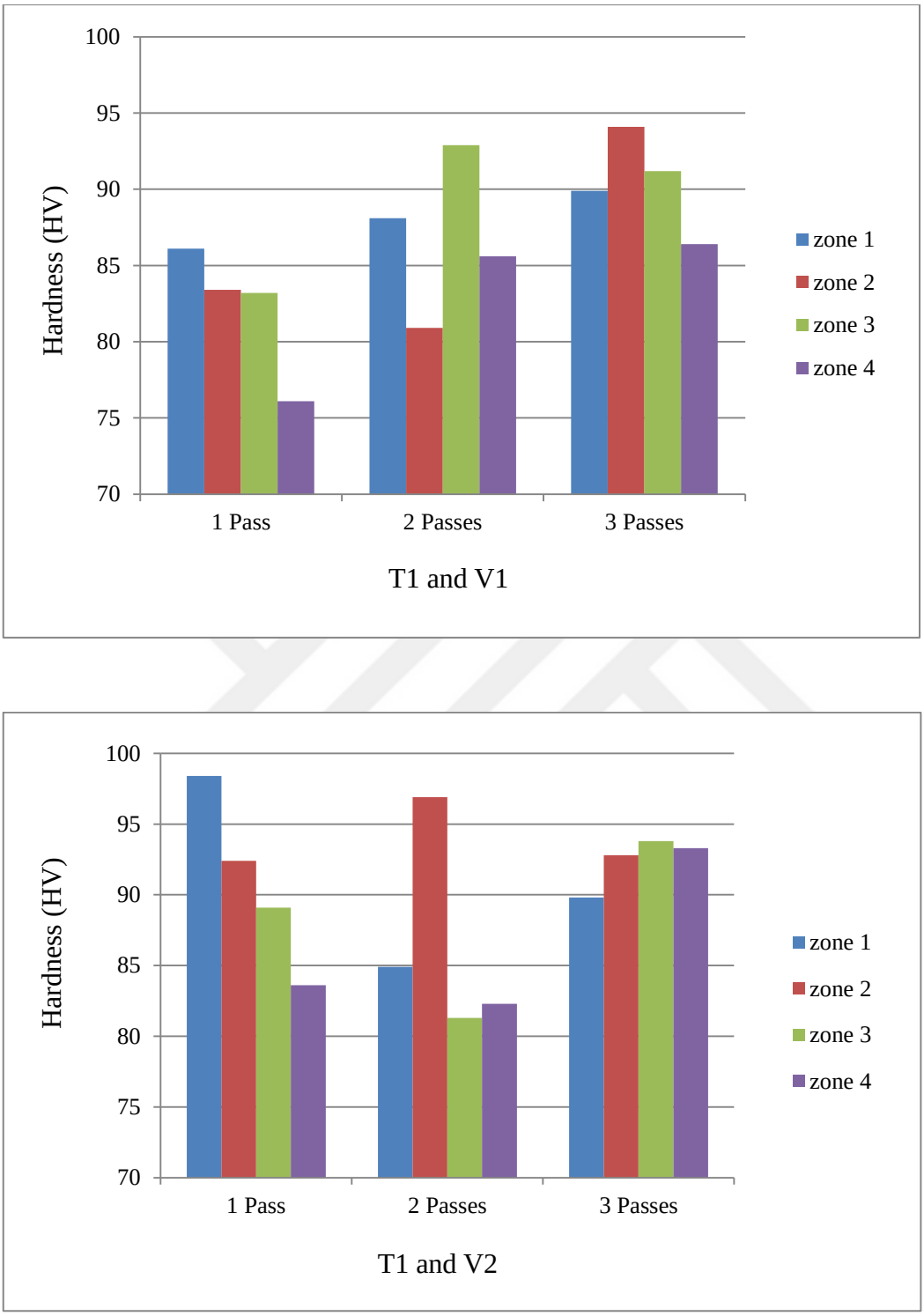

Figure 6.30: Hardness at T1 = 275°C, V1 = 14 mm/s and V2 = 27 mm/s

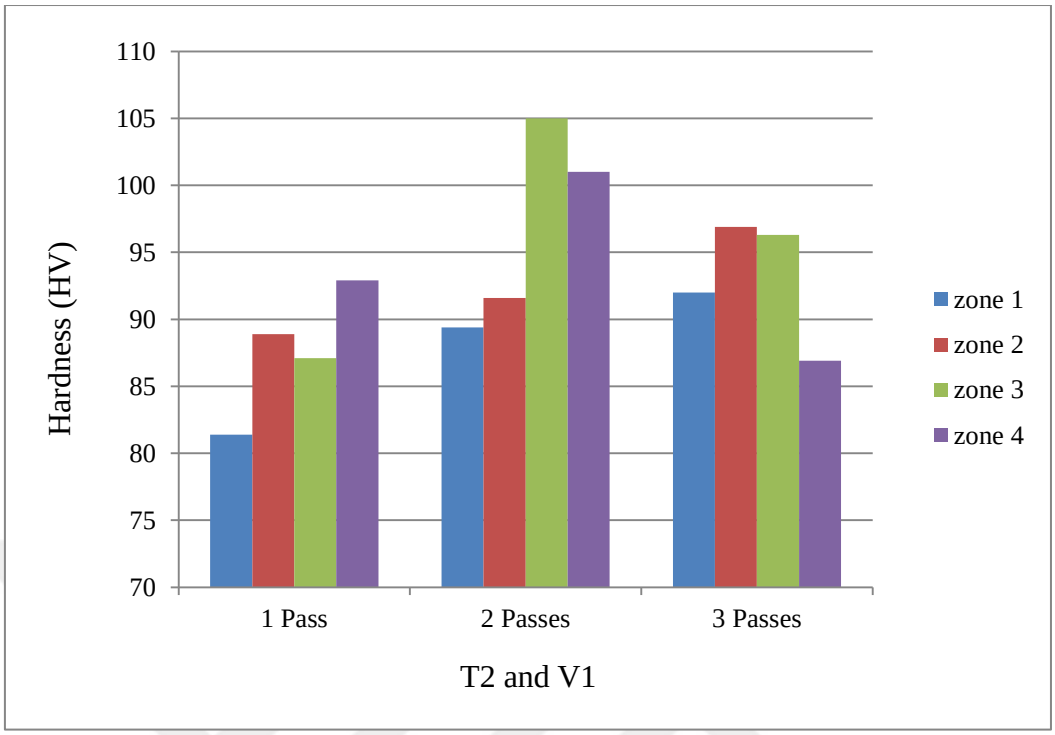

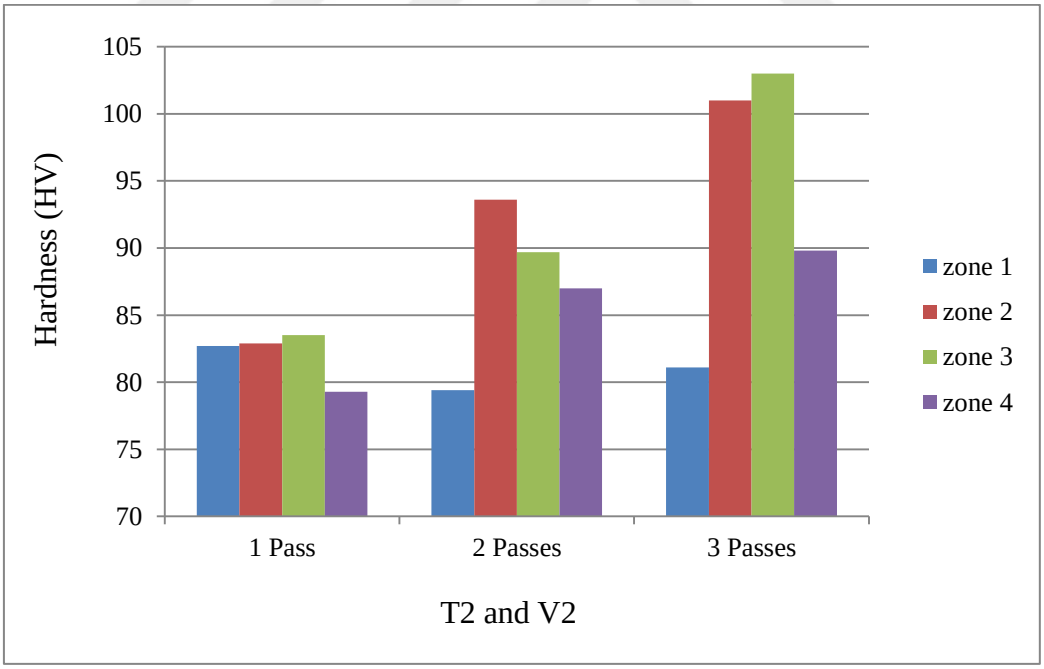

Figure 6.31: Hardness at T2 = 300°C, V1 = 14mm/s and V2 = 27 mm/s

At a constant temperature, the hardness increased at the above velocity.

6.2.4 Load and Time

In the experimental work, the measurements of load and time were taken in the mechanical press during the process, as shown in the table below:

Table 6.17: Load and time measurements at T1 = 275°C

Case 1 T1 = 275°C and V1 = 14 mm/s			
p (kg/cm²)	t (s)	No. of passes	Cases
1300	5.5	1	1 pace
1500	7	1	2 passes
1000	5	2	
750	15	1	3 passes
850	12	2	
1000	6	3	
Case 2 T1 = 275°C and V2 = 27 mm/s			
p (kg/cm²)	t (s)	No. of passes	Cases
1290	3	1	1 pace
1250	5	1	2 passes
950	3.5	2	
1300	5	1	3 passes
1000	4	2	
800	2.5	3	

Table 6.18: Load and Time measurements at T2 = 300°C

Case 3 T2 = 300°C and V1 = 14 mm/s			
p (kg/cm²)	t (s)	No. of passes	Cases
1300	4.5	1	1 pass
1450	4.8	1	2 passes
1100	4.3	2	
1500	5	1	3 passes
1100	4.4	2	
1000	4	3	
Case 4 T2 = 300°C and V2 = 27 mm/s			
p (kg/cm²)	t (s)	No. of passes	Cases
1100	3	1	1 pass
1100	3.4	1	2 passes
1000	2.4	2	
1000	5	1	3 passes
900	4.79	2	
875	4	3	

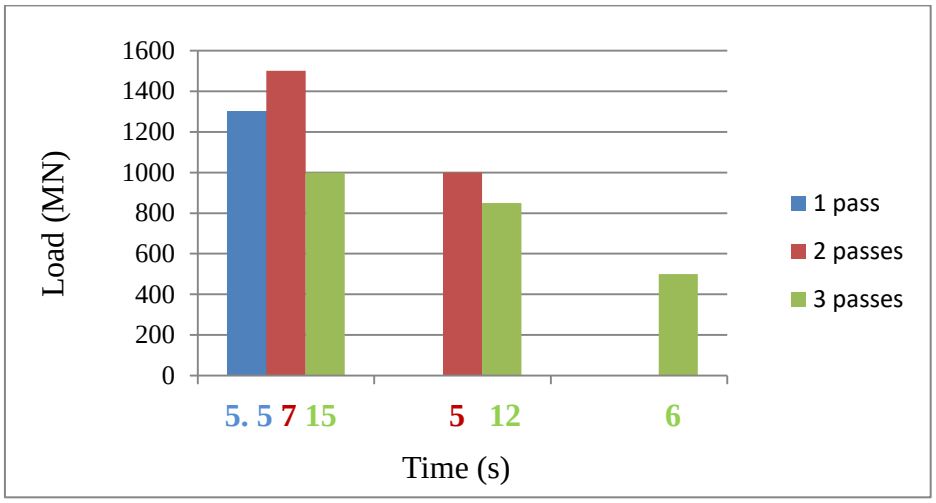

Figure 6.32: Relationship between loads and times at T1 = 275°C and V1 = 14mm/s

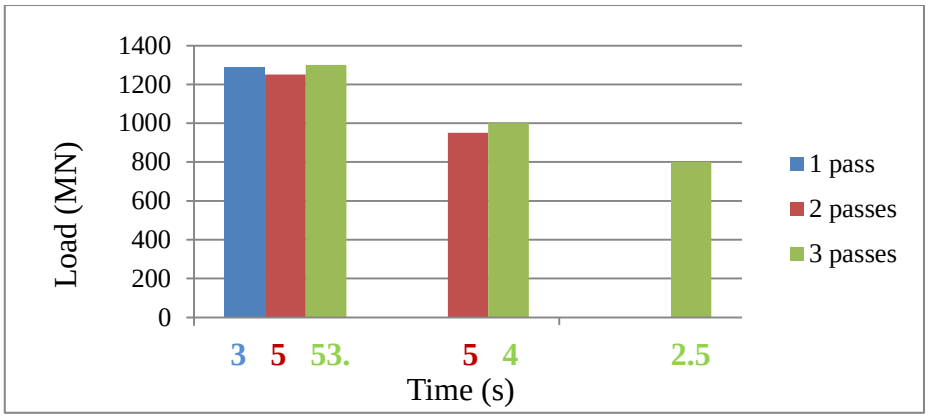

Figure 6.33: Relationship between loads and times at T1 = 275°C and V2 = 27 mm/s

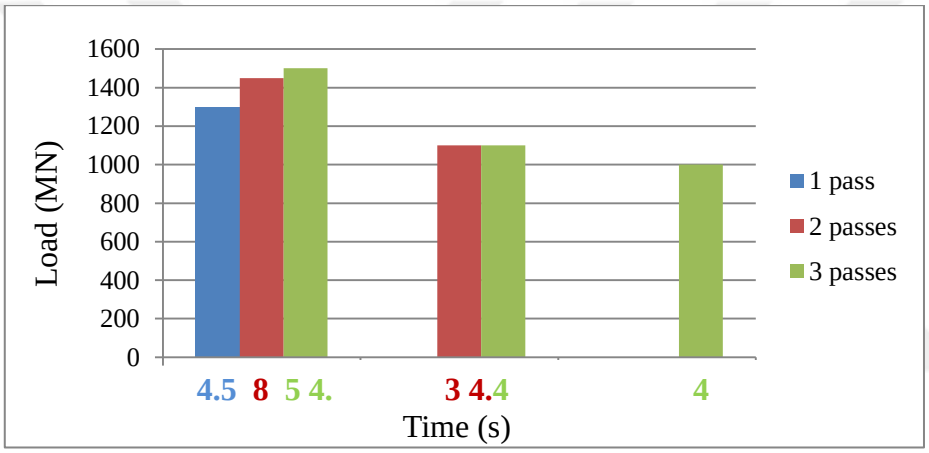

Figure 6.34: Relationship between loads and times at T2 = 300°C and V1 = 14 mm/s

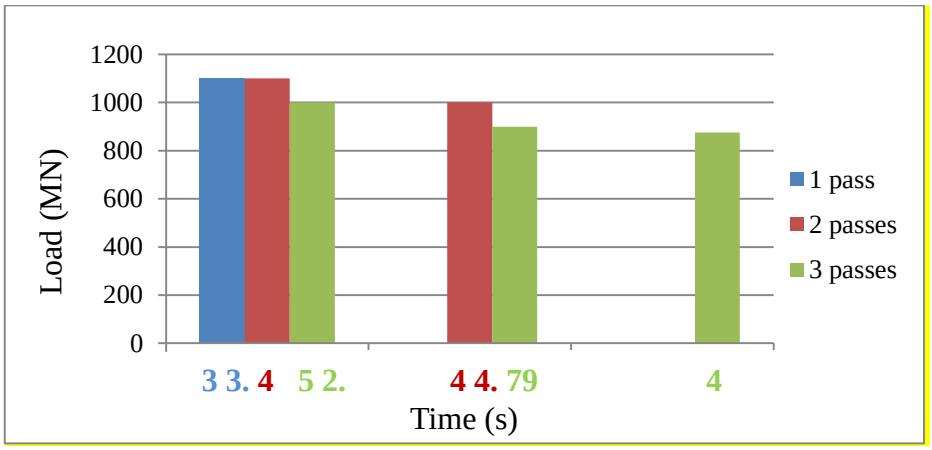

Figure 6.35: Relationship between loads and times at T2 = 300°C and V2 = 27 mm/s

6.3 Comparsion between Experimental and Simulation Results

6.3.1 Grain Size

The figures below show comparsions in grain size between experimental and simulation results.

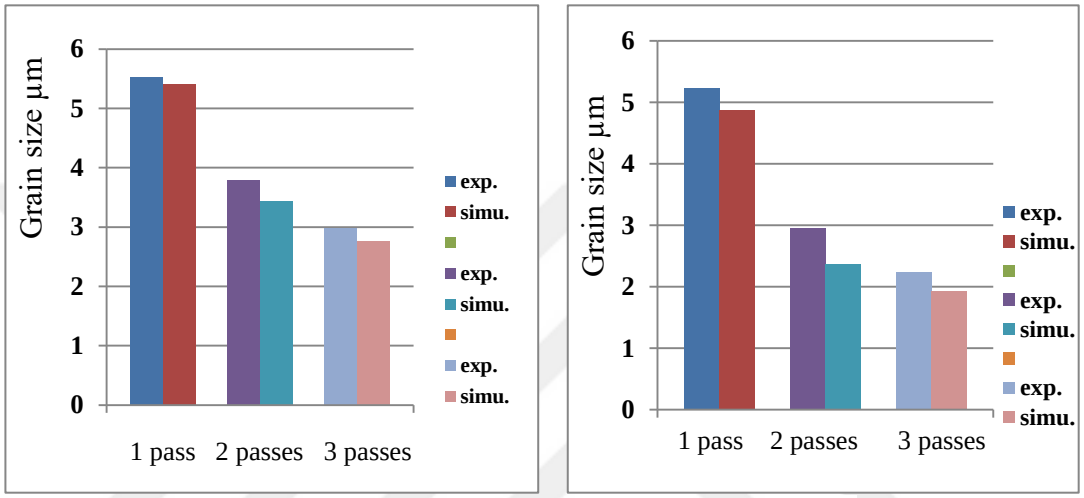

(a) (b)

Figure 6.36: Relationship between simulation and experimental for grain size at constant temperature T1 = 275°C and constant velocity (a) V1 = 14mm/s and (b) V2 = 27 mm/s

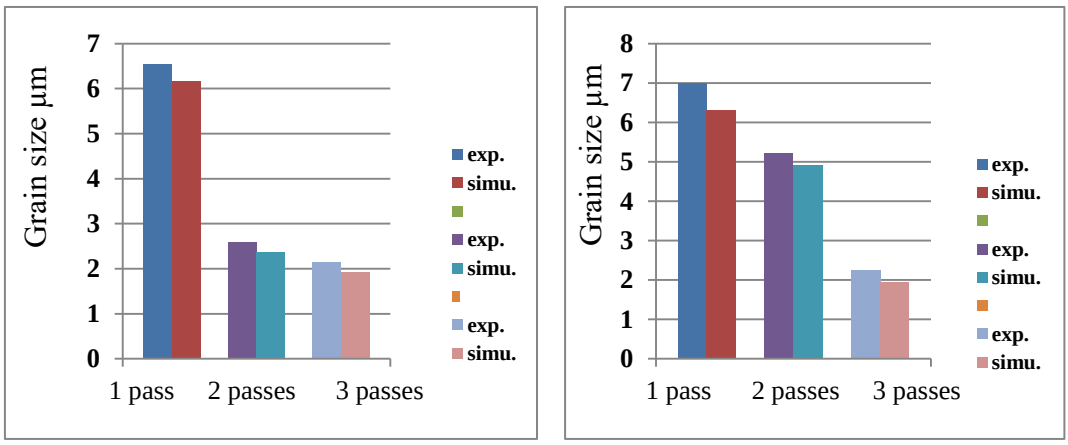

(a) (b)

Figure 6.37: Relationship between simulation and experimental for grain size at constant temperature T2 = 300°C and constant velocity (a) V1 = 14 mm/s and (b) V2 = 27 mm/s

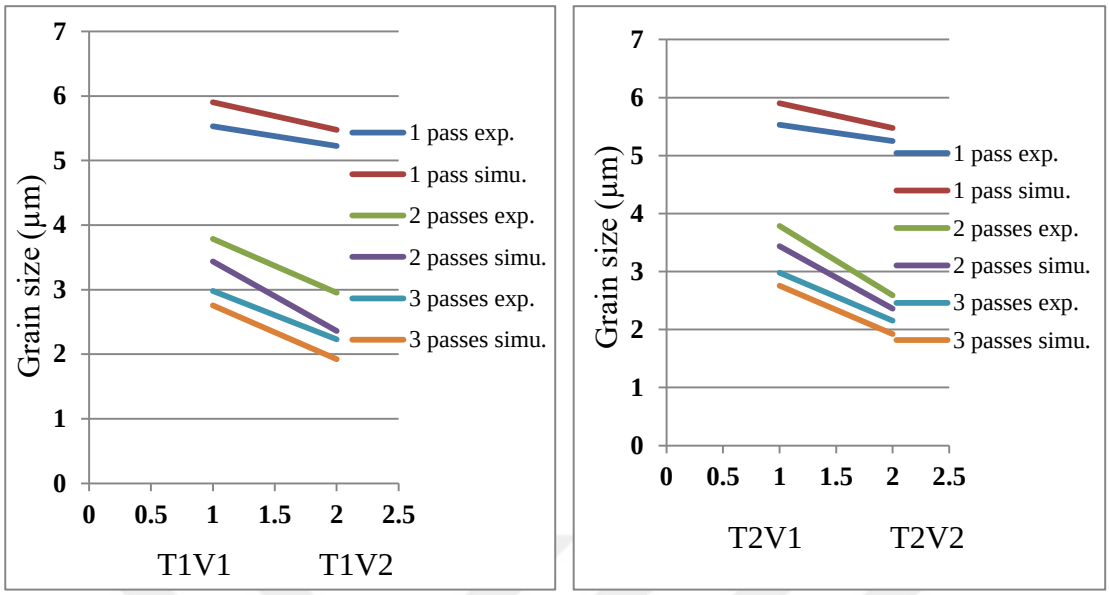

Figure 6.38: Relationship between simulation and experiments for grain size with temperatures (b) T1 = 275°C and (b) T2 = 300°C

The change in velocity between V1 = 14 mm/s and V2 = 27 mm/s with the constant temperature T1 would lead to a grain size decrease (and an increase in the number of grains).

A change in temperature with a constant velocity V1 produced little difference in grain size between the experimental and simulation results.

At a constant temperature T2, the grain size would increase with the higher velocity of V2. Grain sizes at T2 were greater than that of the grain size at T1.

6.3.2 Hardness

The figures below show comparsions in hardness between the experimental work and simulation results.

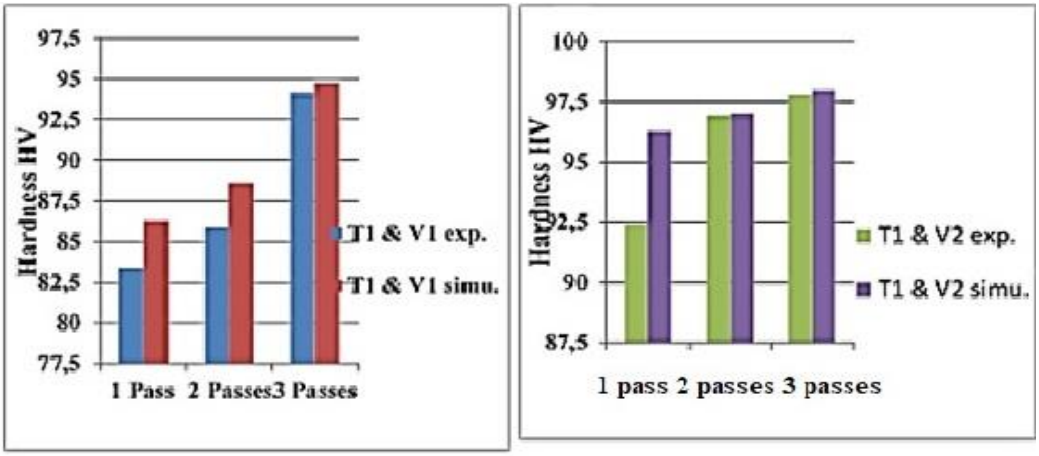

(a) (b)

Figure 6.39: Relationship between simulations and experiments for hardness at constant temperature of T1 = 275°C and constant velocities (a) V1 = 14mm/s and (b) V2 = 27 mm/s

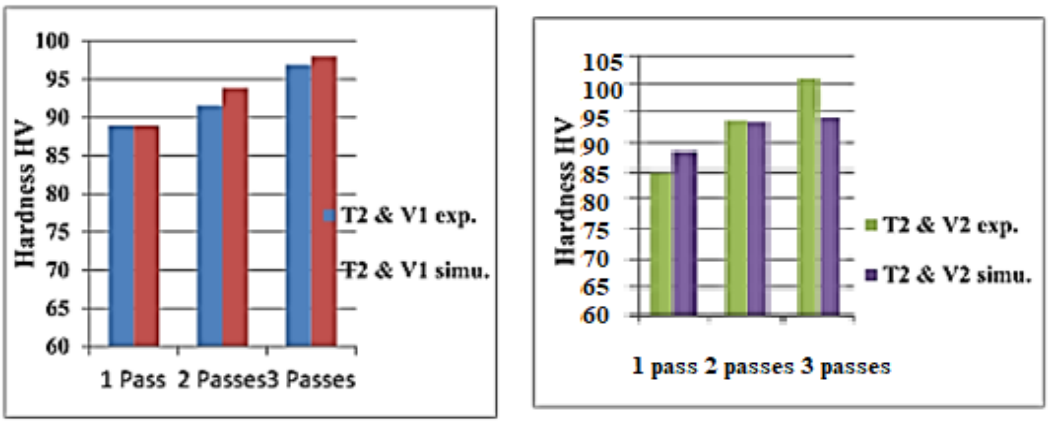

(a) (b)

Figure 6.40: Relationship between simulations and experiments for hardness at constant temperature T2 = 300°C and constant velocities of (a) V1 = 14mm/s and (b) V2 = 27 mm/s

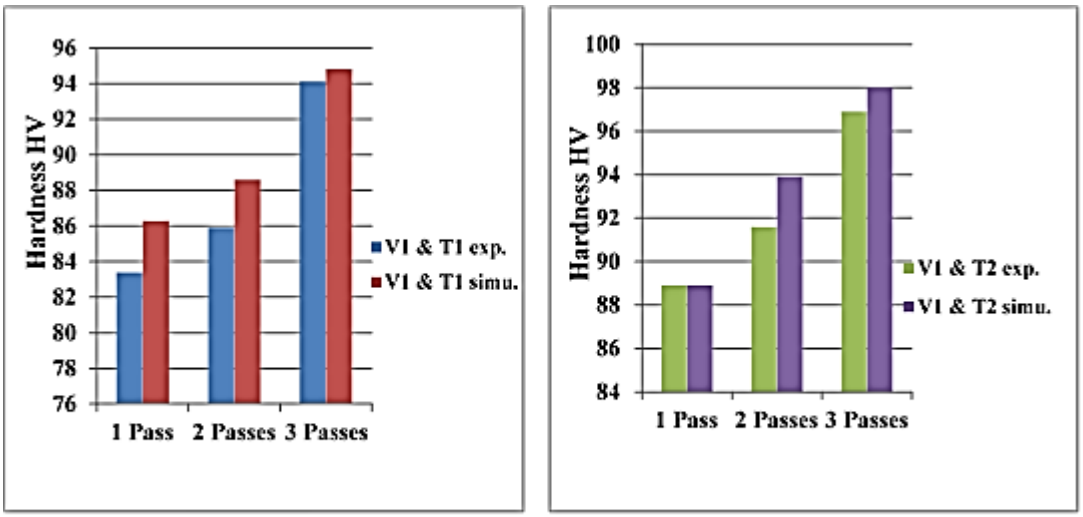

(a) (b)

Figure 6.41: Relationship between simulations and experiments for hardness at constant velocity V1 = 14 mm/s and constant temperatures of (a) T1 = 275°C and (b) T2 = 300°C

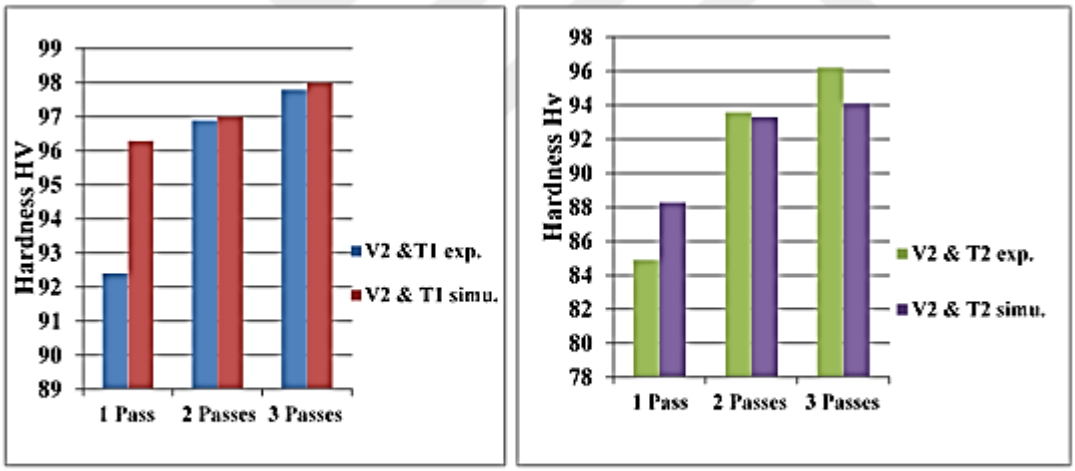

(a) (a)

Figure 6.42: Relationship between simulation sand experiments for hardness at constant velocity V2 = 27 mm/s and constant temperatures of (a) T1 = 275°C and (b) T2 = 300°C

The differences between the hardness values of the experimental work and simulation are such that the simulation results exceed the results of the experiments due to the ideal results of the software program.

6.3.3 Load and Time

Relationships between load and time in the experimental work and simulation results are shown in the figures below.

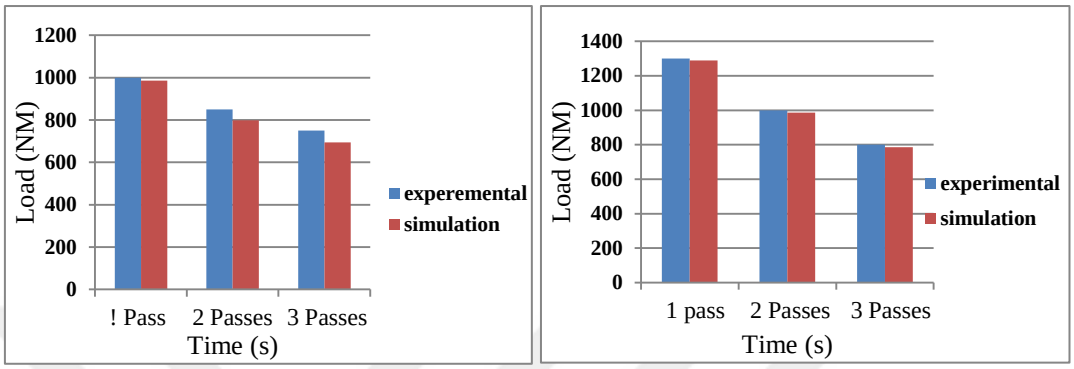

(a) (b)

Figure 6.43: Relationship between the simulation and experiments for loads and times at the constant temperature of T1 = 275°C and velocities (a) V1 = 14 mm/s and (b) V2 = 27 mm/s

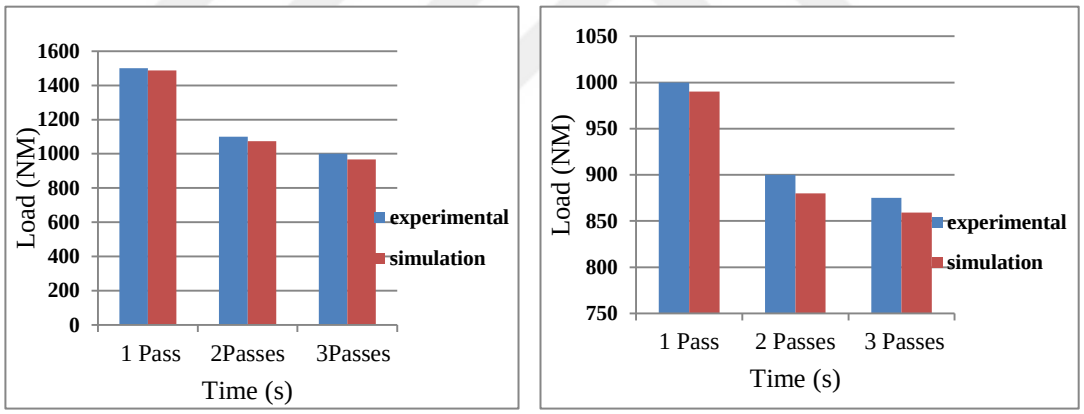

(a) (b)

Figure 6.44: Relationship between the simulation and experiments for loads and times at the constant temperature of T2 = 300°C and velocities (a) V1 = 14 mm/s and (b) V2 = 27 mm/s

6.4 Discussion

Channel angular pressing was performed using both numerical analysis and experimental work to compare results. The numerical work was performed using Q Form, which is efficient for all extrusion processes. The first Q Form analysis

showed some die geometry defects, such as non-uniform deformation as well as shape and dimension defects. The important die fault was the bending angle of the channel angle as it was somewhat sharp such that the simulation would return an error in this region. The die was therefore redesigned by changing the sharp angle into a smooth, curved shape. The simulation was then repeated to give more correct results. The experimental work involved die manufacturing of the ECAP process and magnesium alloy AZ31 as the work piece material. The problem was the insulating system for the die to ensure hot working and keeping the temperature constant during the work. A jacket heater was specially designed and manufactured according to the die dimensions. The most significant problem was the extraction of the product from the die as time was required to do so. The grain size and refinement results show that an increase in the number of passes from pass 1 to pass 3 would increase the refinement by decreasing the grain size. For the effects of velocity, it was shown that the higher velocity provides greater grain refinement and increased hardness. For the microstructure test, the results showed that the temperature of T2 = 300°C had a more uniform structure, especially with velocity increasing to V2 = 27mm/s. The maximum hardness value was 103 HV at pass 3 with T1 = 275°C and V2 = 27 mm/s. On the other hand, the minimum grain size measured was 1.923 μm at T2 and V2. From the simulation, the higher stress value was recorded in the deformation region located at the angle of intersection of the two channels, which was 268 MPa at T1 = 275°C at pass 2 and 386 MPa at pass 3 also with T2 = 300°C. Increasing the velocity sometimes led to broken samples, especially at a high lubrication rate. For the load and pressure, a clear reduction occurred with in increasing in the number of passes due to the ductility increasing each pass as well as due to super plasticity. The results of the simulation and experiments almost identical; however, the experimental values exceeded those of the simulation due to the friction losses and other ideal conditions from the numerical software not present in the experimental work. Flakes, broken samples, non-uniform shapes and poor surface finish were the most significant defects that appeared on the products due to difficulty of controlling the velocity, lubrication and temperature.

The mean stress distribution was at maximum stress at the corner of the angle ϕ because of the shear in the metal layer at this edge. The minimum stress was at the contact area between the punch and work piece.

Figure 6.3 shows that an increase in temperature would lead to a decrease in the mean stresses at a constant velocity because of the increasing friction forces.

Figure 6.4 shows how increasing the velocity with temperature being constant results in an increase in stresses for passes 1 and 2 due to the friction force increasing. For pass 3, increasing the velocity would decrease the stresses because of the increasing in ductility

The effective stress distribution showed the maximum stress was at the corner of angle ϕ and curvature angle ψ because of the movement of the metal layer occurring in this area. The minimum effective stress was in the area far from the corners of the channel at the end of the work piece deformation.

Figure 6.5 shows that increasing the temperature would lead to a decrease in the effective stresses when the velocity is constant, which is due to an increase in ductility and higher friction forces.

Figure 6.6 shows that increasing the velocity with temperature remaining constant would produce and increase in the stresses for passes 1 and 2 due to the friction force increasing. For pass 3, increasing the velocity would decrease the stress because of the increase in ductility

The plastic strain distribution showed maximum strain at the center of the work piece because of the high plastic deformation of the metal in this area. The minimum plastic strain occurred at the end of the work piece for each pass with maximum plastic strain occurring during the third pass.

Figure 6.8 shows that increasing the temperature would lead to increasing the plastic strain when the velocity was constant because of the higher friction forces.

In Figure 6.9, it can be observed that increasing the velocity while temperature remained constant would produce an increase in plastic strain due to an increasing in the dislocation of the material layers, which occurred during every pass.

The minimum grain size in the outer surface of the work piece because of the change in shape and maximum deformation with dislocations would occur more in the corner of the channel than in the center of the work piece.

Grain sizes decreased when the temperature increased and the finest grain size occurred at T = 300°C, while the highest value was recorded at T = 275°C. This result is in agreement with the previewed studies [7].

For velocity increasing with the temperature being constant, the grain size would decrease and obtain the best refinement at V = 27 mm/s during pass 3 after three occurrences of pressing.

The maximum temperature occurred in the work piece while passing through the channel angle at the shape changes because of the shear zone and greatest deformation occurring in those regions. The minimum temperature was observed at the end of the process when the friction force was at a minimum

Figures 6.13 and 6.14 show how increasing the velocity with temperature T1 = 275°C being constant would occur with loads and times decreasing because of the dislocation between the material layers with increasing velocities. Moreover, the dislocation would decrease with an increase in the number of passes.

Figures 6.15 and 6.16 show that increasing the velocity while maintaining a constant temperature (T2 = 300°C) produced a situation where the loads and times would decrease because of the dislocation between the material layers when increasing the velocity. Moreover, load would decrease with an increase in the number of passes.

Figure 6.17 shows that at a constant temperature (T1 = 275°C), the hardness values would increase when the velocity increased because of the grain size decreasing and the velocity would increase with an increasing number of passes.

Figure 6.18 shows how at a constant temperature of T2 = 300°C, the hardness values would increase when the velocity decreased due to the grain size decreasing at low velocity. At high velocity, grain growth would occur. Moreover, grain growth would increase with an increase in the number of passes.

Figure 6.19 shows how at constant velocity V1, the hardness values would increase when the temperature increased due to grain size decreasing. There was an increase with an increase in the number of passes.

Figure 6.20 shows how at constant velocity V2, the hardness values would increase when the temperature decreased due to grain growth at the higher temperature when hardness decreased. Moreover, it would increase with an increase in the number of passes.

Increasing the number of passes would lead to an increase in the refinement and hardness value, which is in agreement with the other studies [14]

CHAPTER 7

CONCLUSIONS AND RECOMMENDATIONS

7.1 Conclusions

1- Severe plastic deformation in the ECAP process shows good results with magnesium alloy AZ31.
2- The Q Form software is an appropriate numerical analysis tool when dealing with manufacturing processes, especially extrusion, the ECAP process and forging processes.
3- There is good agreement between simulations and experimental work.
4- The results of the experimental work are higher in value than the results of the simulation because of the friction between the punch, die, and work piece.
5- Excessive lubrication for the die and work piece lubrication lead to many defects in the samples.
6- Many defects appeared during the experimental work, such as broken samples, flakes and non-uniform shapes.
7- The reasons for the defects depended on punch velocity control, smoothness of the die and billets surfaces as well as the amount and type of lubrication.
8- The manufactured ECAP die was suitable and efficient to achieve the process and deformation to produce high product quality.
9- The insulation of the jacket heaters resulted in insulation efficiency to maintain the temperature and reduce time of heating.
10- The greatest difficulties occurring during the experimental work were the die opening and product extraction due to the high temperatures and occasional cohesion between samples and die surfaces.
11- Q Form analysis showed many defects in die designs leading to modifications being made prior to die manufacturing.

12- Many tests were applied, such as on microstructure, grain size measurement and hardness, the results of which are as follows:

Grain Size

- Changing the velocity between V1 = 14 mm/s and V2 = 27 mm/s at the same temperature of T1 = 300°C led to a grain size decrease (and an increase in the number of grains).
- Upon changing the temperature between T1 = 300°C and T2 = 275°C at the same velocity of V1 = 14 mm/s, there was little difference in grain size; therefore, increasing the velocity would lead to more refinement.
- During the first pass, the grain size decreased until pass three, at which time it was shown that the best grain refinement would occur.
- A higher reduction of grains occurred at a higher temperature T2.

Hardness

- At a constant temperature of T1 = 275°C and at different velocities, the hardness increased as velocity increased, as observed in both the experimental and simulation results.
- At the temperature of T2 = 300°C with different velocities, the hardness would increase at the constant velocity of V1 = 14 mm/s.
- At the constant velocity of V2 = 27 mm/s and at different temperatures, the hardness would increase more at T2 than at T1 in both the experimental and simulation results.

Load

- The results showed that for the increase in the pass numbers from pass 1 to pass 3, the load would decrease and the time of deformation would decrease.
- At the higher temperature of T3 = 300°C, the pressure required to deform the work piece fell more than the pressure required at T1 = 275°C.

- As velocity increased to V2 = 27 mm/s, a reduction in the pressure values occurred.

7.2 Recommendations

1- Choosing other light materials for the ECAP process, such as aluminum alloy.
2- Changing boundary conditions while using higher temperature values.
3- Using different velocities, be they lower or higher.
4- Choosing other types of the lubrication for the ECAP process.
5- Increasing the number of passes in the experimental work.
6- Applying other numerical analyses for simulations and comparing them with Q Form results.
7- New die geometries could be used with different channel angles, such as 90°, and compared with the ECAP process.
8- Applying other isolation systems by using suitable furnace in spite of heater jackets.
9- Calculating the effects of velocity, number of passes and temperature on residual stresses and tensile strength.

REFERENCES

[1] L. Lin, Z. Liu, L. Chen, T. Liu and S. Wu, "Microstructure evolution and low Temperature super plasticity of ZK40 Magnesium alloy subjected to ECAP," Metals and Materials International, vol. 10, no. 6, pp. 501-506, 2004.

[2] F.S.J. Poggiali, R.B. Figueiredo, M.T.P. Aguilar and P. Cetlin, "Grain refinement of commercial purity magnesium processed by ECAP," Materials Research, vol. 15, no. 2, pp. 312-316, 2012.

[3] Y. Estrin and A. Vinogradov, "Extreme grain refinement by severe plastic deformation: A wealth of challenging science," Acta Materialia, vol. 61, no. 3, pp. 782-817, 2013.

[4] R.B. Figueiredo and T.G. Langdon, "Grain refinement and mechanical behavior of magnesium alloy processed by ECAP," Springer Science Journal of Materials Science, vol. 45, no. 17, pp. 4827-4836, 2010.

[5] M. Gzyl, A. Rosochowski, R. Pesci, L. Olejnik, E. Yakushina and P. Wood, "Mechanical properties and microstructure of AZ31B Magnesium alloy processed by I-ECAP," Metallurgical and Materials Transactions A, vol. 45,no. 3, pp. 1609-1620, 2013.

[6] R.Z. Valiev and T.G. Langdon, "Principles of equal-channel angular pressing as a processing tool for grain refinement," ELSEVIER Progress in Materials Science, vol. 51, pp. 881-981, 2006.

[7] P. Lukáč, R. Kocich, M. Greger, O. Padalka and Z. Száraz, "Microstructure of AZ31 and AZ61 Mg alloys prepared by rolling and ECAP," Kovove Mater, vol. 45, pp. 115-120, 2007.

[8] Y. Estrin S.B. Yi, H.G. Brokmeier, Z. Zúberová, S.C. Yoon, H.S. Kim and R.J. Hellmig, "Microstructure, texture and mechanical properties of the magnesium alloy AZ31 processed by ECAP," International Journal of Materials Research, vol. 99, no. 1, pp. 50-55, 2008.

[9] R.B. Figueiredo and T.G. Langdon, "Developing superplasticity in a magnesium AZ31 alloy by ECAP," Journal of Materials Science, vol. 43, no. 23-24, pp. 7366-7371, 2008.

[10] R.B. Figueiredo and T.G. Langdon, "Record Superplastic ductility in a Magnesium alloy processed by equal –channel angular pressing," Advanced Engineering Materials, vol. 10, no. 1-2, pp. 37-40, 2008.

[11] R.B. Figueiredo, I.J. Beyerlein, A.P. Zhilyaev and T.G. Langdon, "Evolution of texture in a magnesium alloy processed by ECAP through dies with different angles," Materials Science and Engineering A, vol. 527, no. 7-8, pp. 1709-1718, Elsevier, 2010.

[12] R. Ding, C. Chung, Y. Chiu and P. Lyon, “Effect of ECAP on microstructure and mechanical properties of ZE41 magnesium alloy,” ELSEVIER Materials Science and Engineering A, vol. 527, no. 16-17, pp. 3777-3784, 2010.

[13] Y.K.S.Y.B. Jing and X.U.E. Feng, “Effects of rotary-die ECAP routes on microstructure and mechanical property of AZ31 Magnesium alloy,” Acta Metall Sin, vol. 46, no. 1, pp. 27-33, 2010.

[14] K. Bryla, T. Dutkiewicz, L. Lityńska-Dobrzyńska, L.L. Rokhlin and P. Kurtyka, “Influence of number of ECAP passes on microstructures and mechanical properties of AZ31 Magnesium alloy,” Archives of Metallurgy and Materials, vol., 57, pp. 711-717, 2012.

[15] G.D. Fan, M.Y. Zheng, C.H. Ju, X.S. Hu, K. Wu, W.M. Gan and H.G. Brokmeier, “Effect of grain size on cyclic micro plasticity of ECAP processed commercial pure magnesium,” Journal of Materials Science Springer, vol. 48, no. 3, pp. 1239-1248, 2013.

[16] Y. Ogushi, E. Mostaed, D. Dellasega, M. Vedani, H. Miyamoto and H. Fujiwara, “Aging behavior of ECAP processed AZ80 Mg alloy,” The International Conference on Nanomaterial's by Severe Plastic Deformation, Materials Science and Engineering, vol. 63, no. 1, pp. 012076, 2014.

[17] G. Qiang, E. Mostaed, C. Zanella, Y. Zhentao and M. Vedani, “Ultra –fine grained degradable Magnesium for biomedical applications,” Rare Metal Materials and Engineering, vol. 43, no. 11, pp. 2561-2566, 2014.

[18] E. Mostaed, M. Hashempour, A. Fabrizi, D. Dellasega, M. Bestetti, F. Bonollo and M. Vedani, “Microstructure, texture evolution, mechanical properties and corrosion behavior of ECAP processed ZK60 magnesium alloy for biodegradable applications,” ELSEVIER Journal of the Mechanical Behavior of Biomedical Materials, vol. 37, pp. 307-322, 2014.

[19] E. Mostaed, A. Fabrizi, D. Dellasega, F. Bonollo and M. Vedani, “Microstructure,mechanical behavior and low temperature super plasticity of ECAP processed ZM21 Mg alloy,” ELSEVIER Journal of Alloys and Compounds, vol. 638, pp. 267-276, 2015.

[20] V.V. Ramalingam, P. Ramasamy, M.D. Kovukkal and G. Myilsamy, “Research and development in magnesium alloy for industrial and biomedical applications: a review,” Metals and Materials International, pp. 1-22, 2019.

[21] J. Zrnik, S.V. Dobatkin and I. Mamuzić, “Processing of metals by sever plastic deformation (SPD)-structure and mechanical properties respond,” Metalurgiha, vol. 47, no. 3, pp. 211-216, 2008.

[22] D. Verma, N.K. Mukhopadhyay, G.V.S. Sastry and R. Manna, "Microstructure and mechanical properties of ultrafine-grained interstitial-free steel processed by ECAP," Transactions of the Indian Institute of Metals, vol. 70, no. 4, pp. 917-926, 2017.

[23] Y. Beygelzimer, "How to make strong metals with high ductility," https://slideplayer.com/slide/5139713/, 2019.

[24] R. Kapoor, "Severe plastic deformation of materials," Materials Under Extreme Conditions. Elsevier, pp. 717-754, 2017.

[25] P. Thakur, P. Surve and S. Sanas, "Advancement in die design of equi-channel angular pressing (ECAP) process: a review," International Journal of Scientific & Engineering Research, vol. 5, no. 12, pp. 93-96, 2014.

[26] A. Fadaei, F. Farahafshan and S. Sepahi-Boroujeni, "Spiral equal channel angular extrusion (Sp-ECAE) as a modified ECAE process," Materials & Design, vol. 113, pp. 361-368, 2017.

[27] O. Sanusi, D. Makinde and J. Oliver, "Equal channel angular pressing technique for the formation of ultra-fine grained structures," South African Journal of Science, vol. 108, no. 9-10, pp. 1-7, 2012.

[28] B. Ravisankar, "Equal-channel angular pressing (ECAP)," Handbook of Mechanical Nanostructuring, pp. 277-297, 2015.

[29] R.S. Namur, L.M. Feitosa, A.C.K. Ferreira, A.G. Bueno, K.D. Zilnyk and O.M. Cintho, "Ecap consolidation and heat treatment of blended elemental powders of iron, chromium, nickel and manganese," Materials Research 22, 2019.

[30] I. Balasundar and T. Raghu, "Effect of friction model in numerical analysis of equal channel angular pressing process," Materials & Design, vol. 31, no. 1, pp. 449-457, 2010.

[31] I. Balasundar, M.S. Rao and T. Raghu, "Equal channel angular pressing die to extrude a variety of materials," Materials & Design, vol. 30, no. 4, pp. 1050-1059, 2009.

[32] T.G. Langdon, "The principles of grain refinement in equal-channel angular pressing," Materials Science and Engineering A, vol. 462, no. 1-2, pp. 3-11, 2007.

[33] A. Pramono, "Investigation of severe plastic deformation processes for aluminum based composites," Department Mechanical Engineering, 2016.

[34] S. Ahmadzadeh, O. Keles and N. Camuscu, "Effect of equal channel angular pressing on microstructure and mechanical properties of aluminum based composite materials," Gazi University Journal of Science, vol. 30, no. 3, pp. 51-61, 2017.

[35] R.B. Figueiredo, A.L.D.M. Costa, M.S. Andrade, M.T.P. Aguilar and P.R. Cetlin, "Microstructure and mechanical properties of Pb-4% Sb alloy processed by equal channel angular pressing," Materials Research, vol. 9, no. 1, pp. 101-106, 2006.

[36] J.C. Werenskiold, "Equal channel angular pressing (ECAP) of AA6082: mechanical properties, texture and microstructural development," 2004.

[37] R. Melicher, "Numerical simulation of plastic deformation of aluminium work piece induced by ECAP technology," Applied and Computational Mechanics, vol. 3, no. 2, 2009.

[38] H.S. Kim, S.I. Hong and M.H. Seo, "Effects of strain hardenability and strain-rate sensitivity on the plastic flow and deformation homogeneity during equal channel angular pressing," Journal of Materials Research, vol. 16, no. 3, pp. 856-864, 2001.

[39] W.Z. Han, Z.F. Zhang, S.D. Wu and S.X. Li, "Influences of crystallographic orientations on deformation mechanism and grain refinement of Al single crystals subjected to one-pass equal-channel angular pressing," Acta Materialia, vol. 55, no. 17, pp. 5889-5900, 2007.

[40] O. Sanusi, D. Makinde and J. Oliver, "Equal channel angular pressing technique for the formation of ultra-fine grained structures," South African Journal of Science, vol. 108, no. 9-10, pp. 1-7, 2012.

[41] T. Sakai, A. Belyakov, R. Kaibyshev, H. Miura and J.J. Jonas, "Dynamic and post-dynamic recrystallization under hot, cold and severe plastic deformation conditions," Progress in Materials Science, vol. 60, pp. 130–207, 2014.

[42] M.H. Shaeri, M. Shaeri, M. Ebrahimi, M.T. Salehi and S.H. Seyyedein, "Effect of ECAP temperature on microstructure and mechanical properties of Al–Zn–Mg–Cu alloy," Progress in Natural Science: Materials International, vol. 26, no. 2, pp. 182–191, 2016.

[43] O. Sanusi, D. Makinde and J. Oliver, "Equal channel angular pressing technique for the formation of ultra-fine grained structures," South African Journal of Science, vol. 108, no. 9-10, pp. 1-7, 2012.

[44] R.Z. Valiev, "Superior strength in ultrafine-grained materials produced by SPD processing," Materials Transactions, vol. 55, no. 1, pp. 13-18, 2014.

[45] K.R. Cardoso, M.A. Muñoz-Morris, M. Lieblichb and D. Morris "Effect of equal channel angular pressing (ECAP) on microstructure and properties of Al-FeAlCr intermetallic phase composites," Materials Research, vol. 17, no. 3, pp. 775-780, 2014.

[46] A.P. Zhilyaev and T.G. Langdon, "Using high-pressure torsion for metal processing: Fundamentals and applications," Progress in Materials Science, vol. 53, no. 6, pp. 893-979, 2008.

[47] R. Z. Valiev and T.G. Langdon, “Developments in the use of ECAP processing for grain refinement,” Journal Reviews on Advanced Materials Science, vol. 13, no. 1, pp. 15-26, 2006.

[48] M. O. Görtan, “Analytical and experimental investigation of process loads on incremental severe plastic deformation,” 7th International Conference on Nanomaterials by Severe Plastic Deformation IOP Publishing: Materials Science and Engineering, vol. 194, no. 1, 2017.

[49] S. S. Murugan, “Equal channel angular pressing: a novel technique for the production of ultra-fine grained structure in materials– a mini review,” International Journal of Modern Studies in Mechanical Engineering (IJMSME), vol. 3, no. 1, pp. 6-14, 2017.

[50] Y. C. Chen, Y.Y. Huang, C.P. Chang and P.W. Kao, “The effect extrusion temperature on the development of deformation microstructure in 5052 aluminum alloy processed by equal channel angular extrusion,” Acta Materialia, vol. 51, no. 7, pp. 2005-2015, 2003.

[51] G. J. Sevillano, P. van Houtte and E. Aernoudt, “Large strain work hardening and textures,” Progress Materials Science, vol. 25, no. 4-2, pp. 69-134, 1980.

[52] R. Ding, C. Chung, Y. Chiu and P. Lyon, “Effect of ECAP on microstructure and mechanical properties of ZE41 magnesium alloy,” Materials Science and Engineering, A, vol. 527, no. 16-17, pp. 3777-3784, 2010.

[53] J. Lin, W. Ren, Q. Wang, L. Ma and Y. Chen, “Influence of grain size and texture on the yield strength of Mg alloys processed by severe plastic deformation,” Advances in Materials Science and Engineering, 2014.

[54] F. S. J. Poggiali, C.L.P. Silva, P.H.R. Pereira, R.B. Figueiredo and P.R. Cetlin, “Determination of mechanical anisotropy of magnesium processed by ECAP,” Journal of Materials Research and Technology, vol. 3, no. 4, pp. 331-337, 2014.

[55] N. N. M. Ishak, M.S. Salleh, S.H. Yahaya, E. Mohamad and M.A. Sulaiman, “The effect of equal channel angular pressing (ECAP) on the microstructure and hardness of a 356 aluminum alloy,” Journal of Advanced Manufacturing Technology (JAMT), vol. 11, no. 2, pp. 47-58, 2017.

[56] H. X. Khoa, S. Bae, S. Bae, B.W. Kim and J.S. Kim, “Planetary ball mill process in aspect of milling energy,” Journal of Korean Powder Metallurgy Institute, vol. 21, no. 2, pp. 155-164, 2014.

[57] Y. Mazaheri, F. Karimzadeh and M.H. Enayati, “Nanoindentation study of Al356-Al2O3 nanocomposite prepared by ball milling,” Materials Sciences and Applications, vol. 1, no. 04, pp. 217-222, 2010.

[58] R. Z. Valiev, “Superior strength in ultrafine-grained materials produced by SPD processing,” Materials Transactions, vol. 55, no. 1, pp. 13-18, 2014.

[59] Quantor Form Ltd, “The program of simulation of metal forming,” Q Form 2D/3D Version V8 part 4, www.qform3d.com, 2015.

[60] A. Güral, S. Tekeli, A. Aytac and C. Karatas, “Construction of an equal channel angular pressing unit and determination of optimum. parameters for AL-Zn–Mg-Cu alloy chosen as a modal material,” Journal of Polytechnic, vol. 14, no. 4, pp. 243-248, 2011.

[61] M. Elektron, “Service and innovation in magnesium,” Ultimo Acesso em, vol. 19.no. 1, 2015.

[62] M. Gupta and S.N.M. Ling, “Magnesium, magnesium alloys, and magnesium composites,” John Wiley & Sons, 2011.

[63] K. Gudimetla, B. Tejaswi and B. Ravisankar. “Effect of microstructure and mechanical properties of Al–Mg alloy processed by ECAP at room temperature and cryo temperature,” Transactions of the Indian Institute of Metals, vol. 70, no. 3, pp. 639-648, 2017.

[64] P. Minarik and R. Král, J. Pešička and F. Chmelík, “Evolution of mechanical properties of LAE442 magnesium alloy processed by extrusion and ECAP,” Journal of Materials Research and Technology ELSEVIER, vol. 4, no. 1, pp. 75-78, 2015.

[65] J. JIANG and A. MA, “Bulk ultrafine-grained magnesium alloys by SPD processing: technique, microstructures and properties,” Magnesium Alloys – Design, Processing and Properties, 2011.

PUBLICATIONS

1. Haitham Al-Jawad, Cetin Karataş, Faruk Mert and Ban Al-Amer, "Effect of die angle on temperature distribution for Al6061 in ECAP process," International Symposium on Innovative Technologies in the 2018 Published in 6 Engineering and Science 09-11 November 2018 (ISITES2018 Alanya-Antalya. Turkey)

2. Haitham Al-Jawad, Ban Al-Amer, Faruk Mert and Cetin Karataş, "Investigation for lubrication effect on stress distribution during ECAP process by QForm analysis to improve mechanical properties for aluminum alloy," International Symposium on Automotive Science and Technology 5-6 September 2019 Ankara, Turkey.

3. Haitham Al-Jawad, Ban Al-Amer, Faruk Mert and Cetia Karataş, "Effect of curvature angle on ECAP process results for copper alloys," 3nd International Conference on Material Science and Technology in Cappadocia (IMSTEC'18), September 17-19, 2018, Nevsehir, Turkey.

4. Haitham Al-Jawad, Ban Al-Amer, Faruk Mert and Çetin Karataş, "Velocity and die angle influence on stress distribution during ECAP process for aluminum alloy," The International Conference on Materials Science, Mechanical and Automotive Engineering and Technology in Cappadocia/Turkey (IMSMATEC'19), June 21-23 2019.

5. Haitham Al-Jawad, Ban Al-Amer, Faruk Mert and Çetin Karataş, "Evaluation of ECAP process of magnesium alloys for biomedical applications," 1st International Symposium on Light Alloys and Composite Materials (ISLAC'18), March 22-24, 2018, Karabuk, Turkey.

6. Haitham Al-Jawad, Ban Al-Amer, Faruk Mert and Çetin Karataş, "The influence of curvature angle of ECAP process on the residual stresses for the copoer (OFE)," 4th International Conference on Material Science and Technology in Kızılcahamam /Ankara (IMSTEC) & 18-20 October 2019.

7. Haitham Al-Jawad, Ban Al-Amer, Faruk Mert and Çetin Karataş, “Investigation of the effect of velocity on stress for ECAP process of aluminum alloy 7075 by QForm,” 2nd International Congress on Engineering and Architecture, Marmaris/Turkey, 22-24 April 2019.

8. Haitham Al-Jawad, Ban Al-Amer, Faruk Mert and Çetin Karataş, “Numerical analysis to investigate the effect of friction factor and lubrication on load in ECAP process of aluminum alloy 6061,” 2nd International Congress on Engineering and Architecture, Marmaris/Turkey, 22-24 April 2019.